STUDIES ON BIOPOLYMER-BASED NANOCOMPOSITES AND THEIR APPLICATIONS

By

JAGRAM MEENA

2K18/Ph.D/AC/13

Department of Applied Chemistry

Submitted Under the Supervision of

Prof. Sudhir G. Warkar

In fulfilment of the requirements for the degree of

DOCTOR OF PHILOSOPHY

DEPARTMENT OF APPLIED CHEMISTRY

DELHI TECHNOLOGICAL UNIVERSITY

DELHI-110042 (INDIA)

2022

Dedication

To my Parents
Mr. & Mrs. Meena

To my wife and children
Divya Meena, Rudra Meena &
Kiara Meena

Thanks for your endless sacrifices,
love, support and prayers

DELHI TECHNOLOGICAL UNIVERSITY

(Formerly Delhi College of Engineering)

Department of Applied Chemistry Shahbad Daulatpur, Bawana Road, Delhi – 110042, India

DECLARATION

I declare that the research work reported in the thesis entitled **"Studies on biopolymer-based nanocomposites and their applications"** for the award of degree of Doctoral of Philosophy in Chemistry has been carried out by me under the supervision of Prof. Sudhir G. Warkar, Department of Applied Chemistry, Delhi Technological University, India. The research work embodied in this thesis, except where otherwise indicate, is my original research. This thesis has not been submitted by me in part or full to any other University for the award of any degree or diploma. This thesis does not contain other person's data, graphs or other information, unless specifically acknowledged.

Mr. Jagram Meena
(Research Scholar)
2K18/PhD/AC/13

This is to certify that the above statement made by the candidate is correct to the best of our knowledge.

Prof. Sudhir G. Warkar
Supervisor

Prof. Sudhir G. Warkar
Head of Department
Applied Chemistry, DTU

DELHI TECHNOLOGICAL UNIVERSITY

(Formerly Delhi College of Engineering)

Department of Applied Chemistry Shahbad Daulatpur, Bawana Road, Delhi – 110042, India

CERTIFICATE

This is to certify that the Ph.D. thesis entitled **"Studies on biopolymer based nanocomposites and their applications"** submitted to Delhi Technological University, New Delhi, for the award of Doctoral of Philosophy in Chemistry, is based on original research work carried out by me, under the supervision of Prof. Sudhir G. Warkar, Department of Applied Chemistry, Delhi Technological University, Delhi, India. It is further certified that the work embodied in this thesis has neither partially or fully submitted to any other university or institution for the award of any degree or diploma.

Mr. Jagram Meena
(Research Scholar)
2K18/PhD/AC/13

This is to certify that the above statement made by the candidate is correct to the best of our knowledge.

Prof. Sudhir G. Warkar
(Supervisor)

Prof. Sudhir G. Warkar
(Head of Department)
Applied Chemistry, DTU

ACKNOWLEDGEMENT

I have no words to express my deep sense of gratitude for adeptness and heartiest respect to my revered supervisor **Prof. Sudhir G. Warkar,** Department of Applied Chemistry, Delhi Technological University, for his surveillance, learned guidance, worthy encouragement, and heart touching inspirations throughout this work which help me to make this work as complete as possible. I will always be needed for his guidance for techniques of presentation, a positive attitude to the work, and necessary about developmental progress that is shown by full and heartily attention and interest to the latest technologies of the science and active support related programs

I am also thankful to faculty members, Prof. D. Kumar Prof. R. K Gupta Prof. R.C Sharma, Prof. Archna Rani, Prof. Anil Kumar, Prof. Roli Purwar, Prof. Ram Singh, Dr. Richa Srivastava, Dr. Raminder Kaur, Dr. Saurabh Mehta, Dr. D Santhiya, Dr. Poonam, Dr. Manish, Jain, and Dr. Yogendra Kumar Meena for providing necessary help during Thesis work.

I express my thanks to the technical, library, and office staff of the Department of Applied Chemistry, Delhi Technological University, for their help at various stages of the present especially thanks to SAIF Laboratory Punjab University, Chandigarh & Indian institute of Petroleum, Dehradun for helping in testing.

I especially thank to working place Department of Chemistry, Gurukul Kangri (Deemed to be University), Haridwar Uttarakhand, India for providing infrastructural and instrumentation facilities and thanks to Dr. Harish Chandra Assistant Professor Department of Botany and Microbiology, Gurukul Kangri (Deemed to be University), Haridwar, Uttarakhand for providing microbiology testing facility

All my thanks are to my mentors and guide, my respected mother Smt. Jhuma Devi and my Honourable father Shri Mohar Singh Meena, my wife Divya Meena and my son Rudra Meena and daughter Kiara Meena for their great trust in me for their encouragement and pertinence and understanding for educating me to become the person I am. It is that confidence given by my parents which help me to sail through this important part of my life. I am truly blessed to be their son. Finally, my acknowledgment shall remain incomplete if I do not express my sincere gratitude to the almighty God that is always with me when I feel alone, happy sorrowful rows.

Mr. Jagram Meena

Place: New Delhi
Date: November 03, 2022

LIST OF CONTENTS

Chapter 5: Synthesis and Characterizations of carboxymethyl tamarind kernel gum /ZnO nanocomposites and their application in chromium metal removal and antifungal activity

Chapter 7: Conclusion and future prospects

LIST OF TABLES

LIST OF FIGURES

LIST OF ABBREVIATIONS

^0C	Degree centigrade
b	Langmuir adsorption equilibrium constant
BMNCs	Biopolymer Metal Nano Composite
BMNPs	Biopolymer Metal Nano Particles
C_0	Initial concentrations
C_e	Final Concentrations
CMTKG	Carboxymethyl tamarind kernel gum
DDW	Double Distilled water
DMSO	Dimethyl Sulfoxide
g	Gram
GG-	Guar gum
mg/g	Milligram per gram
ml/g	Milli litre gram per
MPa	Mega Pascal Pressure
MTCC	Multi-type Culture Collection
MW	Molecular weight
NA	No Activity
NC	Negative Control
NG	No Growth
nm	Nanometre
NP	Nano Particle
PAA	Polyacrylic acid
PC	Positive Control

PHBV	Poly(3-hydroxybutyrate-co-3-hydroxy valerate)
PLA	Polylactic Acid
PPM	Part Per Million
PVA	Polyvinyl Alcohol
q_e	sAmount of Cr adsorbed
R_L	Separation factor or equilibrium parameter
SPR	Surface Plasma Resonance
TKG	Tamarind kernel gum
V	Volume
V/V	Volume ratio volume
W/V	Weight ratio volume
X	Amount adsorbed per unit weight
X_{max}	Maximum adsorption at monolayer coverage

ABSTRACT

This research focusses on the development of carboxymethyl tamarind kernel gum modified metal nanocomposites. The scientific literature on the synthesized metal and metallic oxide biopolymer nanocomposite used for antibacterial, antifungal, antioxidant, biosensor antifouling, and organic/inorganic contaminant removal from wastewater biosensor activity. The experimental methods used to carry out the research work are discussed in the thesis, which includes information on the materials utilized, approved by the research, and the descriptions and parameters of several characterization techniques XRD, FTIR, HRTEM, FESEM, TGA, DLS, UV. employed to fulfil the research effort's goal.

In seven chapters, the complete thesis is summarized.

The thesis's first chapter provides a brief overview of the study work's contemporary scientific significance, as well as the thesis's objective. It also summarizes the scientific literature on the synthesized metal and metallic oxide biopolymer nanocomposite used for antibacterial, antifungal, antioxidant, biosensor, antifouling, and organic/inorganic contaminant removal from wastewater.

Study Chapter second of the thesis discusses the experimental techniques used to conduct the research work. It also provides information on the materials used, approved for the research, and the descriptions and parameters of a number of characterization techniques used to achieve the objectives of the research effort.

Study Chapter 3 explains the purpose and parameters of the research that was done for this thesis**.**

Chapter four. The use of carboxymethyl tamarind kernel Gum/iron oxide nanocomposites in liquid ammonia sensors and antibacterial activity has been developed and characterised in study These Nano composites exhibited excellent antibacterial activity against both *Enterococcus faecalis* and hence can be considered for applications in antibacterial textiles for personal and hospital uses. The sensing properties of the synthesized nanocomposite solution across rising ammonia concentrations in the range of 1–100 ppm by observing the changes in SPR situations and magnitude with a UV-Visible Spectrophotometer have been notified

The synthesis and characterization of carboxymethyl tamarind kernel gum/ZnO nanocomposites, as well as their utilisation in chromium metal removal and antifungal

activities, are covered in Chapter five. The removal of hexavalent chromium ions from water was studied in relation to pH, concentration, time, and amount of adsorbent. Compared to other biopolymers with zinc oxide modification, carboxymethyl tamarind kernel gum/zinc oxide nanocomposites were found to be more effective adsorbents for Cr (VI) ions. Furthermore, we utilised the CMTKG/ZnO for antifungal activities.

The synthesis and characterization of carboxymethyl tamarind kernel gum nanoparticles and their antioxidant properties are discussed in this Chapter six. The antioxidant capabilities of the produced CMTKG nanoparticles composites were demonstrated by a radical scavenging model system. All of the outcomes were perfectly matched, just as they had been in the literature. CMTKG nanoparticles created in this manner could be employed as antioxidants.

The chapter seven summarizes the entire research study as well as the research's prospects and includes the publications out of the thesis.

Chapter-1

Introduction

1.1 Introduction

The research of a novel class of materials known as "bio nanocomposites" has been prompted by recent developments in nanotechnology and the rising demand for environmentally friendly goods [1–4]. These hybrid materials combine biopolymers—often naturally occurring—with synthetic elements that have at least one nanoscale dimension. Under favourable conditions like oxygen, moisture, and temperature, natural microbe's breakdown biopolymers rather quickly and without causing any environmental problems [5,6]. Studies have shown that modified products made from biopolymer, tamarind kernel gum (TKG) have been investigated in a number of industries, including textiles, explosives, food, agriculture, plywood, and medicine [7–10]. It is an excellent alternative biopolymer for synthetic polymers due to its biodegradability, varied solubility, non-toxicity, and susceptibility to microbial breakdown. TKG is a high-molecular-weight neutral branching polysaccharide made up of cellulose, xylose, and galactoxylose that is derived from tamarind seeds. It is a naturally occurring polysaccharide that degrades quickly, and preferred because of its natural origins and low production costs, as well as the fact that it has few side effects [11,12].

Biopolymer chemical modification has drawn a lot of attention in the last ten years since it allows for both the retention of natural polymers' full potential and the addition of desirable qualities without changing the fundamental structure of the polymer backbone [13–17]. One such excellent example of chemical modification derived from TKG is carboxymethyl tamarind kernel gum (CMTKG) [18–21]. The molar ratio of its constituent sugars is 1:2:3 (D-xylose, D-galactose, and D-glucose). This polysaccharide is composed of a main chain of carboxymethylated glucopyranosyl units linked by β-D-(1 → 4) links and a side chain containing a single xylopyranosyl unit that is further connected to each subsequent second, third, and fourth D-glucopyranosyl unit by α-D-(1 → 6) linkage. Whereas a β-D-(1 → 2) linkage connects one xylopyranosyl unit to one of the D-galactopyranosyl units. The presence of hydroxyl groups, which permits modifications in structure, formula, and functionalization, is the most unique characteristic of CMTKG and its derivatives.

However, the applicability of CMTKG-based polysaccharides remains limited because to their unpleasant odour, rapid biodegradability, low solubility in cold water, dull colour, and poor barrier, mechanical, and thermal properties [22]. As a result, there is a need to enhance and optimize CMTKG's pharmacological and physicochemical properties in order to increase action and, as a result, expand its potential uses. Extensive research has been conducted on CMTKG to modify its physical and chemical properties through grafting, mixing nanoparticles, and nanocomposites with synthetic and natural polymers [23–28].

According to several studies, the mechanical, thermal, barrier, and antibacterial properties of the material were all improved by the inclusion of nanoparticles at low concentrations. Metallic nanoparticles have been employed as reinforcing agents in polysaccharide-based films, such as silver [24,29,30], graphene oxide [18], titanium dioxide [31], and cupric oxide [32]. Of which, Magnetite [33,34] and ZnO [35–37] nanoparticle impregnation can be potential candidates among these nanoparticles. In addition to their inherent characteristics, biopolymer-based nanocomposite materials frequently exhibit great stability, maximum accessibility, and even intriguing enhancements brought on by the interaction of nanoparticles and matrix. They are widely used as adsorbents for the removal of organic and inorganic impurities from effluent water solutions [38–44] and as biosensors [45–50], antifungal [51–54], antioxidant [55–62], antimicrobial [63–68], antifouling [69–75], and drug delivery agents [76–81].

Researchers and industry professionals can benefit from a useful reference source on the properties and applications of biopolymer-based nanocomposite in a variety of industries, including textiles, explosives, food, agriculture, plywood, and medicine. As a result, the goal of the study is to identify the best synthesis method while also examining the features, structural characteristics, and morphology of a biopolymer-based nanocomposite made of magnetite and ZnO metal nanoparticles that have been mixed with CMTKG matrix.

This chapter provides a general review of composites and their different types. The fundamental use of nanocomposites, the current state of biopolymer metallic nanocomposites processing, and use of Fe and Zn oxide nanocomposites in various applications are all explored. The fundamentals of TKG and CMTKG is also covered in this chapter. An outline of this thesis’s content is also included.

1.2 Biopolymers

The polymers that come from plants, animals, and microorganisms are known as biopolymers [82–84]. Commercially, biopolymers are manufactured in enormous quantities for a variety of uses. Except for a small number, most biopolymers may degrade microbiologically into carbon dioxide (CO_2), water (H_2O), methane (CH_4), and inorganic chemicals. Biopolymers are natural polymer alternatives that are widely used in the medical, agricultural, and environmental fields, as well as pharmaceuticals, due to their renewable, sustainable, and non-toxic properties, as well as their biocompatibility and low-cost availability [85–90]. Biopolymers with potential applications include tamarind [91–96], starch [97–102], pectin [103–110], cellulose [111–115], chitin [116–118], and chitosan [119–126]. Because their chains contain a large number of hydroxyl groups that interact well with metal ions and provide a favorable environment for metal and semiconductor nanoparticle development. Biopolymer is also mucoadhesive, biocompatible, and non-irritant, making it useful in biomedical applications such as drug delivery, bio nanoreactors, nanofiltration, biosensors, and antimicrobial properties.

In accordance with their place of origin and synthesis, biopolymers can be categorized into three groups. The first category consists of organic polymers found in plants and animals, such as proteins, polysaccharides, and lipids [127]. The most prevalent carbohydrate, cellulose, is a potential biodegradable polymer that is present in nearly all plant components. Cellulose is environmentally beneficial, requires little energy during production, exhibits exceptional film-forming capabilities, and is simple to recycle by burning. A structural polysaccharide, cellulose is composed of microfibrils that are joined to form cellulose fibres [128,129]. A hydrophobic polymer with an acidic or neutral nature, Chitin is insoluble in water and a wide range of organic solvents [130,131]. Chitosan is the second most prevalent natural amino polysaccharide. Native Chitin extracted from shrimp and other crustaceans is deacetylated to produce it. The storage polysaccharide known as Starch is made up of branched and linear amylopectin chains that are between 0.1 and 1 nm in length. Cereals, tubers, and roots are the primary sources of starches [132].

The second category consists of man-made polymers, which can be created using various condensation or ring-opening polymerization processes. Polylactide, often known as PLA, is a potential synthetic biopolymer that can replace traditional polymers due to its strong clarity and high stiffness. It is a hydrophobic aliphatic polyester that is biodegradable, renewable,

and recyclable and has great processing capabilities [133]. Lactic acid generation is the first stage in the multi-step process that results in PLA. The third category includes biopolymers generated by various bacteria and other microorganisms in a specific medium with the necessary ingredients.

Functionalized biopolymers are a type of organic material that is both robust and chemically resistant, as well as responsive to a variety of chemical modifications [134]. These synthetic and semi-synthetic functionalized materials, also known as reactive biopolymers or ion exchangers, have exploded in popularity over the last five decades, spawning a slew of scientific pursuits ranging from mining to microelectronics, deionization, decontamination, sensing, drug delivery, and desalination, to name a few [135–138].

1.2.1 Tamarind kernel gum

The tamarind tree (*Tamarindus indica*, family: Leguminosae) is generally well known as the "Imli", in Hindi; "Indian date" [139]. It is an African tropical tree that is grown in tropical Asia for the pulp of its pods [140]. This evergreen tree is planted virtually everywhere in India, as well in as other Southeast Asian countries. Tamarind is harvested in India at a rate of around 0.30 million tonnes annually [141]. Tamarind gum is made from the plant's seed endosperm. It is separated from the ground-up tamarind seed kernel powder using a variety of proven techniques. It is present as a cell-wall storage unit in tamarind seed endosperm [139]. The mature and harvested tamarind seeds were processed into tamarind seed kernel powder using a number of stages, including choosing raw seeds, removing the seed coat, separating the seed kernels, milling, grinding, and sieving [7]. It is classified as a galactoxyloglucan and is a water-soluble bio polysaccharide. Tamarind gum's molecules have the following composition: (1 → 4) -β- d-xylopyranose and α-d-galactopyranosyl side chains have been replaced for the α-d-xylopyranose and β-d-galactopyranosyl (1 → 2) -α-d-xylopyranose is attached (1 → 6) to glucose residues with a glucose : xylose : galactose ratio of 2.8 : 2.25 : 1.0 (Figure 1.1) [142,143].

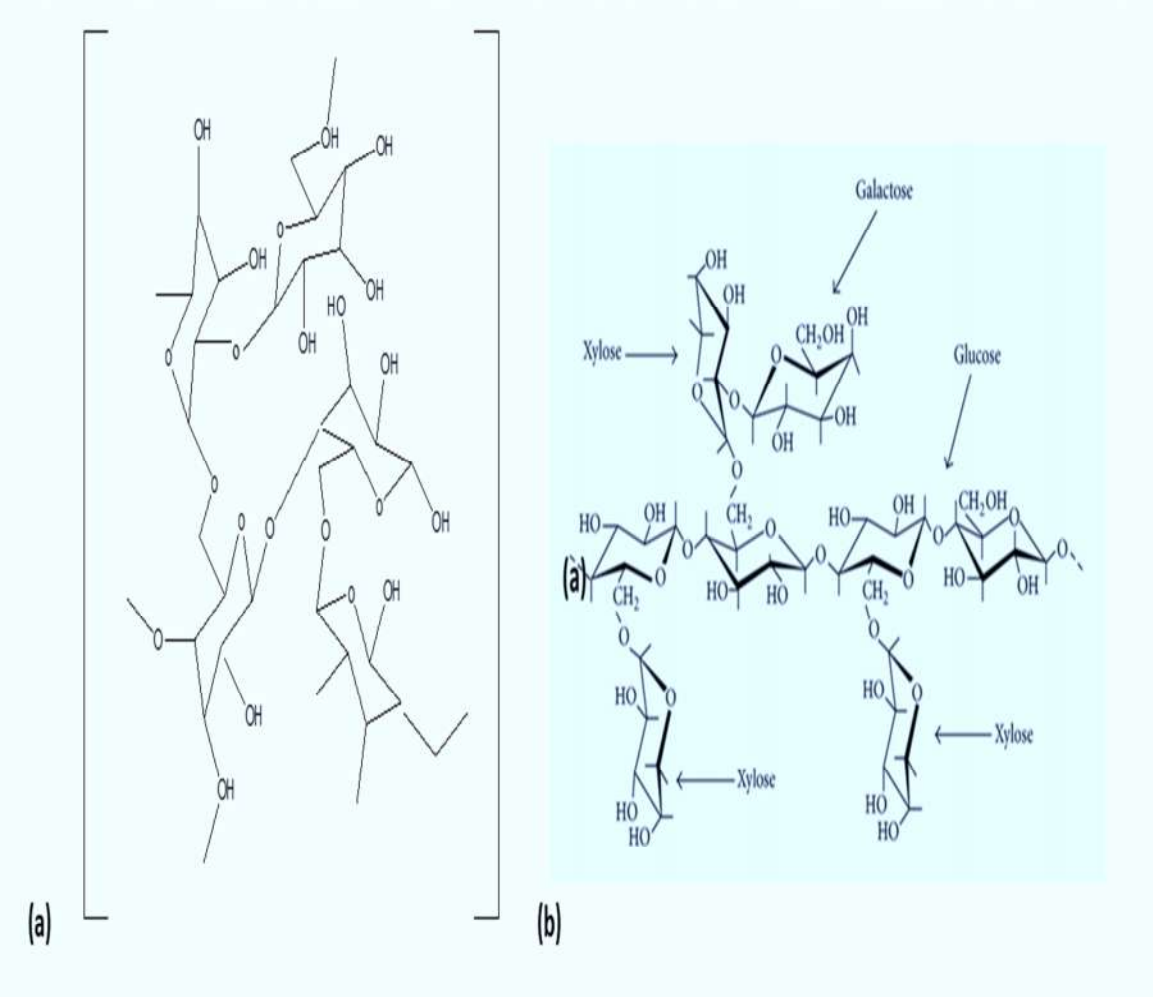

Figure 1.1: Chemical structure of Tamarind gum

Tamarind gum is naturally water soluble, hydrophilic, stable in low pH (acidic environment), biodegradable, and biocompatible. It is employed as binding agents, gelling agents, dissolving agents, sustaining agents in matrix tablets, film-forming agents, thickening agent suspending agents, emulsifying agents, and sola utilizing agents [144–150]. Additionally, it is used as a matrix-former in the fabrication of prolonged drug-releasing matrix tablets for a variety of medications [151,152]. Additionally, tamarind gum is employed in the development of several types of bio mucoadhesive systems for drug administration due to its outstanding hydrophilic and bio mucoadhesive qualities [153–155]. Tamarind gum has recently undergone a number of changes that have been tested for use as medicinal excipients in various dosage forms. Table 1.1 below lists a few recent studies on tamarind gum.

Table 1.1: Tamarind gum as a potential pharmaceutical excipient

Formulations	Drug	Uses	References
Matrix tablets	Aspirin	Sustained releasing agent	[156]
Mucoadhesive buccal films	Rizatriptan benzoate	Mucoadhesive agent	[157]
Mucoadhesive beads	Metformin HCl	Mucoadhesive agent	[158]
Microparticles	Aceclofenac	Sustained releasing agent	[159]
Buoyant beads	Risperidone	Mucoadhesive agent	[160]
Ophthalmic delivery	Tropicamide	Sustained releasing agent	[161]
Matrix tablets	Propranolol HCl	Colon targeting agent	[162]
Cryogels	Metronidazole	Sustained releasing agent	[163]
Hydrogel	5-Fluorouracil	Colon specific anti-cancer drug delivery	[164]
Mucoadhesive buccal tablets	Resperidone	Sustained releasing agent	[165]

1.3 Biopolymer composites

1.3.1 Composites and types

Combining two or more materials with radically dissimilar characteristics produces composite materials [127]. The dispersion phase and the matrix phase are the two phases that make up a composite in general. The matrix phase is continuous and surrounds the dispersion phase. A matrix phase appears consistently. In comparison to the crystalline phase, the matrix

phase is more ductile and less rigid. It is in charge of dispersing the load and bringing the scattered phase back together. On the other hand, the second phase is regarded as the dispersed (reinforcing) phase. In the second stage, a discontinuous matrix embedding is utilized. The scattered phase is also referred to as the reinforcing phase since it often has greater strength than the matrix [166]. Many common materials (metal alloys, doped ceramics, and polymers with additives) are not classified as composite materials even if they include a small number of dispersed phases in their structures since their properties are identical to those of their constituents (the physical character of metals is similar to those of pure iron).

Based on their matrix materials, composites can be categorized into three groups [167] (Figure 1.2):

1. **Metal matrix composites** are composed of a dispersed ceramic (oxides, carbides) or metallic phase (lead, tungsten, molybdenum) and a metallic matrix (aluminum, magnesium, iron, cobalt, copper, zinc, etc.). Despite having a relatively high specific mass, metal fibres are often inexpensive. They are used to strengthen metal matrices. They are not in great demand because of their high density. The high fiber-matrix compatibility makes it possible to perform the primary function in the creation of the metal-metal composite. Metal matrices are strengthened with carbon steel fibres to withstand temperatures of up to 300°C. Fibers composed of metals with great heat resistance, such as tungsten or molybdenum, are used to strengthen metal matrices so they can tolerate even higher temperatures [166].
2. **Ceramic matrix composites** are composed of a ceramic matrix with ceramic fibers inserted in it (dispersed phase).
3. **Polymer matrix composite materials** are further subdivided into thermosetting resin-based composite materials and thermoplastic resin-based composite materials. For example, thermoplastic polymers such as Polycarbonate, Polyvinylchloride, Nylon, Polystyrene or thermoset resins such as Unsaturated Polyester, Epoxy matrix with glass, carbon, metal, or Kevlar fibers incorporated in it (dispersed phase). [166,168,169].

Depending on the type of reinforcement, composites can be categorized into three groups [167] (Figure 1.2).

1. **Fibre reinforced composites– continuous or discontinuous:** When the properties of

a discontinuous fiber or short fiber composite change with its length, it is referred to as a discontinuous fiber or short fiber composite. In contrast, the composite is classified as continuous or long fiber composites. Fiber-reinforced when the fiber length is such that any additional length increase does not increase the elastic modulus of the composite.

2. **Laminar composites:** Laminar composites are as different as the constituent components. These materials are composites made up of bonded layers of different parts. These can consist of numerous layers of two or more metal components arranged alternately or in a certain order as many times as necessary for a given purpose.

3. **Particulate composites:** Particles reinforced composites are metal and ceramic composite microstructures with particulates from one phase spread over the other. All sides of the square, triangular, and circular reinforcement shapes appear to have approximately the same proportions. The size and volume concentration of the dispersion distinguish it from dispersion hardened materials. Particulate composites have a dispersion size of a few microns and a volume concentration of more than a quarter of a percent. As a result, there is no substantial difference between particle composites and dispersion-strengthened composites. They each have a unique mechanism for enhancing their forces. The distribution of dispersion-strengthening materials reinforces the matrix alloy by preventing dislocation motion, and fracture requires high forces.

   Each has a system in place to strengthen its defenses. The diffusion components dispersed throughout the matrix alloy strengthen it by preventing dislocation movement and requiring significant forces to overcome the dispersion constraint. In particulate composites, the hydrostatic pressure of the filler in the matrix and the hardness of the particulates in proportion to the matrix reinforce the system. Three-dimensional reinforcement in composites has isotropic properties because it has three consistently orthogonal planes. Because the array is not homogeneous, the material properties, as well as the array's interfacial properties and geometric shapes, become sensitive to the constituent attributes. Particle diameter, inter-particle spacing, and volume proportion are all important considerations. The reinforcing has an impact on the strength is of the composite. The matrix properties influence the behavior of particle composites.

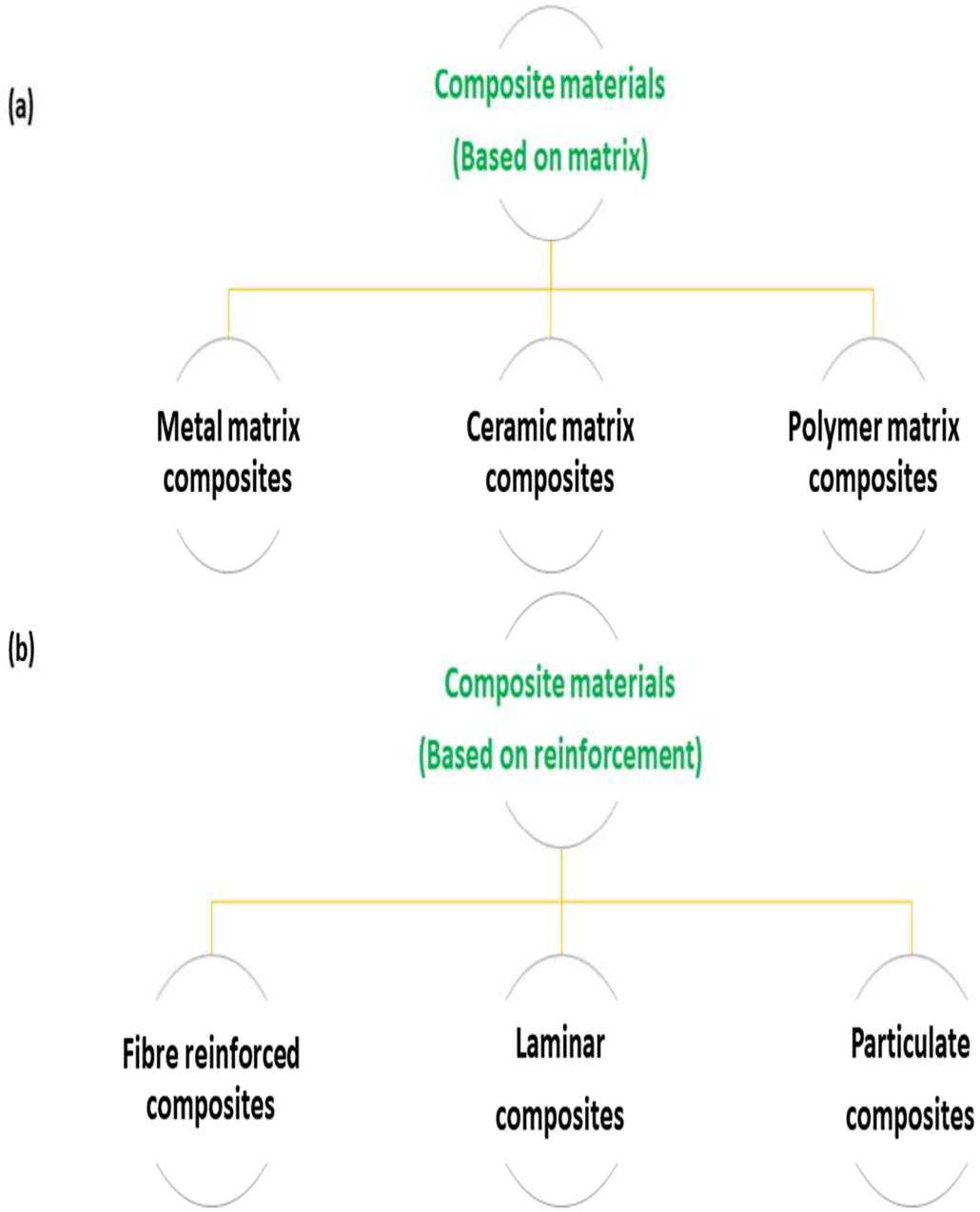

Figure 1.2: Types of composites based on (a) matrix and (b) reinforcement

1.3.2 Biopolymer composites

The terminology "biopolymer composites" refers to biodegradable composites that are reinforced using a variety of natural fibres derived from plant and animal sources and/or natural and/or manufactured biopolymers [170,171]. The resultant composite is given more stiffness and tensile strength by the addition of natural fibre (reinforcement agent) in discontinuous phase to the continuous biopolymer matrix. By using natural fibre and biopolymer, respectively, this type of composite is intended to produce a product with high mechanical behaviour and durability performance [127]. Biocomposites typically have maximum stiffness and tensile strengths between 1 and 4 GPa and 20 and 200 MPa, respectively [172]. Sustainability, economic viability, lightweight properties, exceptional specific strength, biodegradability, environmental friendliness of renewable resources, health and safety of the manufacturer and customers are some notable advantages of adopting biopolymer composites. [173].

The type of fibre, percentage of fibre content, moisture absorption of the fibre, technique used to modify the fibre surface, composite structure and design, interfacial adhesion between the fibre and matrix, presence of voids, and incorporation of additives like plasticizers, compatibilizers, nanofillers, and binding agents all have an effect on the properties of biopolymer composites. [174,175]. Different reinforcing materials and plasticizers have an impact on the biopolymer composites' density, water sensitivity, gas permeability, degradability, and shelf life. Depending on the kind of processing, the processing needs, and the ambient circumstances, biopolymer composites' performance can be enhanced chemically [176].

1.3.3 Biopolymer-based metal/metal oxide nanoparticle and nanocomposites

Metal or metallic oxide nanoparticles produced by biopolymers are a novel type of hybrid inorganic/biopolymer materials with unique features and uses that cannot be found in either inorganic nanoparticles or biopolymer host materials alone [177,178]. These hybrid materials are referred to as biopolymer-synthesized nanoparticles (BSNPs). Biopolymer based nanocomposites, which are biopolymers reinforced by nanoparticles, have improved mechanical and barrier properties. However, these characteristics are influenced by the kind, degree of dispersion, and quantity of nanoparticles present in a polymer matrix. Using in-situ and ex-situ techniques, metal and metal oxide nanoparticles are dispersed within the polymer phase in biopolymer based nano composites. The biopolymers' morphology, or physical

organisation, can take the form of granules, membranes, threads, or spherical beads, among other shapes and sizes. Even at the nanoscale level, the biopolymer and metal/metallic oxide nanoparticles maintain their intrinsic properties, but they can be easily altered to enhance the overall qualities in a variety of ways.

Metal and metallic oxide nanoparticles have unique characteristics such as chemical stability and mechanical strength. Hence, attempts are being made to employ them in a number of applications. Additionally, nanoparticles often convert their high surface area to low volumes with reduced effectiveness. This method of synthesizing metal precursor nanoparticles has been documented in the literature using a variety of metals and metallic oxides, including gold, silver, magnetite, cobalt, zinc, etc. Biosensing, drug delivery, novel time-temperature indicator, antimicrobial, environmental remediation, chemical-pharmaceutical, food industries, DNA carriers, biosensing, drug delivery, antifouling, wound healing, drug delivery, and adsorption of organic/inorganic impurities are just a few of the many applications for the emergence of unique biopolymer-metal nanocomposites (BMNCs) [181–187]. Some biopolymer-metal/metallic oxide nanocomposites and their applications are enlisted in Table 1.2.

Table 1.2: Data from the literature on the synthesis of various biopolymer-metal/metallic oxide nanocomposites

Biopolymer	**Metal/metal oxide**	**Applications**	**Reference**
Sodium Alginate	Fe	Environmental remediation	[186]
Sodium Alginate	Ag	Chemical pharmaceutical and food industries	[187]
Alginate	Ti	As sorbent for heavy metal removal	[188]
Pectin	Au	Theranostic applications	[189]
Guar gum	Au	Ammonia sensor	[190]
Guar gum	Ag/Cu	Food packing	[191]
Guar gum /Chitosan	Pd	Synthesis of biaryl compound	[192]
Guar gum	Se	Anticancer activity	[193]
Gelatin	Au	Time–temperature indicator	[194]
Cellulose	Au, Pd, and Pt	Functionalized textile substrates	[195]
Chitosan	Fe	Removal of Cr(IV) metal	[196]
Chitosan	Fe	Removal of humic acid	[197]

Chitosan	Fe	Dye removal	[198]
Chitosan	Au	Anticoagulant activity	[199]
Chitosan	Cu	Antibacterial activity	[200]
Chitosan	Ni	Pollutants degradation.	[201]
Chitosan	Co	Apoptosis in human leukemic cells	[202]
Chitosan	Cr	Decreases the glucose absorption and liver glycogen content	[203]
Chitosan	Au	DNA carriers	[204]
Chitosan	Au	Heavy metal ion sensors	[205]
Chitosan	Au	Indicates temperature abuse in frozen stored products	[206]
Chitosan	Zn	Antimicrobial activity	[207]

1.4 Processing technique of biopolymer metallic nanocomposites

There are several methods of making biopolymer metal nanoparticles, including green synthesis, combustion, electrodeposition, in-situ, ex-situ, wet method, coprecipitation, and hydrothermal [208,209]. The two basic approaches for producing biopolymer-supported nanoparticles are ex-situ and in-situ [210]. By first synthesizing the inorganic nanoparticles and then distributing them in a polymer solution or three-dimensional matrix, an ex-situ process of synthesis can be carried out. This synthesis technique is well-liked since it allows for the use of any kind of host polymer and nanoparticle. Contrarily, it is challenging to combine polymers with nanoparticles so that the inorganic element is uniformly distributed throughout the polymer. An alternative technique, called in-situ synthesis, is applied to address these problems. The prepared polymer phase serves as a micro-reactor in this procedure, where a sequence of reactions converts a precursor into the required nanoparticles. In the polymer phase, metal and metal oxide nanoparticles are produced. The technique is becoming more popular because it has technological benefits over ex-situ methods, such as the ability to easily regulate particle size and shape. Numerous different types of nanocomposites may be produced using the in-situ approach.

1.4.1 In-situ technique

The combination of the large number of functionalized biopolymers accessible with the wide range of ordered nanoparticles increases the number of different BSNPs that can be produced utilizing the in-situ technique [208]. The type of supporting polymer, the type of nanoparticle precursor, the response that bureaucratizes the nanoparticles, and the composition of the metal and metal oxide nanoparticles are the factors that influence the properties of BSNPs. In this method, the polymers serve as nano-reactors, providing a constrained synthesis medium. They also prevent the aggregation of the synthesized nanoparticles by stabilizing and isolating them [211,212]. Although there are many differences between the various techniques of synthesis, the in-situ method may be split into two groups: (a) sorption observed through redox and/or precipitation reaction, and (b) impregnation observed by precipitation and/or redox reaction.

1.4.2 Ex-situ technique

Physical entrapment of metal or metallic oxide nanoparticles within the polymer or biopolymer framework is used in the ex-situ technique. Casting and solvent evaporation, chemical bio polymerization, or co-precipitation may be used to maintain the physical entrapment. This type of nanoparticle encapsulation also aids in the stabilization of nanoparticles by preventing them from agglomerating and forming big particles. This is a common problem with the conventional approach of producing nanoparticles, which produces nanoparticles in a bulk solution. In commonly, ex-situ synthesis involves blending metallic salts or pre-shaped nanoparticles with the biopolymer solution, which is accomplished by casting the suspension inside a membrane or crosslinking the suspension to generate a three-dimensional network. The film or framework is then put through an oxidation/reduction process, which forms the precursor nanoparticles. [213,214].

1.4.3 Co-precipitation

Co-precipitation is a highly efficient technique for generating metallic oxide nanoparticles, but it is frequently unstable and needs to be stabilised with surfactants or functionalized biopolymers. Modifying the testing conditions allows adjustment of the particle form, size, and content of the treated metallic nanoparticles. The production of monodisperse nanoparticles of various sizes has been facilitated by organic additions that were utilized as stabilising or reducing agents. For the stability of metal and metallic oxide nanoparticles,

several biopolymers have been utilised, including chitosan, polyacrylamide, guar gum, cellulose, etc [208].

1.4.4 Green synthesis

Green synthesis, or the creation of stable, sustainable, and environmentally friendly synthetic processes, is necessary to prevent the formation of undesirable or dangerous by-products. To achieve this objective, excellent solvent structures and herbal sources (such as natural systems) are required. By using biopolymers and metal nanoparticles in green synthesis, several organic molecules have been accommodated (e.g., bacteria, fungi, algae, and plant extracts). When compared to microbe and/or fungi-mediated synthesis, the utilisation of plant extracts is an alternate straightforward way to produce nanoparticles on a wide scale for metal/metal oxide nanoparticles. These are known collectively as biogenic nanoparticles. Some gums and natural biopolymers, as well as their derivatives, have been discovered to be useful for the creation of nanoparticles and nanocomposites [215–220]. Moreover, the produced nanocomposites can be used in optical antibacterial, antifungal, sensor, and impurity removal of wastewater activities.

1.5 Biopolymer-Magnetite oxide nanocomposites

Magnetite oxides are utilized extensively because they are cheap and play an important role in a variety of geological and biological processes. A few examples include the use of ore in catalysts, thermite, magnetic materials, long-lasting pigments (colours for paints, varnishes, and concrete), and haemoglobin. The precipitation technique is the most efficient, affordable, and simple approach to generate magnetic particles. Magnetite nanoparticles have regulated form, nucleation, growth, durability, repeatability, scalability, and dispersibility (particularly for building complex magnetic nanostructures). For instance, altering the particle shape of the substance might display the most active catalytic region of FeO, resulting in efficient and reasonably priced catalysts for a variety of processes. Examples of uses for superparamagnetic FeO nanoparticles include adsorbents, catalysts, sensors, reducing agents, and biological activities. Many biological processes, including magnetic resonance imaging, targeted drug administration, cancer hyperthermia therapy, antibacterial activity, and pharmaceutical purposes, benefit from the usage of magnetite nanoparticles.

Due to their rarity, magnetite FeO nanoparticles have most desirable properties, including ease of separation, high surface-to-volume ratio, and paramagnetic behaviour. Natural biopolymers such as chitosan, guar gum,

alginate, dextran, and pectin are also used in the dispersing phase. The creation of magnetic nanoparticles has been made possible by this extraordinary host. The fabrication of biopolymer-based magnetite nanocomposites has used a number of techniques, including co-precipitations, green synthesis, in-situ, hydrothermal, and wet chemical. Researchers are drawn to the properties of biopolymer magnetic nanocomposites for a variety of uses, including the adsorption of inorganic metal, organic impurities, target medication delivery, biosensing, catalysis, antibacterial, antifungal, antioxidant, anti-cancer, energy, environmental remediation, anti-fouling, wastewater treatment, and textiles. Table 1.3 enlists recent studies on synthetic materials that are suitable, biocompatible, non-expansive, eco-friendly, and non-toxic for the creation and stabilization of magnetic nanoparticle biopolymer composites.

Table 1.3: Biopolymer-magnetite nanocomposites and nanoparticles literature

Biopolymer	**Iron/ FeO**	**Method of preparation**	**Applications**	**Reference**
Irish moss	Fe_3O_4	Green synthesis	Synthesis of imidazopyrimidine derivatives	[221]
Agarose/dextran/ gelatin	Fe_2O_3	Green synthesis		[24]
Alginate	FeO	Ex-situ	Improve the detection of liver tumors	[222]
Alginate	Fe (II)	Ex-situ		[35]
Sodium alginate	Fe_3O_4	Hydrothermal		[36]
β-cyclodextrin/ chitosan	Fe_3O_4	Green synthesis	Anticancer drug delivery system	[223]
Chitosan	Fe	Co-precipitation	Cresol and its derivatives removal from waste water	[224]

Chitosan	Fe_3O_4	Ex-situ co-precipitation	Biomedical and therapeutic agent development	[225]
Chitosan	Fe_2O_3	Co-precipitation		[40]
Chitosan	Fe	In-situ		[41]
Chitosan	Fe	Co-precipitation		[42]
Chitosan	Fe_3O_4	Wet chemical	To study enzymatic antioxidant system	[226]
Chitosan	Fe	Wet chemical		[44]
Chitosan	Fe	Hydrothermal		[45]
Chitosan alginate	Magnetite	Ex-situ		[46]
Chitosan	Fe_3O_4	Ex-situ	Detection of phenolic compounds	[227]
Carboxylate polyacrylamide	Fe_3O_4	Co-precipitations		[48]
Guar gum	Fe_3O_4	Co-precipitations		[49]
Nitrocellulose	Fe_2O_3	Combustion waves	Electrochemical applications	[228]
Styrene	Fe_3O_4	Seed-mediated growth method	Magnetic nanoparticles	[229]
Starch-Pectin	Magnetite	Green synthesis		[28]
Polymethylmethacrylate	FeO	Ex-situ	Technological applications	[230]
Poly(methylmethacrylate)	Fe	Microwave plasma technique	Electromagnetic applications	[231]

1.5.1 Applications of biopolymer and magnetic oxide nanocomposites

BMNCs containing magnetite oxide have been used extensively in a range of technical domains in contrast to other ions due of their exceptional biological, chemical, and physical characteristics. Supported metal adsorptions, organic impurities, catalytic activity, sensors and biosensors, biomedical, antibacterial activity, antioxidant activity, anti-cancer activity, coatings, and other measures are some of the applications in a variety of sectors. (Figure 1.3).

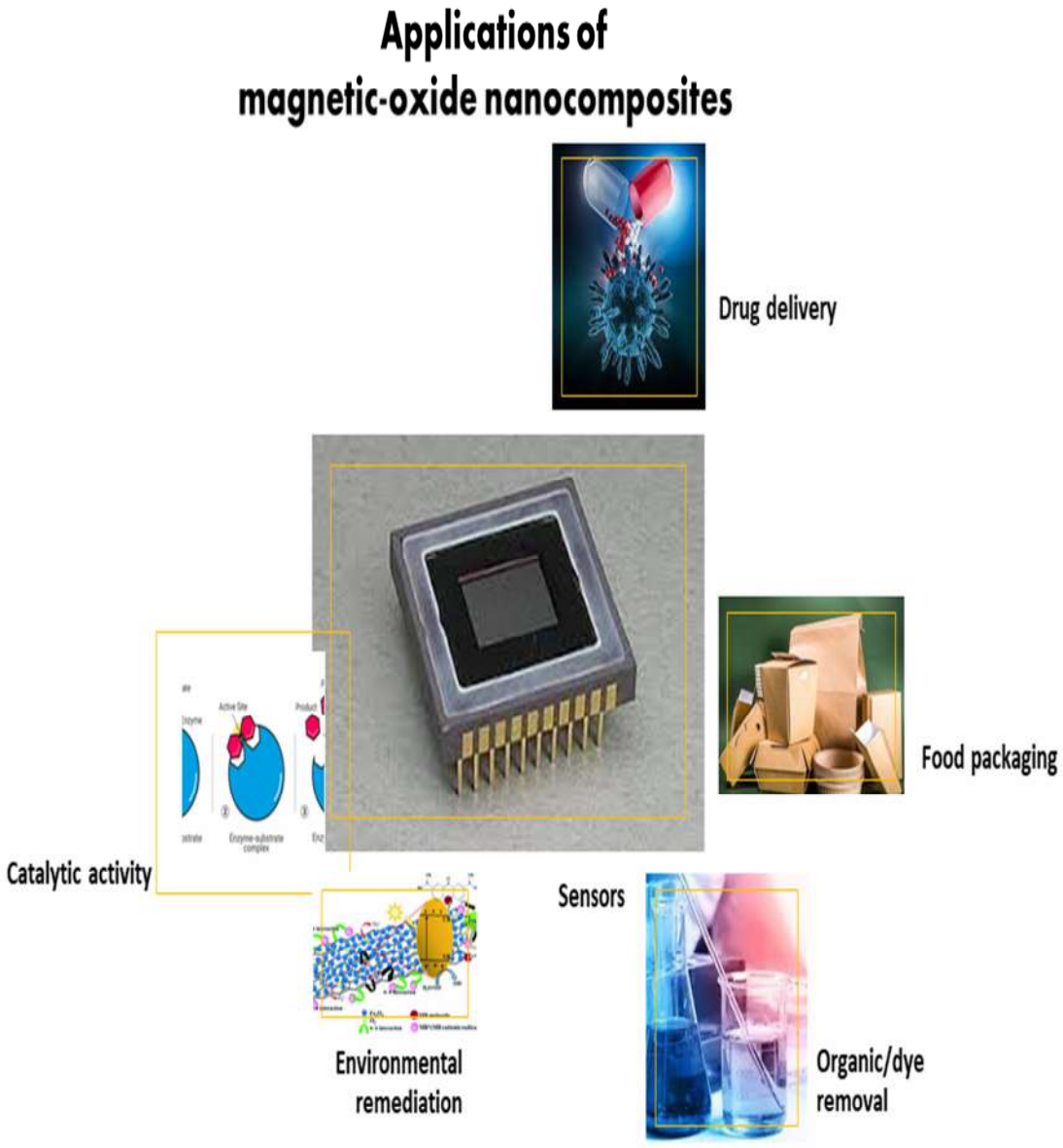

Figure 1.3: Applications of biopolymers-magnetite oxide nanocomposites

1.5.1.1 Organic/inorganic impurity removal

Many conventional and cutting-edge methods, including coagulation, chemical precipitation, adsorption, ion-exchange, complexation, electrodeposition, and membrane operations, are employed to remove organic and inorganic contaminants. Unfortunately, most of these treatments require a lot of energy, have ineffective removal, and produce a lot of trash when employed [232]. Single polymer-based metal biopolymer composites provide the highest possible adsorption value, a wide variety of surface groups, are physically feasible, and have outstanding durability. Applications of biopolymers-magnetite oxide nanocomposites in organic/inorganic impurity removal is discussed in the following section.

It has been found that biological molecules including chitin, chitosan, and lignin are effective adsorbents for the removal of heavy metals [233]. For instance, calcium alginate hydrous (dropped/coated) ferric beads fabricated utilizing an adsorption technique were used to remove As.[61-62] Other studies suggest usage of nanoparticles Fe(III)@Alginate nanoparticles prepared by batch adsorptions method for removal of copper metal (II).[55-56] There is growing evidence that, in several circumstances, increasing the concentration of biopolymer compared to chitosan improves heavy metal adsorption[73]. Research indicate removal of Dy^{3+}, Er^{3+}, and Nd^{3+} from the media using Fe_3O_4-C-18 chitosan-DETA (FCCD) nanoparticles [234]. Another study shows elimination of As (V) by in situ starch/Fe_3O_4 [61].In other studies, thorium ions and rare earth metals were removed from contaminated water using magnetic chitosan nanoparticles.[59] Arsenic metal and a cupper was removed by alginate/Fe nanoparticles prepared using the batch adsorption technique.[58,73]

Diverse organic pollutants, such as basic dye, clove oil, BB, azo dye, methylene blue, humic acid, phenol, and cresol, are removed from wastewater through batch adsorption of synthetic magnetic/chitosan nanoparticles.[67-75]. In a different work, basic dye is extracted out of Fe_3O_4/PAA nanoparticles via batch adsorption.[64]. Using a guar-gum/magnetic oxide nanocomposite, an adsorption approach is used to remove Congo red from waste water [72]Removal of methyl-indole colour from wastewater using F_3O_4/Alginate nanocomposites[73]

Table 1.4: Applications of biopolymers-magnetite oxide nanocomposites in organic/inorganic impurity removal

Biopolymer /Metal	Metal	References
Alginate /Fe (III) /oxide	As (III), As(V)	[235]
Alginate /Fe (III)	As(V)	[236]
Alginate / Fe_3O_4	As (III), As(V)	[34]
Alginate/ Fe_3O_4	Cu (II)	[237]
Alginate/ Fe_3O_4	Cu^{2+}	[238]
Chitosan/ Fe_2O_3	Th(IV)	[239]
Chitosan/Fe	Cr(VI)	[196]
Chitosan /Fe	Cu (II)	[240]
Chitosan/Fe	As	[73]
CS / Fe_3O_4	Pb (II)	[183]
Chitosan /Fe	Rare-earth metal	[59]
CS NPs /Fe_3O_4	Heavy metal	[73]
Chitosan/Fe_3O_4	Hg(II)	[241]
Starch / Fe_3O_4	As(V)	[242]
Poly(methylmethacrylate)/ Fe_2O_3	Pb(II), Hg(II), Cu(II) and Co(II)	[243]
Chitosan/Fe_3O_4	As (III)	[62]
Chitosan/ Fe_3O_4@SiO_2	Hg^{2+}, Pb^{2+}, Cu^{2+}	[244]
Fe_3O_4/PAA	Basic dye	[64]
Chitosan/magnetic	Phenol	[245]
Chitosan / Fe_3O_4	Cresol	[224]
Chitosan / Fe	Methylene blue	[77]
Alginate/ Fe	Dye	[67]
Chitosan / Fe	Basic dye	[68]
Chitosan/Fe	Humic acid	[197]
Chitosan / Fe	Methylene blue	[70]
Chitosan / Fe	Clove oil	[71]
Guar gum/coated FeO	Congo red dye	[246]
Fe_3O_4–alginate, H_2O_2	3-Methyl-indole	[73]
Fe_3O_4/chitosan	BB	[74]
γ-Fe_2O_3/chitosan	Azo dye	[75]
Fe_3O_4-C-18 Chitosan-DETA	Dy^{3+}, Er^{3+}, and Nd^{3+}	[234]

1.5.1.2 Antibacterial activity/anti-oxidant activity/anticancer activity

The most frequent medical conditions are caused by bacterial infections, which have a variety of negative effects on human public health. [95] Unfortunately, pathogenic bacterial and fungal strains that are solely multidrug-resistant have developed drug resistance as a result of these drugs' inferior effectiveness and excessive use. These strains of infections are more difficult to avoid and treat. Hence, it is essential to create novel antibacterial agents with high efficacy and low toxicity as well as an alternate treatment to deal with these problems. Magnetic oxide NPs supported by a range of biopolymers significantly inhibited Gram-positive and Gram-negative bacteria, including spherical *P. aeruginosa, E. faecalis, C. krusei, S. aureus, and B. cereus*.. [79]. Because of their small size, high surface-to-volume ratio, and tuneable Plasmon resonance properties, MNPs FeO have specifically attracted attention among all potential treatments for bacterial infections. [72,99], as displayed in Table 1.5.

Table 1.5 Applications of biopolymers-magnetite oxide nanocomposites in Antimicrobial activity/antioxidant activity /anticancer activity

Biopolymer/metal	Applications	Reference
Chitosan / Fe_2O_3	Antioxidant	[76]
Pectin /Fe_2O_3	Antimicrobial activity	[77]
Agarose-Fe_2O_3, Dextran-Fe_2O_3 Gelatin-Fe_2O_3	Antibacterial activity against gram-positive and gram-negative bacteria species	[78]
Dextran/sucrose Fe	Spherical *E. coli, P. aeruginosa, E. faecalis, C. krusei*	[79]
Agarose/dextran/gelatin Fe_2O_3	10.0 Dumbbell shape *S. aureus, A. hydrophila, S. pyogenes, P. aeruginosa*	[80]
Dextran/ Fe_3O_4	59.0–149.0 Monitoring cancer cells of Micelles magnetic resonance imaging	[81]

1.5.1.3 Electrochemical biosensor activity

A biosensing device is a highly effective and precise analytical tool with a low detection limit for analysis that may transform a biological event into a physicochemical significance. Various biosensors are used nowadays to find proteins, metal ions, and compounds. BMNPs have been widely employed in biosensing due to their exceptional chemical, electrical, and

optical charterers. Table 1.6 shows an arbitrary of the current progress in probes and biosensing.

Table 1.6: Applications of biopolymers-magnetite oxide nanocomposites in electrochemical biosensor activity

Biopolymer/Metal	Function of Activity	Reference
FeO/Chitosan	Glucose biosensor	[82]
Chitosan/ Fe_3O_4	Tyrosine biosensor	[86]
Fe_3O_4 /Chitosan	Herbicide biosensor	[83]
Fe_3O_4 /Chitosan	Glucose biosensor	[84]
Magnetic-chitosan nanocomposite	Electrochemical Geno sensor	[85]
DNA/chitosan-Fe_3O_4magnetic	Electrochemistry and electrocatalysis	[87]

1.5.1.4 Biomedical

Numerous biological applications, such as the immobilisation of proteins and enzymes, bio separation, drug administration, and magnetic resonance imaging, have made extensive use of magnetic nanoparticles [247]. Using synthetic BMNPs as a contrast agent for magnetic resonance imaging during biomedical hypothermic treatment for malignant tumours is one example. [126] The studies focusing on drug release, tissue distribution, pharmacy, kinetics, specific organ delivery, and magnetic resonance imaging contrast agent were the most notable among the numerous super-paramagnetic magnetic oxide applications incapacitate in biopolymer studies. Additionally, nanoparticles performed admirably when used to examine liver tumours. [85]

1.5.1.5 Drug delivery

Many biopolymer/gene-loaded nanoparticles have been produced recently as medication delivery vehicles, and it has been thoroughly studied how these nanoparticles circulate in human systems. In the past few years, biopolymer-magnetic nanoparticles/nanocomposites have demonstrated significant potential in targeted drug delivery applications. Biopolymer-magnetic nanoparticles/nanocomposites were a common targeted delivery method that was

used to deliver anti-cancer medications to the precise locations where cancer cells are located. The magnetic properties of the metallic nanoparticles that resemble anti-cancer medication delivery have been demonstrated when they are combined with biopolymers such as chitosan[97], cyclodextrin[92], k-carrageenan[93] and Mannan[96]. Some of the recent researches of biopolymer-magnetic nanoparticles/nanocomposites in drug delivery are briefly enlisted in Table 1.7.

Table 1.7: Potential applications of biopolymer-magnetic nanoparticles/nanocomposites in drug delivery

Biopolymer/Metal	**Function of Activity**	**Reference**
β-cyclodextrin/ chitosan/Fe	Drug delivery/Prodigiosin delivery	[92]
k-carrageenan/ Fe_3O_4	Drug delivery	[93]
Mannan / Fe_3O_4	Drug delivery	[95]
Alginate / Fe	Reduction activity	[96]
Chitosan/ Fe_3O_4	Drug delivery	[97]
γ-Fe_2O_3/alginate matrix	Drug delivery	[98]
Medicago sativa (alfalfa)/ FeO	Cancer hyperthermia, drug delivery	[99]
Gelatin-coated magnetic FeO nanoparticles	Drug loading and in vitro	[100]
Cyclodextrin conjugated magnetic colloidal nanoparticles	Drug Targeted anticancer drug delivery	[101]

1.6 Biopolymer-ZnO nanocomposite (BZNCs)

Nanocomposites made of biopolymers and ZnO are novel materials with a variety of characteristics. Significant research has been done over the past 10 years on the biosynthesis of nanocomposites using environmentally friendly techniques. This biopolymer/ZnO composite integrates studies that have been application-driven for decades with the most current investigation on crucial synthetic procedures. ZnO nanoparticles can be produced utilizing a variety of synthesis methods including the sol-gel process[20], the hydrothermal

process[21], the wet chemical method, and chemical vaporisation (CVD)[22], co-precipitation[23], micro emulsion, microwave-assisted synthesis[25] , green synthesis[26] etc. Recent research directs fabrication of biopolymer/ZnO nanocomposites by embedding biopolymers such as polyethylene, chitosan [105], starch, alginate, [106] tamarind gum, pectin, cellulose[107], poly(3-hydroxybutyrate-co-3-hydroxy valerate) (PHBV)[112], poly(3-hydroxybutyrate) (PHB)[111], polyacrylic acid (PAA), polyvinyl alcohol (PVA), polylactic acid (PLA) [115] polyethylene [116]. The incorporation of zinc oxide nanoparticles into natural biopolymers broadens their applications, including biomedical [101], adsorption [32], environmental [33], drug delivery, antimicrobial activity [34] antioxidant activity [35] anti-cancer activity [36] and catalytic activity [37] (Figure 1.4).

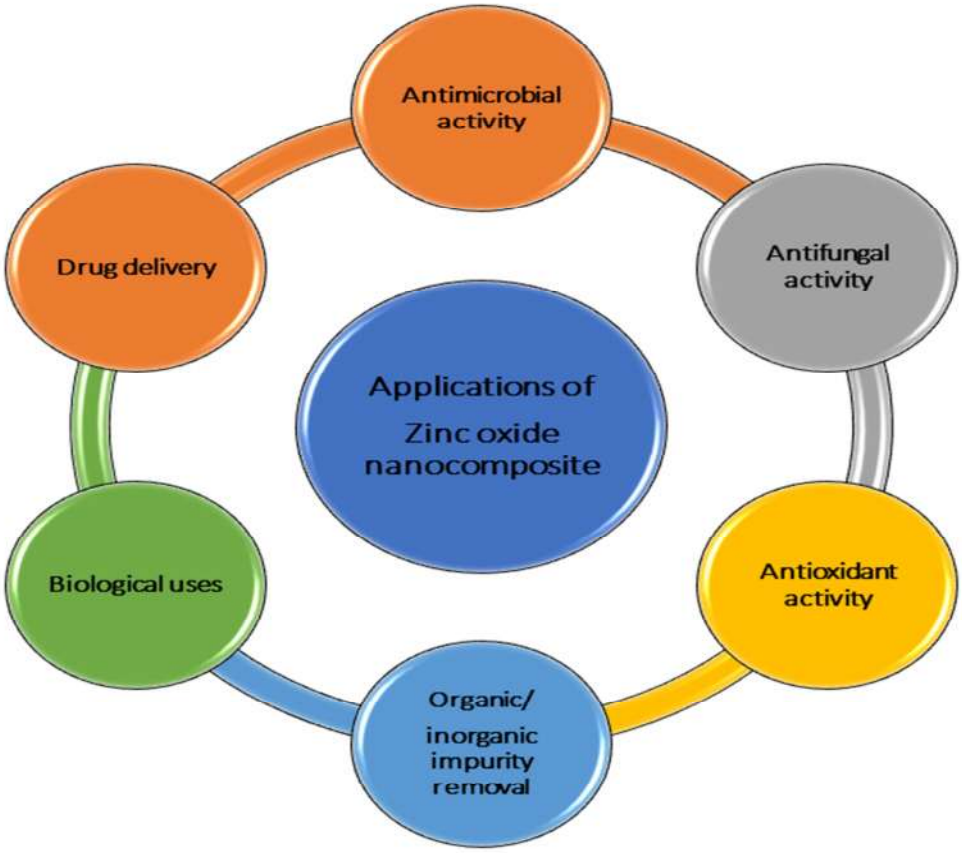

Figure 1.4: Applications of biopolymers-zinc oxide nanocomposites

1.6.1 Applications of biopolymer/ZnO nanocomposite

Biopolymer/ZnO nanocomposite is intriguing because to its high photosensitivity, physical and chemical stability, non-toxicity, and broad band gap. Due to its low in vivo and in vitro toxicity, it also has a wide range of uses in many other industries, including dyes, medicines,

fragrances, biology, petroleum, and agrochemicals. Due to its high biocompatibility, stability, quick electron transfer, and longer life than organic-based disinfectants, the application of Biopolymer/ZnO nanocomposite as antibacterial activity, anticancer activity, metal and dye removal from water has received significant attention recently. Studies have supported its use in food packaging. Table 1.9 lists a few uses for biopolymer/ZnO nanocomposite materials.

1.6.1.1 Antimicrobial /antifungal / Drug delivery / anticancer activity

A literature analysis revealed that the majority of biopolymer/ZnO nanocomposites were initially created for a variety of applications involving the selective adsorption of target contaminants in the presence of other ions. Wide varieties of biopolymer/ZnO nanocomposites/nanoparticles have been synthesised recently and have been shown to possess potent antibacterial activities (Table 1.8). Chitosan/Ag/ZnO nanocomposite showed exceptional antibacterial action against *B. 409 licheniformis, B. cereus, P. vulgaris and V. parahaemolyticus*. The Chitosan-Ag@ZnO nanocomposite effectively inhibited the biofilm formation of bacteria and Candida albicans. Also, chitosan-assembled zinc oxide nanoparticles have been effectively investigated for their anticancer efficacy against cervical cancer cells. [141]

1.6.1.2 Metal removal/organic compound removal

Biopolymer / zinc oxide nanocomposites are being employed in the adsorptions batch method to remove organic and inorganic contaminants from wastewater treatment. In required to remove diverse target species from contaminated water and wastewater, BZNCs have been produced and employed in a number of different ways, as shown in Table 1.9. ZnO nanoparticles incorporated in biopolymer graphene oxide are employed in its application to remove Mn (II) metal. [132]. In addition, graphene oxide with zinc oxide nanoparticles show ability to remove copper and aluminium from acidic conditions. [133]. Using it as an adsorbent, Congo red was recovered from our aqueous solutions.[130]. To enhance the elimination of Cr (VI) from aqueous solution, the adsorbent guar gum-nano and zinc oxide (GG/ZnO) nanocomposite has been used [138]. According to another study of the literature, complex contaminants may be eliminated using nanomaterials like graphene oxide (GO). This study presents the initial findings of Mn (II) ion removal from acidic solutions utilising GO functionalized with zinc oxide nanoparticles (ZnO).[132]. In terms of organic dye degradation and heavy metal ion removal, nano-engineered ZnO NR-rGO nanocomposites

show effective water remediation. The synthesis of ZnO NR-rGO nanocomposite via a simple template-free hydrothermal approach is described here to boost visible photo catalytic efficiency [127].

According to the findings, ZnO@Chitosan core/organically shell nanocomposite (ZOCS) may be used to remove Pb (II), Cd (II), and Cu (II) ions from polluted water [135]. The study presents the development of a Zeolite/Zinc Oxide Nanocomposite. Using a co-precipitation technique, (Zeolite/ZnO NCs) were produced. The adsorption of Lead (II) and Arsenic (V) from aqueous solution was then investigated on the produced Nanocomposite. Nano-ZnO/Chitosan composite beads (nano-ZnO/CT-CB) were used to remove Reactive Black 5 (RB-5) from an aqueous solution in this investigation.[134]. Another work used sodium tripolyphosphate as the cross-linker to produce ZnO nanoparticles in situ while making physically cross-linked chitosan hydrogel beads., "Polyaniline/ZnO nanocomposite: a new adsorbent for the removal of Cr (VI) from aqueous solution [138].

Table 1.8: Applications of biopolymer/ZnO nanocomposite

Biopolymer	**Metal/Metallic oxide**	**Application**	**Reference**
Alginate and chitosan	ZnO	Antimicrobial activity	[103]
Carrageenan	ZnO	Food packing activity	[104]
Chitosan	ZnO	Antimicrobial activity	[105]
Sodium alginate	ZnO	Food packing activity	[106]
Carboxymethyl cellulose	ZnO	Food packing activity	[107]
3-Methacryloxypropyl trimethoxysilane treated	ZnO	-	[109]
Poly (3-hydroxybutyrate)	ZnO	Antibacterial activity	[111]
Poly (3-hydroxybutyrate-co-3-hydroxy valerate	ZnO	Food packing activity	[112]
PBAT	ZnO	Food packing activity	[113]
Poly-lactic acid	ZnO	Food packing activity	[115]
Linear-low-density polyethylene	ZnO	Food packing activity	[116]
modified cellulosic	ZnO	-	[118]
Polyaniline	ZnO	-	[119]

Poly (lactic acid) or polylactide (PLA)	ZnO	-	[120]
Chitosan Ag/	ZnO	Antibacterial activity	[121]
Chitosan	Zn complex	Antibacterial activity	[122]
Gelatin	ZnO	Antibacterial activity	[124]
Carboxymethyl starch/cellulose	ZnO/Zn	Photo degradation of dyes	[125]
Chitosan/ corn starch/ sodium alginate	ZnO	Photocatalytic reaction	[126]
Carboxymethyl cellulose-chitosan-	ZnO	Food packing's	[127]
Gelatin- Nanocomposite	ZnO	Application in Spinach Packaging.	[164]
Graphene-oxide nanocomposite w	ZnO	Photocatalytic	[127]
Poly(styrene-*co*-acrylonitrile)	ZnO	Efficient Ligand Exchange Strategy	[128]
Graphene Oxide–Nanocomposites	ZnO	Aluminium and Copper Ions from Acid Mine Drainage Wastewater	[129]
Chitosan	ZnO	Removal Congo red dye	[130]
Guar-gum	ZnO		[131]
Graphene Oxide–nanocomposites	ZnO	Removal of Mn (II) from Acidic Wastewaters	[132]
Graphene oxide hybrids nanocomposites	ZnO	Metal removal	[133]

chitosan–polyaniline hybrid composite	ZnO	Orange 16 dye	[134]
Chitosan	ZnO	Cu (II), Pb (II) and Cd (II	[135]
Zeolite/ Nanocomposite	ZnO	Lead Pb (II) and Arsenic As (V)	[136]
Polyaniline/ nanocomposites is a novel	ZnO	Removal of Cr (VI) from Aqueous Solution	[138]
Facile synthesis of chitosan/ bio-nanocomposite	ZnO	Drug delivery	[139]
-polystyrene nanocomposite for	ZnO	UV-shielding applications	[140]
Chitosan-based nanoparticle	ZnO	Anticancer activity	[141]

1.7 Carboxymethyl tamarind kernel gum composites

Tamarind kernel gum with carboxymethyl is one of its derivatives (CMTKG), as shown in Figure 1.5. This polysaccharide has been extensively employed in a range of applications because to its exceptional ability to alter the rheological properties, the thickening, and the viscosity of an aqueous solution.

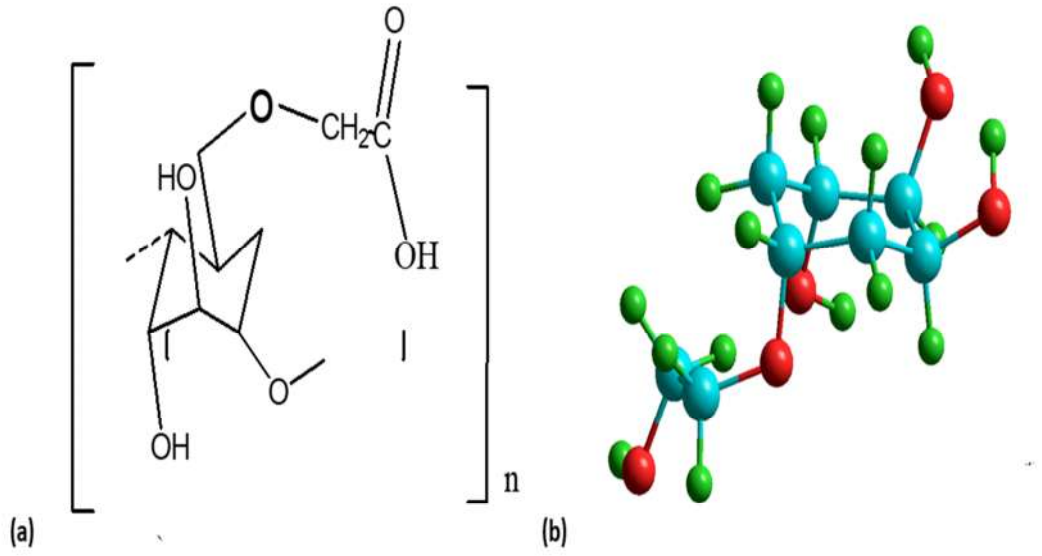

Figure 1.5: Chemical structure of carboxymethyl tamarind kernel gum

1.7.1 Applications of carboxymethyl tamarind kernel gum composites

The usage of gradual medication delivery using aceclofenac medicine is shown to be beneficial for the interpenetrating network bio-composite of CMTKG and gelatin. In HCl arrangements, CMTKG in any bio-composites slowed down the rate of medicine release; nevertheless, the same elevation occurred in 6.8 pH buffer solution. The scientists suggested that their drug-stacked bio-composites may be used as soothing treatments (Jana, Banerjee, et al., 2016). To consider a composite made of a microwave-aided join of polyacrylonitrile and CMTKG, a 4-factor, 3-level focal composite plan was adopted. The ammonium persulfate convergence was altered by the response surface approach, indicating a synergistic effect, but the unifying efficiency decreased as the amount of acrylonitrile increased. The grafting increased the conferred pH-subordinate growth properties, upgraded the crystallinity, and improved thermal stability, according to the authors, who concluded that it was useful for developing pH-responsive applications [160,163] created erlotinib-stacked semi-interpenetrating network nanocomposites using CMTKG, poly (N-isopropyl acrylamide), and montmorillonite [160]. These nanoscale composites were demonstrated for the administration of ERL for the treatment of NSCLC (non-small cell lung cancer). Be a result, this synthesis might be referred to as an exceptional method of treating NSCLC.

1.8 Background and Significance

Even while tamarind gum is ideally suited for pharmaceutical purposes, it may have significant disadvantages. TKG's functional groups have had to be modified by scientists due to its dull colour, bad odour, insolubility in water, and degradation in an aqueous environment.[20],Carboxymethylation [24], acetylation [25], hydroxyl alkylation, and thiolation [31] are some of the alterations that have been carried out to far. Tamarind kernel gum thiolation, Tamarind kernel gum crosslinking, number [27], Tamarind kernel gum that has partially decomposed [28,30]. Graft-modified Tamarind kernel gum [35]. Tamarind kernel gum that has been oxidised. Tamarind kernel gum's solubility, viscosity, swelling, and stability have all changed as a result of these alterations.

TKG's polysaccharide structure is broken by carboxymethylation, which exposes the hydration network and gives the polymer an anionic character. This results in higher viscosity and lesser biodegradability than TKG, ultimately increasing shelf life. The inclusion of carboxymethyl groups makes the molecule resistant to enzymatic assault. Carboxymethyl xyloglucan has improved qualities that are essential for drug release retardation, assisting in

achieving sustained release action. [10] Moreover, incorporation of magnetic and zinc oxide nanomaterials with CMTKG may lead to the formation of an improved composite. The resultant biocomposite not only carry the inherent character but also often show high stability, maximum accessibility, and even interesting enhancement caused through the interaction of nanoparticle–matrix. Synthesized biocomposite have been a high achievement, biosensor, antifungal, antioxidant, antimicrobial antifouling, drug delivery activity, and adsorbents for removal of organic/inorganic impurity wastewater water solution that has comprehensive future utility.

1.9 Overview of thesis

In seven chapters, the complete thesis is summarized.

Chapter 1: The thesis's first chapter provides a brief overview of the study work's contemporary scientific significance, as well as the thesis's objective. It also summarizes the scientific literature on the synthesized metal and metallic oxide biopolymer nanocomposite used for antibacterial, antifungal, antioxidant, biosensor antifouling, and organic/inorganic contaminant removal from wastewater.

Chapter 2: The experimental methods used to carry out the research work are discussed in this chapter of the thesis, which includes information on the materials utilized, approved by the research, and the descriptions and parameters of several characterization techniques employed to fulfill the research effort's goal.

Chapter 3: This chapter include the rationale as well as scope behind the research work conducted in this thesis.

Chapter 4: The utilization of carboxymethyl tamarind kernel Gum/FeO nanocomposites in liquid ammonia sensors and antimicrobial activity has been prepared and characterized.

Chapter 5: This chapter covers the synthesis and characterization of carboxymethyl tamarind kernel gum/ZnO nanocomposites, as well as their use in chromium metal removal and antifungal activities.

Chapter 6: The synthesis and characterization of carboxymethyl tamarind kernel gum nanoparticles and their antioxidant properties are discussed in this Chapter.

Chapter 7: This chapter summarizes the entire research study as well as the research's prospects.

References

[1] V. Nimbagal, N.R. Banapurmath, A.M. Sajjan, A.Y. Patil, S. V. Ganachari, Studies on Hybrid Bio-Nanocomposites for Structural Applications, J. Mater. Eng. Perform. 30 (2021) 6461–6480. https://doi.org/10.1007/s11665-021-05843-9.

[2] J. Puiggalí, R. Katsarava, Bionanocomposites, in: Clay-Polymer Nanocomposites, Elsevier, 2017: pp. 239–272. https://doi.org/10.1016/B978-0-323-46153-5.00007-0.

[3] E.S. Medeiros, A.S.F. Santos, A. Dufresne, W.J. Orts, L.H.C. Mattoso, Bionanocomposites, in: Polym. Compos. Biocomposites, John Wiley & Sons, Ltd, 2013: pp. 361–430. https://doi.org/10.1002/9783527674220.ch11.

[4] M. Darder, P. Aranda, E. Ruiz-Hitzky, Bionanocomposites: A new concept of ecological, bioinspired, and functional hybrid materials, Adv. Mater. 19 (2007) 1309–1319. https://doi.org/10.1002/adma.200602328.

[5] V. Siracusa, Microbial degradation of synthetic biopolymers waste, Polymers (Basel). 11 (2019) 1066. https://doi.org/10.3390/polym11061066.

[6] E.M.N. Polman, G.J.M. Gruter, J.R. Parsons, A. Tietema, Comparison of the aerobic biodegradation of biopolymers and the corresponding bioplastics: A review, Sci. Total Environ. 753 (2021) 141953. https://doi.org/10.1016/j.scitotenv.2020.141953.

[7] C.S. Kumar, S. Bhattacharya, Tamarind seed: Properties, processing and utilization, Crit. Rev. Food Sci. Nutr. 48 (2008) 1–20. https://doi.org/10.1080/10408390600948600.

[8] S. Babel, H. Upadhayay, R. Gupta, Optimization of Thickening Agent Based on Tamarind Seed Gum for Printing of Cotton and Its Impact on Physical Parameters, Int. J. Fiber Text. Res. 5 (2015) 5–8. http://www.urpjournals.com (accessed July 19, 2022).

[9] S. Dey, B. Chandra Nandy, J. Narayan De, M.S. Hasnain, A.K. Nayak, Tamarind gum in drug delivery applications, in: Nat. Polysaccharides Drug Deliv. Biomed. Appl., Academic Press, 2019: pp. 285–306. https://doi.org/10.1016/B978-0-12-817055-7.00012-1.

[10] C.K. Nagar, S.K. Dash, K. Rayaguru, Tamarind seed: Composition, applications, and value addition: A comprehensive review, J. Food Process. Preserv. (2022) e16872. https://doi.org/10.1111/JFPP.16872.

[11] S. Gupta, S. Jain, G. Rao, V. Gupta, R. Puri, Tamarind kernel gum: An upcoming natural polysaccharide, Syst. Rev. Pharm. 1 (2010) 50. https://doi.org/10.4103/0975-8453.59512.

[12] H. Shao, H. Zhang, Y. Tian, Z. Song, P.F.H. Lai, L. Ai, Composition and rheological

properties of polysaccharide extracted from tamarind (Tamarindus indica L.) seed, Molecules. 24 (2019). https://doi.org/10.3390/molecules24071218.

[13] A.S. Singha, A. Guleria, Chemical modification of cellulosic biopolymer and its use in removal of heavy metal ions from wastewater, Int. J. Biol. Macromol. 67 (2014) 409–417. https://doi.org/10.1016/j.ijbiomac.2014.03.046.

[14] N.A. Negm, H.H.H. Hefni, A.A.A. Abd-Elaal, E.A. Badr, M.T.H. Abou Kana, Advancement on modification of chitosan biopolymer and its potential applications, Int. J. Biol. Macromol. 152 (2020) 681–702. https://doi.org/10.1016/j.ijbiomac.2020.02.196.

[15] B.R. Reddy, R. Patil, S. Patil, Chemical modification of biopolymers to design cement slurries with temperature-activated viscosification, in: Proc. - SPE Int. Symp. Oilf. Chem., OnePetro, 2011: pp. 236–246. https://doi.org/10.2118/141005-ms.

[16] Y. Pei, L. Wang, K. Tang, D.L. Kaplan, Biopolymer Nanoscale Assemblies as Building Blocks for New Materials: A Review, Adv. Funct. Mater. 31 (2021) 2008552. https://doi.org/10.1002/adfm.202008552.

[17] R.J.N. Tiozon, A.P. Bonto, N. Sreenivasulu, Enhancing the functional properties of rice starch through biopolymer blending for industrial applications: A review, Int. J. Biol. Macromol. 192 (2021) 100–117. https://doi.org/10.1016/j.ijbiomac.2021.09.194.

[18] Khushbu, S.G. Warkar, Potential applications and various aspects of polyfunctional macromolecule- carboxymethyl tamarind kernel gum, Eur. Polym. J. 140 (2020) 110042. https://doi.org/10.1016/j.eurpolymj.2020.110042.

[19] P. Goyal, V. Kumar, P. Sharma, Carboxymethylation of Tamarind kernel powder, Carbohydr. Polym. 69 (2007) 251–255. https://doi.org/10.1016/j.carbpol.2006.10.001.

[20] K.K. Mali, S.C. Dhawale, R.J. Dias, Extraction, characterization and functionalization of tamarind gum, Res. J. Pharm. Technol. 12 (2019) 1745–1752. https://doi.org/10.5958/0974-360X.2019.00292.0.

[21] H. Prabhanjan, Studies on Modified Tamarind Kernel Powder. Part I: Preparation and Physicochemical Properties of Sodium Salt of Carboxymethyl Derivatives, Starch □ Stärke. 41 (1989) 409–414. https://doi.org/10.1002/star.19890411102.

[22] A.K. Nayak, D. Pal, Functionalization of Tamarind Gum for Drug Delivery, in: Funct. Biopolym., Springer, Cham, 2018: pp. 25–56. https://doi.org/10.1007/978-3-319-66417-0_2.

[23] B.B. Mansingh, J.S. Binoj, N.P. Sai, S.A. Hassan, S. Siengchin, M.R. Sanjay, Y.C. Liu, Sustainable development in utilization of Tamarindus indica L. and its by-

products in industries: A review, Curr. Res. Green Sustain. Chem. 4 (2021) 100207. https://doi.org/10.1016/j.crgsc.2021.100207.

[24] A. Deep, N. Rani, A. Kumar, R. Nandal, P.C. Sharma, A.K. Sharma, Prospective of Natural Gum Nanoparticulate Against Cardiovascular Disorders, Curr. Chem. Biol. 13 (2019) 197–211. https://doi.org/10.2174/2212796813666190328194825.

[25] V. Dagar, R. Pahwa, M. Ahuja, Preparation and Characterization of Calcium Cross-linked Carboxymethyl Tamarind Kernel Polysaccharide as Release Retardant Polymer in Matrix, Biointerface Res. Appl. Chem. 13 (2023) 111. https://doi.org/10.33263/BRIAC132.111.

[26] R. Malik, R. Saxena, S.G. Warkar, Biopolymer-Based Biomatrices – Organic Strategies to Combat Micronutrient Deficit for Dynamic Agronomy, ChemistrySelect. 7 (2022) e202200006. https://doi.org/10.1002/slct.202200006.

[27] M.M. Rahman, H. Ihara, M. Takafuji, Nanomaterial Hybridized Hydrogels as a Potential Adsorbent for Toxic Remediation of Substances from Wastewater, Recent Trends Wastewater Treat. (2022) 365–393. https://doi.org/10.1007/978-3-030-99858-5_16.

[28] V. Malik, L. Saya, D. Gautam, S. Sachdeva, N. Dheer, D.K. Arya, G. Gambhir, S. Hooda, Review on adsorptive removal of metal ions and dyes from wastewater using tamarind-based bio-composites, Polym. Bull. (2022) 1–36. https://doi.org/10.1007/s00289-021-03991-5.

[29] E. Nazarzadeh Zare, P. Makvandi, A. Borzacchiello, F.R. Tay, B. Ashtari, V.T.V. Padil, Antimicrobial gum bio-based nanocomposites and their industrial and biomedical applications, Chem. Commun. 55 (2019) 14871–14885. https://doi.org/10.1039/c9cc08207g.

[30] K. Nagaraja, K.S.V. Krishna Rao, S. Zo, S.S. Han, K.M. Rao, Synthesis of novel tamarind gum-co-poly(Acrylamidoglycolic acid)-based ph responsive semi-ipn hydrogels and their ag nanocomposites for controlled release of chemotherapeutics and inactivation of multi-drug-resistant bacteria, Gels. 7 (2021) 237. https://doi.org/10.3390/gels7040237.

[31] S. Iravani, Plant gums for sustainable and eco-friendly synthesis of nanoparticles: recent advances, Inorg. Nano-Metal Chem. 50 (2020) 469–488. https://doi.org/10.1080/24701556.2020.1719155.

[32] N.R. Bali, M.N. Karemore, S.S. Jadhav, R.M. Bondre, N.Y. Yenorkar, Nanomedicine approaches and strategies for gum-based stealth nanocarriers, in: Micro- Nanoeng.

Gum-Based Biomater. Drug Deliv. Biomed. Appl., Elsevier, 2022: pp. 1–33. https://doi.org/10.1016/B978-0-323-90986-0.00018-2.

[33] E. Alpizar-Reyes, S. Cortés-Camargo, A. Román-Guerrero, C. Pérez-Alonso, Tamarind gum as a wall material in the microencapsulation of drugs and natural products, in: Micro- Nanoeng. Gum-Based Biomater. Drug Deliv. Biomed. Appl., Elsevier, 2022: pp. 347–382. https://doi.org/10.1016/B978-0-323-90986-0.00016-9.

[34] V. Singh, P. Kumar, Carboxymethyl tamarind gum-silica nanohybrids for effective immobilization of amylase, J. Mol. Catal. B Enzym. 70 (2011) 67–73. https://doi.org/10.1016/j.molcatb.2011.02.006.

[35] M. Hoque, P. Sarkar, J. Ahmed, Preparation and characterization of tamarind kernel powder/ZnO nanoparticle-based food packaging films, Ind. Crops Prod. 178 (2022) 114670. https://doi.org/10.1016/j.indcrop.2022.114670.

[36] R. Santhosh, P. Sarkar, Jackfruit seed starch/tamarind kernel xyloglucan/zinc oxide nanoparticles-based composite films: Preparation, characterization, and application on tomato (Solanum lycopersicum) fruits, in: Food Hydrocoll., Elsevier, 2022: p. 107917. https://doi.org/10.1016/J.FOODHYD.2022.107917.

[37] S. Padhi, A. Behera, M.S. Hasnain, A.K. Nayak, Chitosan in colon-targeted drug delivery, Chitosan Drug Deliv. (2022) 107–132. https://doi.org/10.1016/B978-0-12-819336-5.00019-4.

[38] K. Gupta, P. Joshi, O.P. Khatri, Carbon Nanomaterials and Biopolymers Derived Aerogels for Wastewater Remediation, Liq. Cryst. Nanomater. Water Pollut. Remediat. (2022) 119–139. https://doi.org/10.1201/9781003091486-6.

[39] A. Balakrishnan, S. Appunni, M. Chinthala, D.V.N. Vo, Biopolymer-supported TiO2 as a sustainable photocatalyst for wastewater treatment: a review, Environ. Chem. Lett. 2022. 1 (2022) 1–28. https://doi.org/10.1007/S10311-022-01443-8.

[40] A. Amini Herab, D. Salari, A. Ostadrahimi, A. Olad, Synthesis of innovative TiO2-inulin-Fe_3O_4 nanocomposite for removal of Ni (II), Cr (III), crystal violet and malachite green from aqueous solutions, J. Polym. Res. 2022 298. 29 (2022) 1–23. https://doi.org/10.1007/S10965-022-03186-0.

[41] A.H. Naeini, M. Kalaee, O. Moradi, R. Khajavi, M. Abdouss, Eco-friendly inorganic-organic bionanocomposite (Copper oxide — Carboxyl methyl cellulose — Guar gum): Preparation and effective removal of dye from aqueous solution, Korean J. Chem. Eng. 2022. 39 (2022) 1–10. https://doi.org/10.1007/S11814-022-1074-7.

[42] S. Singh, K.L. Wasewar, S.K. Kansal, Low-cost adsorbents for removal of inorganic

impurities from wastewater, Inorg. Pollut. Water. (2020) 173–203. https://doi.org/10.1016/B978-0-12-818965-8.00010-X.

[43] M.S. Samuel, E. Selvarajan, A. Sarswat, H. Muthukumar, J.M. Jacob, M. Mukesh, A. Pugazhendhi, Nanomaterials as adsorbents for As(III) and As(V) removal from water: A review, J. Hazard. Mater. 424 (2022) 127572. https://doi.org/10.1016/J.JHAZMAT.2021.127572.

[44] U. Chadha, P. Bhardwaj, S.K. Selvaraj, K. Kumari, T.S. Isaac, M. Panjwani, K. Kulkarni, R.M. Mathew, A.M. Satheesh, A. Pal, N. Gunreddy, O. Dubey, S. Singh, S. Latha, A. Chakravorty, B. Badoni, M. Banavoth, P. Sonar, M. Manoharan, V. Paramasivam, Advances in chitosan biopolymer composite materials: from bioengineering, wastewater treatment to agricultural applications, Mater. Res. Express. 9 (2022) 052002. https://doi.org/10.1088/2053-1591/AC5A9D.

[45] V. Andal, K. Kannan, Z.E. Kennedy, Biodegradable Composites for Conductive and Sensor Applications, in: Biodegrad. Compos. Packag. Appl., CRC Press, 2022: pp. 97–113. https://doi.org/10.1201/9781003227908-7.

[46] M. Tavassoli, M. Alizadeh Sani, A. Khezerlou, A. Ehsani, G. Jahed-Khaniki, D.J. McClements, Smart Biopolymer-Based Nanocomposite Materials Containing pH-Sensing Colorimetric Indicators for Food Freshness Monitoring, Molecules. 27 (2022) 3168. https://doi.org/10.3390/molecules27103168.

[47] N. Bhanu, M.E. Harikumar, S.K. Batabyal, Self-powered low-range pressure sensor using biopolymer composites, Appl. Phys. A Mater. Sci. Process. 128 (2022) 1–9. https://doi.org/10.1007/s00339-022-05320-7.

[48] M. Krebsz, T. Pasinszki, T.T. Tung, D. Losic, Development of Vapor/Gas Sensors from Biopolymer Composites, in: Biopolym. Compos. Electron., Elsevier, 2017: pp. 385–403. https://doi.org/10.1016/B978-0-12-809261-3.00014-0.

[49] Y.A. Anisimov, R.W. Evitts, D.E. Cree, L.D. Wilson, Polyaniline/biopolymer composite systems for humidity sensor applications: A review, Polymers (Basel). 13 (2021) 2722. https://doi.org/10.3390/polym13162722.

[50] K. Li, K. Dai, X. Xu, G. Zheng, C. Liu, J. Chen, C. Shen, Organic vapor sensing behaviors of carbon black/poly (lactic acid) conductive biopolymer composite, Colloid Polym. Sci. 291 (2013) 2871–2878. https://doi.org/10.1007/s00396-013-3038-2.

[51] A.P. Martínez-Camacho, M.O. Cortez-Rocha, J.M. Ezquerra-Brauer, A.Z. Graciano-Verdugo, F. Rodriguez-Félix, M.M. Castillo-Ortega, M.S. Yépiz-Gómez, M. Plascencia-Jatomea, Chitosan composite films: Thermal, structural, mechanical and

antifungal properties, Carbohydr. Polym. 82 (2010) 305–315. https://doi.org/10.1016/J.CARBPOL.2010.04.069.

[52] A. Shehabeldine, H. El-Hamshary, M. Hasanin, A. El-Faham, M. Al-Sahly, Enhancing the antifungal activity of griseofulvin by incorporation a green biopolymer-based nanocomposite, Polymers (Basel). 13 (2021) 1–12. https://doi.org/10.3390/polym13040542.

[53] M.F. Salem, W.A. Abd-Elraoof, A.A. Tayel, F.M. Alzuaibr, O.M. Abonama, Antifungal application of biosynthesized selenium nanoparticles with pomegranate peels and nanochitosan as edible coatings for citrus green mold protection, J. Nanobiotechnology. 20 (2022) 1–12. https://doi.org/10.1186/s12951-022-01393-x.

[54] X. Hu, J. Wang, X. Wu, X. Gao, F. Mo, Y. Ding, R. Li, M. Li, Preparation and characterization of sustainable osthole@guar gum composite film and antifungal mechanism against Ustilaginoidea virens, Ind. Crops Prod. 185 (2022). https://www.mdpi.com/2304-8158/11/8/1083/htm (accessed July 20, 2022).

[55] J. Jacob, S. Thomas, S. Loganathan, R.B. Valapa, Antioxidant incorporated biopolymer composites for active packaging, in: Process. Dev. Polysaccharide-Based Biopolym. Packag. Appl., Elsevier, 2020: pp. 239–260. https://doi.org/10.1016/b978-0-12-818795-1.00010-1.

[56] N.A. Negm, M.T.H.A. Kana, S.A. Abubshait, M.A. Betiha, Effectuality of chitosan biopolymer and its derivatives during antioxidant applications, Int. J. Biol. Macromol. 164 (2020) 1342–1369. https://doi.org/10.1016/J.IJBIOMAC.2020.07.197.

[57] Y. Zou, Y. Qian, X. Rong, K. Cao, D.J. McClements, K. Hu, Encapsulation of quercetin in biopolymer-coated zein nanoparticles: Formation, stability, antioxidant capacity, and bioaccessibility, Food Hydrocoll. 120 (2021) 106980. https://doi.org/10.1016/j.foodhyd.2021.106980.

[58] M.I. Alvarez Echazú, C.E. Olivetti, I. Peralta, M.R. Alonso, C. Anesini, C.J. Perez, G.S. Alvarez, M.F. Desimone, Development of pH-responsive biopolymer-silica composites loaded with Larrea divaricata Cav. extract with antioxidant activity, Colloids Surfaces B Biointerfaces. 169 (2018) 82–91. https://doi.org/10.1016/J.COLSURFB.2018.05.015.

[59] S. Roy, J.W. Rhim, Agar-based antioxidant composite films incorporated with melanin nanoparticles, Food Hydrocoll. 94 (2019) 391–398. https://doi.org/10.1016/j.foodhyd.2019.03.038.

[60] J. Domínguez-Robles, E. Larrañeta, M.L. Fong, N.K. Martin, N.J. Irwin, P. Mutjé, Q.

Tarrés, M. Delgado-Aguilar, Lignin/poly(butylene succinate) composites with antioxidant and antibacterial properties for potential biomedical applications, Int. J. Biol. Macromol. 145 (2020) 92–99. https://doi.org/10.1016/j.ijbiomac.2019.12.146.

[61] M. Pirnia, K. Shirani, F. Tabatabaee Yazdi, S.A. Moratazavi, M. Mohebbi, Characterization of antioxidant active biopolymer bilayer film based on gelatin-frankincense incorporated with ascorbic acid and Hyssopus officinalis essential oil, Food Chem. X. 14 (2022) 100300. https://doi.org/10.1016/j.fochx.2022.100300.

[62] N. Panneerselvam, D. Sundaramurthy, A. Maruthapillai, Antibacterial/Antioxidant Activity of CuO Impacted Xanthan Gum/Chitosan @Ascorbic Acid Nanocomposite Films, J. Polym. Environ. 30 (2022) 3239–3249. https://doi.org/10.1007/s10924-022-02429-x.

[63] J. Tarique, S.M. Sapuan, A. Khalina, R.A. Ilyas, E.S. Zainudin, Thermal, flammability, and antimicrobial properties of arrowroot (Maranta arundinacea) fiber reinforced arrowroot starch biopolymer composites for food packaging applications, Int. J. Biol. Macromol. 213 (2022) 1–10. https://doi.org/10.1016/J.IJBIOMAC.2022.05.104.

[64] S. Roy, P. Ezati, J.W. Rhim, Fabrication of Antioxidant and Antimicrobial Pullulan/Gelatin Films Integrated with Grape Seed Extract and Sulfur Nanoparticles, ACS Appl. Bio Mater. (2022). https://doi.org/10.1021/ACSABM.2C00148/SUPPL_FILE/MT2C00148_SI_001.PDF.

[65] T. Todhanakasem, S. Panjapiyakul, P. Koombhongse, Novel pineapple leaf fibre composites coating with antimicrobial compound as a potential food packaging, Packag. Technol. Sci. 35 (2022) 97–105. https://doi.org/10.1002/PTS.2612.

[66] R. Priyadarshi, S. Roy, T. Ghosh, D. Biswas, J.W. Rhim, Antimicrobial nanofillers reinforced biopolymer composite films for active food packaging applications - A review, Sustain. Mater. Technol. 32 (2022) e00353. https://doi.org/10.1016/J.SUSMAT.2021.E00353.

[67] R. Syafiq, S.M. Sapuan, M.Y.M. Zuhri, R.A. Ilyas, A. Nazrin, S.F.K. Sherwani, A. Khalina, Antimicrobial activities of starch-based biopolymers and biocomposites incorporated with plant essential oils: A review, Polymers (Basel). 12 (2020) 1–26. https://doi.org/10.3390/polym12102403.

[68] J.H. Lee, D. Jeong, P. Kanmani, Study on physical and mechanical properties of the biopolymer/silver based active nanocomposite films with antimicrobial activity, Carbohydr. Polym. 224 (2019) 50. https://doi.org/10.1016/j.carbpol.2019.115159.

[69] M. Darya, M.H. Abdolrasouli, M. Yousefzadi, M.M. Sajjadi, I. Sourinejad, M. Zarei,

Antifouling coating based on biopolymers (PCL/ PLA) and bioactive extract from the sea cucumber Stichopus herrmanni, AMB Express. 12 (2022) 1–12. https://doi.org/10.1186/S13568-022-01364-3/TABLES/5.

[70] C. Jansen, N.M. Tran-Cong, C. Schlüsener, A. Schmitz, P. Proksch, C. Janiak, MOF@chitosan Composites with Potential Antifouling Properties for Open-Environment Applications of Metal-Organic Frameworks, Solids. 3 (2022) 35–54. https://doi.org/10.3390/solids3010004.

[71] L. Li, G. Li, Y. Wu, Y. Lin, Y. Qu, Y. Wu, K. Lu, Y. Zou, H. Chen, Q. Yu, Y. Zhang, Dual-functional bacterial cellulose modified with phase-transitioned proteins and gold nanorods combining antifouling and photothermal bactericidal properties, J. Mater. Sci. Technol. 110 (2022) 14–23. https://doi.org/10.1016/j.jmst.2021.10.011.

[72] R. Cao, S. Shi, H. Cao, Y. Li, F. Duan, Y. Li, Surface composite modification of anion exchange membrane by electrodeposition and self-polymerization for improved antifouling performance, Colloids Surfaces A Physicochem. Eng. Asp. 648 (2022) 129402. https://doi.org/10.1016/j.colsurfa.2022.129402.

[73] R.F.M. Elshaarawy, J. Dechnik, H.M.A. Hassan, D. Dietrich, M.A. Betiha, S. Schmidt, C. Janiak, Novel high throughput mixed matrix membranes embracing poly ionic liquid-grafted biopolymer: Fabrication, characterization, permeation and antifouling performance, J. Mol. Liq. 266 (2018) 484–494. https://doi.org/10.1016/J.MOLLIQ.2018.06.100.

[74] P. Asuri, S.S. Karajanagi, R.S. Kane, J.S. Dordick, Polymer-nanotube-enzyme composites as active antifouling films, Small. 3 (2007) 50–53. https://doi.org/10.1002/smll.200600312.

[75] E. Bagheripour, A.R. Moghadassi, S.M. Hosseini, B. Van der Bruggen, F. Parvizian, Novel composite graphene oxide/chitosan nanoplates incorporated into PES based nanofiltration membrane: Chromium removal and antifouling enhancement, J. Ind. Eng. Chem. 62 (2018) 311–320. https://doi.org/10.1016/j.jiec.2018.01.009.

[76] S. Gopi, A. Amalraj, N.P. Sukumaran, J.T. Haponiuk, S. Thomas, Biopolymers and Their Composites for Drug Delivery: A Brief Review, Macromol. Symp. 380 (2018) 1800114. https://doi.org/10.1002/MASY.201800114.

[77] Y.E. Miao, H. Zhu, D. Chen, R. Wang, W.W. Tjiu, T. Liu, Electrospun fibers of layered double hydroxide/biopolymer nanocomposites as effective drug delivery systems, Mater. Chem. Phys. 134 (2012) 623–630. https://doi.org/10.1016/J.MATCHEMPHYS.2012.03.041.

[78] E. Abdullayev, Y. Lvov, Halloysite clay nanotubes as a ceramic “skeleton” for functional biopolymer composites with sustained drug release, J. Mater. Chem. B. 1 (2013) 2894–2903. https://doi.org/10.1039/C3TB20059K.

[79] A. Koyyada, P. Orsu, Natural gum polysaccharides as efficient tissue engineering and drug delivery biopolymers, J. Drug Deliv. Sci. Technol. 63 (2021) 102431. https://doi.org/10.1016/J.JDDST.2021.102431.

[80] M.H. Kim, S. An, K. Won, H.J. Kim, S.H. Lee, Entrapment of enzymes into cellulose–biopolymer composite hydrogel beads using biocompatible ionic liquid, J. Mol. Catal. B Enzym. 75 (2012) 68–72. https://doi.org/10.1016/J.MOLCATB.2011.11.011.

[81] H. Yadav, R. Agrawal, A. Panday, J. Patel, S. Maiti, Polysaccharide-silicate composite hydrogels: Review on synthesis and drug delivery credentials, J. Drug Deliv. Sci. Technol. 74 (2022) 103573. https://doi.org/10.1016/J.JDDST.2022.103573.

[82] S. Doppalapudi, S. Katiyar, A.J. Domb, W. Khan, Biodegradable Natural Polymers, Adv. Polym. Med. (2015) 33–66. https://doi.org/10.1007/978-3-319-12478-0_2.

[83] V. Wankhade, Animal-derived biopolymers in food and biomedical technology, Biopolym. Formul. Biomed. Food Appl. (2020) 139–152. https://doi.org/10.1016/B978-0-12-816897-4.00006-0.

[84] J. Baranwal, B. Barse, A. Fais, G.L. Delogu, A. Kumar, Biopolymer: A Sustainable Material for Food and Medical Applications, Polymers (Basel). 14 (2022) 983. https://doi.org/10.3390/polym14050983.

[85] J. Li, X. Yu, E.E. Martinez, J. Zhu, T. Wang, S. Shi, S.R. Shin, S. Hassan, C. Guo, Emerging Biopolymer-Based Bioadhesives, Macromol. Biosci. 22 (2022) 2100340. https://doi.org/10.1002/MABI.202100340.

[86] S. Ling, W. Chen, Y. Fan, K. Zheng, K. Jin, H. Yu, M.J. Buehler, D.L. Kaplan, Biopolymer nanofibrils: Structure, modeling, preparation, and applications, Prog. Polym. Sci. 85 (2018) 1–56. https://doi.org/10.1016/J.PROGPOLYMSCI.2018.06.004.

[87] N. Fijoł, A. Aguilar-Sánchez, A.P. Mathew, 3D-printable biopolymer-based materials for water treatment: A review, Chem. Eng. J. 430 (2022) 132964. https://doi.org/10.1016/J.CEJ.2021.132964.

[88] I.B. Basumatary, A. Mukherjee, V. Katiyar, S. Kumar, Biopolymer-based nanocomposite films and coatings: recent advances in shelf-life improvement of fruits and vegetables, Crit. Rev. Food Sci. Nutr. 62 (2022) 1912–1935. https://doi.org/10.1080/10408398.2020.1848789.

[89] A. Apriyanto, J. Compart, J. Fettke, A review of starch, a unique biopolymer –

Structure, metabolism and in planta modifications, Plant Sci. 318 (2022) 111223. https://doi.org/10.1016/J.PLANTSCI.2022.111223.

[90] D.; ; Patel, B.; Hickson, J.; Desrochers, X. Hu, A. Mahmood, D. Patel, B. Hickson, J. Desrochers, X. Hu, Recent Progress in Biopolymer-Based Hydrogel Materials for Biomedical Applications, Int. J. Mol. Sci. 2022, Vol. 23, Page 1415. 23 (2022) 1415. https://doi.org/10.3390/IJMS23031415.

[91] M. Premalatha, T. Mathavan, S. Selvasekarapandian, S. Monisha, D.V. Pandi, S. Selvalakshmi, Investigations on proton conducting biopolymer membranes based on tamarind seed polysaccharide incorporated with ammonium thiocyanate, J. Non. Cryst. Solids. 453 (2016) 131–140. https://doi.org/10.1016/J.JNONCRYSOL.2016.10.008.

[92] R. Malviya, S. Sundram, S. Fuloria, V. Subramaniyan, K. V. Sathasivam, A.K. Azad, M. Sekar, D.H. Kumar, S. Chakravarthi, O. Porwal, D.U. Meenakshi, N.K. Fuloria, Evaluation and characterization of tamarind gum polysaccharide: The biopolymer, Polymers (Basel). 13 (2021) 3023. https://doi.org/10.3390/polym13183023.

[93] L. Sampathkumar, P. Christopher Selvin, S. Selvasekarapandian, P. Perumal, R. Chitra, M. Muthukrishnan, Synthesis and characterization of biopolymer electrolyte based on tamarind seed polysaccharide, lithium perchlorate and ethylene carbonate for electrochemical applications, Ionics (Kiel). 25 (2019) 1067–1082. https://doi.org/10.1007/S11581-019-02857-1/TABLES/7.

[94] L.S. Kumar, P.C. Selvin, S. Selvasekarapandian, R. Manjuladevi, S. Monisha, P. Perumal, Tamarind seed polysaccharide biopolymer membrane for lithium-ion conducting battery, Ionics (Kiel). 24 (2018) 3793–3803. https://doi.org/10.1007/S11581-018-2541-3/TABLES/5.

[95] J. Kochumalayil, H. Sehaqui, Q. Zhou, L.A. Berglund, Tamarind seed xyloglucan – a thermostable high-performance biopolymer from non-food feedstock, J. Mater. Chem. 20 (2010) 4321–4327. https://doi.org/10.1039/C0JM00367K.

[96] K. Maithilee, P. Sathya, S. Selvasekarapandian, R. Chitra, M.V. Krishna, S. Meyvel, Na-ion conducting biopolymer electrolyte based on tamarind seed polysaccharide incorporated with sodium perchlorate for primary sodium-ion batteries, Ionics (Kiel). 28 (2022) 1783–1790. https://doi.org/10.1007/S11581-022-04440-7/FIGURES/10.

[97] R.A. Ilyas, S.M. Sapuan, M.N.F. Norrrahim, T.A.T. Yasim-Anuar, A. Kadier, M.S. Kalil, M.S.N. Atikah, R. Ibrahim, M. Asrofi, H. Abral, A. Nazrin, R. Syafiq, H.A. Aisyah, M.R.M. Asyraf, Nanocellulose/Starch Biopolymer Nanocomposites: Processing, Manufacturing, and Applications, Adv. Process. Prop. Appl. Starch Other

Bio-Based Polym. (2020) 65–88. https://doi.org/10.1016/B978-0-12-819661-8.00006-8.

[98] T.A. Fernandes, I.F.M. Costa, P. Jorge, A.C. Sousa, V. André, R.G. Cabral, N. Cerca, A.M. Kirillov, Hybrid Silver(I)-Doped Soybean Oil and Potato Starch Biopolymer Films to Combat Bacterial Biofilms, ACS Appl. Mater. Interfaces. (2022). https://doi.org/10.1021/ACSAMI.2C03010/SUPPL_FILE/AM2C03010_SI_001.PDF.

[99] A. Gamage, A. Liyanapathiranage, A. Manamperi, C. Gunathilake, S. Mani, O. Merah, T. Madhujith, Applications of Starch Biopolymers for a Sustainable Modern Agriculture, Sustainability. 14 (2022) 6085. https://doi.org/10.3390/su14106085.

[100] F.Z. Semlali Aouragh Hassani, M.H. Salim, Z. Kassab, H. Sehaqui, E.H. Ablouh, R. Bouhfid, A.E.K. Qaiss, M. El Achaby, Crosslinked starch-coated cellulosic papers as alternative food-packaging materials, RSC Adv. 12 (2022) 8536–8546. https://doi.org/10.1039/D2RA00536K.

[101] J. Tarique, E.S. Zainudin, S.M. Sapuan, R.A. Ilyas, A. Khalina, Physical, Mechanical, and Morphological Performances of Arrowroot (Maranta arundinacea) Fiber Reinforced Arrowroot Starch Biopolymer Composites, Polymers (Basel). 14 (2022) 388. https://doi.org/10.3390/polym14030388.

[102] S. Sethi, Saruchi, Medha, S. Thakur, B.S. Kaith, N. Sharma, S. Ansar, S. Pandey, V. Kuma, Biopolymer starch-gelatin embedded with silver nanoparticle–based hydrogel composites for antibacterial application, Biomass Convers. Biorefinery. (2022) 1–22. https://doi.org/10.1007/S13399-022-02437-W/FIGURES/15.

[103] A.F. Pierce, B.S. Liu, M. Liao, W.L. Wagner, H.A. Khalil, Z. Chen, M. Ackermann, S.J. Mentzer, Optical and Mechanical Properties of Self-Repairing Pectin Biopolymers, Polymers (Basel). 14 (2022) 1345. https://doi.org/10.3390/polym14071345.

[104] M.A. Jothi, D. Vanitha, N. Nallamuthu, K. Sundaramahalingam, Optical and dielectric characterization of biopolymer pectin based electrolytes with NaCl, J. Elastomers Plast. (2022). https://doi.org/10.1177/00952443221087380.

[105] J. Chu, P. Metcalfe, H. V. Linford, S. Zhao, F.M. Goycoolea, S. Chen, X. Ye, M. Holmes, C. Orfila, Short-time acoustic and hydrodynamic cavitation improves dispersibility and functionality of pectin-rich biopolymers from citrus waste., J. Clean. Prod. 330 (2022) 129789. https://doi.org/10.1016/J.JCLEPRO.2021.129789.

[106] A. Pierce, Y. Zheng, W.L. Wagner, H. V. Scheller, D. Mohnen, A. Tsuda, M. Ackermann, S.J. Mentzer, Pectin biopolymer mechanics and microstructure associated

with polysaccharide phase transitions, J. Biomed. Mater. Res. Part A. 108 (2020) 246–253. https://doi.org/10.1002/JBM.A.36811.

[107] P. Perumal, P. Christopher Selvin, S. Selvasekarapandian, Characterization of biopolymer pectin with lithium chloride and its applications to electrochemical devices, Ionics (Kiel). 24 (2018) 3259–3270. https://doi.org/10.1007/S11581-018-2507-5/TABLES/5.

[108] H.B. Ahmed, M.K. Zahran, H.E. Emam, Heatless synthesis of well dispersible Au nanoparticles using pectin biopolymer, Int. J. Biol. Macromol. 91 (2016) 208–219. https://doi.org/10.1016/J.IJBIOMAC.2016.05.060.

[109] B. Khodashenas, M. Ardjmand, M.S. Baei, A.S. Rad, A. Akbarzadeh, Conjugation of pectin biopolymer with Au-nanoparticles as a drug delivery system: Experimental and DFT studies, Appl. Organomet. Chem. 34 (2020) e5609. https://doi.org/10.1002/AOC.5609.

[110] R. Basak, R. Bandyopadhyay, Formation and rupture of Ca^{2+} induced pectin biopolymer gels, Soft Matter. 10 (2014) 7225–7233. https://doi.org/10.1039/C4SM00748D.

[111] S. Bhaladhare, D. Das, Cellulose: a fascinating biopolymer for hydrogel synthesis, J. Mater. Chem. B. 10 (2022) 1923–1945. https://doi.org/10.1039/D1TB02848K.

[112] P. Shrivastav, S. Pramanik, G. Vaidya, M.A. Abdelgawad, M.M. Ghoneim, A. Singh, B.M. Abualsoud, L.S. Amaral, M.A.S. Abourehab, Bacterial cellulose as a potential biopolymer in biomedical applications: a state-of-the-art review, J. Mater. Chem. B. 10 (2022) 3199–3241. https://doi.org/10.1039/D1TB02709C.

[113] L.T. Yogarathinam, P.S. Goh, A.F. Ismail, A. Gangasalam, N.A. Ahmad, A. Samavati, S.C. Mamah, M.N. Zainol Abidin, B.C. Ng, B. Gopal, Nanocrystalline cellulose incorporated biopolymer tailored polyethersulfone mixed matrix membranes for efficient treatment of produced water, Chemosphere. 293 (2022) 133561. https://doi.org/10.1016/J.CHEMOSPHERE.2022.133561.

[114] R. Portela, C.R. Leal, P.L. Almeida, R.G. Sobral, Bacterial cellulose: a versatile biopolymer for wound dressing applications, Microb. Biotechnol. 12 (2019) 586–610. https://doi.org/10.1111/1751-7915.13392.

[115] J. Koliyoor, Ismayil, S. Hegde, R. Vasachar, G. Sanjeev, Novel solid biopolymer electrolyte based on methyl cellulose with enhanced ion transport properties, J. Appl. Polym. Sci. 139 (2022) 51826. https://doi.org/10.1002/APP.51826.

[116] G. Wei, Y. Chen, N. Zhou, Q. Lu, S. Xu, A. Zhang, K. Chen, P. Ouyang, Chitin

biopolymer mediates self-sufficient biocatalyst of pyridoxal 5′-phosphate and L-lysine decarboxylase, Chem. Eng. J. 427 (2022) 132030. https://doi.org/10.1016/J.CEJ.2021.132030.

[117] O. Aguilar-Rosas, S. Blanco, M. Flores, K. Shirai, L.I. Farfan-Cabrera, Partially Deacetylated and Fibrillated Shrimp Waste-Derived Chitin as Biopolymer Emulsifier for Green Cutting Fluids—Towards a Cleaner Production, Polymers (Basel). 14 (2022) 525. https://doi.org/10.3390/polym14030525.

[118] E. Longhinotti, F. Pozza, L. Furlan, M.D.N.D.M. Sanchez, M. Klug, M.C.M. Laranjeira, V.T. Fávere, Adsorption of Anionic Dyes on the Biopolymer Chitin, J. Braz. Chem. Soc. 9 (1998) 435–440. https://doi.org/10.1590/S0103-50531998000500005.

[119] J. Ma, Y. Sahai, Chitosan biopolymer for fuel cell applications, Carbohydr. Polym. 92 (2013) 955–975. https://doi.org/10.1016/J.CARBPOL.2012.10.015.

[120] J. Ruhsing Pan, C. Huang, S. Chen, Y.C. Chung, Evaluation of a modified chitosan biopolymer for coagulation of colloidal particles, Colloids Surfaces A Physicochem. Eng. Asp. 147 (1999) 359–364. https://doi.org/10.1016/S0927-7757(98)00588-3.

[121] N. Hataf, P. Ghadir, N. Ranjbar, Investigation of soil stabilization using chitosan biopolymer, J. Clean. Prod. 170 (2018) 1493–1500. https://doi.org/10.1016/J.JCLEPRO.2017.09.256.

[122] I. Bano, M. Arshad, T. Yasin, M.A. Ghauri, M. Younus, Chitosan: A potential biopolymer for wound management, Int. J. Biol. Macromol. 102 (2017) 380–383. https://doi.org/10.1016/J.IJBIOMAC.2017.04.047.

[123] A. Detsi, E. Kavetsou, I. Kostopoulou, I. Pitterou, A.R.N. Pontillo, A. Tzani, P. Christodoulou, A. Siliachli, P. Zoumpoulakis, Nanosystems for the encapsulation of natural products: The case of chitosan biopolymer as a matrix, Pharmaceutics. 12 (2020) 1–68. https://doi.org/10.3390/pharmaceutics12070669.

[124] H. Huang, N. Hu, Y. Zeng, G. Zhou, Electrochemistry and electrocatalysis with heme proteins in chitosan biopolymer films, Anal. Biochem. 308 (2002) 141–151. https://doi.org/10.1016/S0003-2697(02)00242-7.

[125] S.K. Mondal, C. Wu, F.C. Nwadire, A. Rownaghi, A. Kumar, Y. Adewuyi, M.U. Okoronkwo, Examining the Effect of a Chitosan Biopolymer on Alkali-Activated Inorganic Material for Aqueous Pb(II) and Zn(II) Sorption, Langmuir. 38 (2022) 903–913.
https://doi.org/10.1021/ACS.LANGMUIR.1C01829/ASSET/IMAGES/MEDIUM/LA

1C01829_0009.GIF.

[126] Z. Tang, Z. Qiu, H. Zhong, Y. Kang, B. Guo, Wellbore Stability through Novel Catechol-Chitosan Biopolymer Encapsulator-Based Drilling Mud, Gels. 8 (2022) 307. https://doi.org/10.3390/gels8050307.

[127] B. Aaliya, K. Valiyapeediyekkal Sunooj, M. Lackner, Biopolymer composites: a review, Int. J. Biobased Plast. 3 (2021) 40–84. https://doi.org/10.1080/24759651.2021.1881214.

[128] R.M. Brown, I.M. Saxena, Cellulose biosynthesis: A model for understanding the assembly of biopolymers, Plant Physiol. Biochem. 38 (2000) 57–67. https://doi.org/10.1016/S0981-9428(00)00168-6.

[129] H.P.S. Abdul Khalil, Y.Y. Tye, C.K. Saurabh, C.P. Leh, T.K. Lai, E.W.N. Chong, M.R. Nurul Fazita, J.M. Hafiidz, A. Banerjee, M.I. Syakir, Biodegradable polymer films from seaweed polysaccharides: A review on cellulose as a reinforcement material, Express Polym. Lett. 11 (2017) 244–265. https://doi.org/10.3144/expresspolymlett.2017.26.

[130] D. Klemm, B. Heublein, H.P. Fink, A. Bohn, Cellulose: Fascinating Biopolymer and Sustainable Raw Material, Angew. Chemie Int. Ed. 44 (2005) 3358–3393. https://doi.org/10.1002/ANIE.200460587.

[131] Y. Liu, S. Ahmed, D.E. Sameen, Y. Wang, R. Lu, J. Dai, S. Li, W. Qin, A review of cellulose and its derivatives in biopolymer-based for food packaging application, Trends Food Sci. Technol. 112 (2021) 532–546. https://doi.org/10.1016/J.TIFS.2021.04.016.

[132] I.A.M. Appelqvist, M.R.M. Debet, Starch-biopolymer interactions - A review, Food Rev. Int. 13 (1997) 163–224. https://doi.org/10.1080/87559129709541105.

[133] E. Vatansever, D. Arslan, M. Nofar, Polylactide cellulose-based nanocomposites, Int. J. Biol. Macromol. 137 (2019) 912–938. https://doi.org/10.1016/J.IJBIOMAC.2019.06.205.

[134] Qurat-ul-Ain, K.M. Zia, F. Zia, M. Ali, S. Rehman, M. Zuber, Lipid functionalized biopolymers: A review, Int. J. Biol. Macromol. 93 (2016) 1057–1068. https://doi.org/10.1016/J.IJBIOMAC.2016.09.071.

[135] V.K. Thakur, M.K. Thakur, R.K. Gupta, Development of functionalized cellulosic biopolymers by graft copolymerization, Int. J. Biol. Macromol. 62 (2013) 44–51. https://doi.org/10.1016/J.IJBIOMAC.2013.08.026.

[136] L.A. Grischenko, L.N. Parshina, L. V. Kanitskaya, L.I. Larina, L.N. Novikova, B.A.

Trofimov, Propargylation of arabinogalactan with propargyl halides—a facile route to new functionalized biopolymers, Carbohydr. Res. 376 (2013) 7–14. https://doi.org/10.1016/J.CARRES.2013.04.031.

[137] K.K. Tadi, N.M. Reddy, C.G. Chandaluri, G.P. Sakala, G. V. Ramesh, Functionalized Biopolymer Nanocomposites for the Degradation of Textile Dyes, Springer Ser. Mater. Sci. 323 (2022) 175–200. https://doi.org/10.1007/978-3-030-94995-2_6/COVER/.

[138] S. Singh, W. Chunglok, O.F. Nwabor, Y. V. Ushir, S. Singh, W. Panpipat, Hydrophilic Biopolymer Matrix Antibacterial Peel-off Facial Mask Functionalized with Biogenic Nanostructured Material for Cosmeceutical Applications, J. Polym. Environ. 30 (2022) 938–953. https://doi.org/10.1007/S10924-021-02249-5/FIGURES/7.

[139] C.C. Kandar, M.S. Hasnain, A.K. Nayak, Natural polymers as useful pharmaceutical excipients, in: Adv. Challenges Pharm. Technol., Elsevier, 2021: pp. 1–44. https://doi.org/10.1016/B978-0-12-820043-8.00012-8.

[140] R.J. du Preez, FRUITS OF TROPICAL CLIMATES | Lesser-known Fruits of Africa, in: Encycl. Food Sci. Nutr., Elsevier, 2003: pp. 2800–2810. https://doi.org/10.1016/B0-12-227055-X/00537-X.

[141] A.K. Nayak, M.S. Hasnain, Tamarind polysaccharide based multiple units for oral drug delivery, SpringerBriefs Appl. Sci. Technol. (2019) 31–59. https://doi.org/10.1007/978-981-10-6784-6_4/COVER/.

[142] P.B. Sarkar, A.K. Mazumdar, The Composition of Tamarind Seed Kernel Powder, J. Text. Inst. Trans. 43 (1952) T453–T454. https://doi.org/10.1080/19447025208659687.

[143] M. Kaur, S. Singh, Physicochemical, Morphological, Pasting, and Rheological Properties of Tamarind (Tamarindus indica L.) Kernel Starch, Int. J. Food Prop. 19 (2016) 2432–2442. https://doi.org/10.1080/10942912.2015.1121495.

[144] A.K. Shukla, R.S. Bishnoi, M. Kumar, V. Fenin, C.P. Jain, Applications of Tamarind seeds Polysaccharide-based copolymers in Controlled Drug Delivery: An overview, Asian J. Pharm. Pharmacol. 4 (2018) 23–30. https://doi.org/10.31024/ajpp.2018.4.1.5.

[145] K. Mali, S. Dhawale, R. Dias, V. Ghorpade, Delivery of drugs using tamarind gum and modified tamarind gum: A review, Bull. Fac. Pharmacy, Cairo Univ. 57 (2019) 1–24. https://doi.org/10.21608/bfpc.2019.47260.

[146] S.S. Shaikh, K.J. Shivsharan, R.K. Pawar, N.S. Misal, H.R. Mene, B.A. More, Tamarind seed polysaccharide: A versatile pharmaceutical excipient and its modification, Int. J. Pharm. Sci. Rev. Res. 33 (2015) 157–164. www.globalresearchonline.net (accessed July 20, 2022).

[147] J. Joseph, S.N. Kanchalochana, G. Rajalakshmi, V. Hari, R.D. Durai, Tamarind seed polysaccharide: A promising natural excipient for pharmaceuticals, Int. J. Green Pharm. 6 (2012). https://doi.org/10.22377/IJGP.V6I4.273.

[148] A.K. Nayak, D. Pal, Tamarind seed polysaccharide: An emerging excipient for pharmaceutical use, Indian J. Pharm. Educ. Res. 51 (2017) S136–S146. https://doi.org/10.5530/ijper.51.2s.60.

[149] S. Jana, S. Jana, Micro- and Nanoengineered Gum-Based Biomaterials for Drug Delivery and Biomedical Applications: A volume in Micro and Nano Technologies, Elsevier, 2022. https://doi.org/10.1016/B978-0-323-90986-0.09988-X.

[150] K.E. Abuelella, H. Abd-Allah, S.M. Soliman, M.M.A. Abdel-Mottaleb, Polysaccharide Based Biomaterials for Dermal Applications, Funct. Biomater. (2022) 105–127. https://doi.org/10.1007/978-981-16-7152-4_4.

[151] M. Razavi, S. Nyamathulla, H. Karimian, S.Z. Moghadamtousi, M.I. Noordin, Hydrogel polysaccharides of tamarind and xanthan to formulate hydrodynamically balanced matrix tablets of famotidine, Molecules. 19 (2014) 13909–13931. https://doi.org/10.3390/molecules190913909.

[152] R. Malviya, P. Srivastava, V. Bansal, P.K. Sharma, Formulation, evaluation and comparison of sustained release matrix tablets of diclofenac sodium using natural polymers as release modifier, Int. J. Pharma Bio Sci. 1 (2010).

[153] A.K. Nayak, D. Pal, K. Santra, Development of calcium pectinate-tamarind seed polysaccharide mucoadhesive beads containing metformin HCl, Carbohydr. Polym. 101 (2014) 220–230. https://doi.org/10.1016/J.CARBPOL.2013.09.024.

[154] H. Kaur, S. Yadav, M. Ahuja, N. Dilbaghi, Synthesis, characterization and evaluation of thiolated tamarind seed polysaccharide as a mucoadhesive polymer, Carbohydr. Polym. 90 (2012) 1543–1549. https://doi.org/10.1016/J.CARBPOL.2012.07.028.

[155] A.K. Nayak, S.S. Nanda, D.K. Yi, M.S. Hasnain, D. Pal, Pharmaceutical Applications of Tamarind Gum, Nat. Polym. Pharm. Appl. (2019) 1–20. https://doi.org/10.1201/9780429328251-1.

[156] S. Ghosh, S. Pal, Modified tamarind kernel polysaccharide: A novel matrix for control release of aspirin, Int. J. Biol. Macromol. 58 (2013) 296–300. https://doi.org/10.1016/j.ijbiomac.2013.04.002.

[157] A.M. Avachat, K.N. Gujar, K. V. Wagh, Development and evaluation of tamarind seed xyloglucan-based mucoadhesive buccal films of rizatriptan benzoate, Carbohydr. Polym. 91 (2013) 537–542. https://doi.org/10.1016/j.carbpol.2012.08.062.

[158] A.K. Nayak, D. Pal, K. Santra, Tamarind seed polysaccharide–gellan mucoadhesive beads for controlled release of metformin HCl, Carbohydr. Polym. 103 (2014) 154–163. https://doi.org/10.1016/j.carbpol.2013.12.031.

[159] S. Jana, A. Saha, A.K. Nayak, K.K. Sen, S.K. Basu, Aceclofenac-loaded chitosan-tamarind seed polysaccharide interpenetrating polymeric network microparticles, Colloids Surfaces B Biointerfaces. 105 (2013) 303–309. https://doi.org/10.1016/j.colsurfb.2013.01.013.

[160] H. Bera, S. Boddupalli, S. Nandikonda, S. Kumar, A.K. Nayak, Alginate gel-coated oil-entrapped alginate–tamarind gum–magnesium stearate buoyant beads of risperidone, Int. J. Biol. Macromol. 78 (2015) 102–111. https://doi.org/10.1016/j.ijbiomac.2015.04.001.

[161] N. Dilbaghi, H. Kaur, M. Ahuja, S. Kumar, Evaluation of tropicamide-loaded tamarind seed xyloglucan nanoaggregates for ophthalmic delivery, Carbohydr. Polym. 94 (2013) 286–291. https://doi.org/10.1016/j.carbpol.2013.01.054.

[162] A.M.J. Newton, V.L. Indana, J. Kumar, Chronotherapeutic drug delivery of Tamarind gum, Chitosan and Okra gum controlled release colon targeted directly compressed Propranolol HCl matrix tablets and in-vitro evaluation, Int. J. Biol. Macromol. 79 (2015) 290–299. https://doi.org/10.1016/j.ijbiomac.2015.03.031.

[163] Meenakshi, M. Ahuja, Metronidazole loaded carboxymethyl tamarind kernel polysaccharide-polyvinyl alcohol cryogels: Preparation and characterization, Int. J. Biol. Macromol. 72 (2015) 931–938. https://doi.org/10.1016/j.ijbiomac.2014.09.040.

[164] K. Nagaraja, K.M. Rao, K.S.V.K. Rao, S.S. Han, Dual responsive tamarind gum-co-poly(N-isopropyl acrylamide-co-ethylene glycol vinyl ether) hydrogel: A promising device for colon specific anti-cancer drug delivery, Colloids Surfaces A Physicochem. Eng. Asp. 641 (2022) 128456. https://doi.org/10.1016/j.colsurfa.2022.128456.

[165] D. Nirmala, V. Harika, M. Sudhakar, Formulation and Evaluation of Mucoadhesive Buccal Tablets of Resperidone, Asian J. Pharm. Technol. (2022) 13–19. https://doi.org/10.52711/2231-5713.2022.00003.

[166] M. M. Dawoud, H. M. Saleh, Introductory Chapter: Background on Composite Materials, in: Charact. Some Compos. Mater., IntechOpen, 2019. https://doi.org/10.5772/intechopen.80960.

[167] A. Felix Sahayaraj, M. Muthukrishnan, R. Prem Kumar, M. Ramesh, M. Kannan, PLA based Bio Composite reinforced with natural fibers – Review, IOP Conf. Ser. Mater. Sci. Eng. 1145 (2021) 012069. https://doi.org/10.1088/1757-899X/1145/1/012069.

[168] E.T. Thostenson, Z. Ren, T.W. Chou, Advances in the science and technology of carbon nanotubes and their composites: a review, Compos. Sci. Technol. 61 (2001) 1899–1912. https://doi.org/10.1016/S0266-3538(01)00094-X.

[169] B. Das, K. Eswar Prasad, U. Ramamurty, C.N.R. Rao, Nano-indentation studies on polymer matrix composites reinforced by few-layergraphene, Nanotechnology. 20 (2009) 125705. https://doi.org/10.1088/0957-4484/20/12/125705.

[170] A.M. Díez-Pascual, Synthesis and Applications of Biopolymer Composites, Int. J. Mol. Sci. 2019, Vol. 20, Page 2321. 20 (2019) 2321. https://doi.org/10.3390/IJMS20092321.

[171] K.K. Sadasivuni, P. Saha, J. Adhikari, K. Deshmukh, M.B. Ahamed, J.J. Cabibihan, Recent advances in mechanical properties of biopolymer composites: a review, Polym. Compos. 41 (2020) 32–59. https://doi.org/10.1002/PC.25356.

[172] S.J. Christian, Natural fibre-reinforced noncementitious composites (biocomposites), Nonconv. Vernac. Constr. Mater. Characterisation, Prop. Appl. (2020) 169–187. https://doi.org/10.1016/B978-0-08-102704-2.00008-1.

[173] S.A.N. Mohamed, E.S. Zainudin, S.M. Sapuan, M.D. Azaman, A.M.T. Arifin, Introduction to Natural Fiber Reinforced Vinyl Ester and Vinyl Polymer Composites, Nat. Fibre Reinf. Vinyl Ester Vinyl Polym. Compos. (2018) 1–25. https://doi.org/10.1016/B978-0-08-102160-6.00001-9.

[174] A.S. Getme, B. Patel, A Review: Bio-fiber's as reinforcement in composites of polylactic acid (PLA), Mater. Today Proc. 26 (2020) 2116–2122. https://doi.org/10.1016/J.MATPR.2020.02.457.

[175] M.M. Kabir, H. Wang, K.T. Lau, F. Cardona, Chemical treatments on plant-based natural fibre reinforced polymer composites: An overview, Compos. Part B Eng. 43 (2012) 2883–2892. https://doi.org/10.1016/J.COMPOSITESB.2012.04.053.

[176] A. Vinod, M.R. Sanjay, S. Suchart, P. Jyotishkumar, Renewable and sustainable biobased materials: An assessment on biofibers, biofilms, biopolymers and biocomposites, J. Clean. Prod. 258 (2020) 120978. https://doi.org/10.1016/J.JCLEPRO.2020.120978.

[177] B. Boury, Biopolymers for biomimetic processing of metal oxides, Extrem. Biomimetics. (2016) 135–189. https://doi.org/10.1007/978-3-319-45340-8_6/COVER/.

[178] Y.Y. Kim, C. Neudeck, D. Walsh, Biopolymer templating as synthetic route to functional metal oxide nanoparticles and porous sponges, Polym. Chem. 1 (2010)

272–275. https://doi.org/10.1039/B9PY00366E.

[179] Y.F. Abbasi, H. Bera, Biopolymer–metal oxide composites in biomedical applications, Tailor-Made Funct. Biopolym. Syst. Drug Deliv. Biomed. Appl. (2021) 203–251. https://doi.org/10.1016/B978-0-12-821437-4.00008-6.

[180] M.A. Mohd Adnan, L.P. Bao, N. Muhd Julkapli, Mitigation of pollutants by chitosan/metallic oxide photocatalyst: A review, J. Clean. Prod. 261 (2020) 121190. https://doi.org/10.1016/J.JCLEPRO.2020.121190.

[181] B. Dhlamini, H.K. Paumo, B.P. Kamdem, L. Katata-Seru, I. Bahadur, Nano-engineering metal-based fertilizers using biopolymers: An innovative strategy for a more sustainable agriculture, J. Environ. Chem. Eng. 10 (2022) 107729. https://doi.org/10.1016/J.JECE.2022.107729.

[182] V. Vijayakumar, S.K. Samal, S. Mohanty, S.K. Nayak, Recent advancements in biopolymer and metal nanoparticle-based materials in diabetic wound healing management, Int. J. Biol. Macromol. 122 (2019) 137–148. https://doi.org/10.1016/J.IJBIOMAC.2018.10.120.

[183] S. Sarkar, E. Guibal, F. Quignard, A.K. SenGupta, Polymer-supported metals and metal oxide nanoparticles: synthesis, characterization, and applications, J. Nanoparticle Res. 2012 142. 14 (2012) 1–24. https://doi.org/10.1007/S11051-011-0715-2.

[184] V.A. Tirado-Kulieva, M. Sánchez-Chero, D.P.P. Jimenez, J. Sánchez-Chero, A.G.Y.S. Cruz, H.H.M. Velayarce, L.A.P. Suclupe, L.O.C. Garcia, A Critical Review on The Integration of Metal Nanoparticles in Biopolymers: An Alternative for Active and Sustainable Food Packaging, Curr. Res. Nutr. Food Sci. 10 (2022) 1–18. https://doi.org/10.12944/CRNFSJ.10.1.01.

[185] M. Rai, A.P. Ingle, I. Gupta, A. Brandelli, Bioactivity of noble metal nanoparticles decorated with biopolymers and their application in drug delivery, Int. J. Pharm. 496 (2015) 159–172. https://doi.org/10.1016/J.IJPHARM.2015.10.059.

[186] A.N. Bezbaruah, S.S. Shanbhogue, S. Simsek, E. Khan, Encapsulation of iron nanoparticles in alginate biopolymer for trichloroethylene remediation, J. Nanoparticle Res. 13 (2011) 6673–6681. https://doi.org/10.1007/S11051-011-0574-X/TABLES/2.

[187] S.K. Balavandy, K. Shameli, Z.Z. Abidin, Rapid and green synthesis of silver nanoparticles via sodium alginate media, Int. J. Electrochem. Sci. 10 (2015) 486–497. www.electrochemsci.org (accessed July 20, 2022).

[188] D. Kołodyńska, M. Gęca, E. Skwarek, O. Goncharuk, Titania-Coated Silica Alone and Modified by Sodium Alginate as Sorbents for Heavy Metal Ions, Nanoscale Res. Lett.

13 (2018) 1–12. https://doi.org/10.1186/S11671-018-2512-7/FIGURES/9.

[189] G.V. Kumari, M.A. Jothirajan, T. Mathavan, Pectin functionalized gold nanoparticles towards singlet oxygen generation, Mater. Res. Express. 5 (2018) 085027. https://doi.org/10.1088/2053-1591/AAB001.

[190] S. Pandey, G.K. Goswami, K.K. Nanda, Green synthesis of polysaccharide/gold nanoparticle nanocomposite: An efficient ammonia sensor, Carbohydr. Polym. 94 (2013) 229–234. https://doi.org/10.1016/J.CARBPOL.2013.01.009.

[191] Y.A. Arfat, M. Ejaz, H. Jacob, J. Ahmed, Deciphering the potential of guar gum/Ag-Cu nanocomposite films as an active food packaging material, Carbohydr. Polym. 157 (2017) 65–71. https://doi.org/10.1016/J.CARBPOL.2016.09.069.

[192] T. BARAN, Highly active and robust palladium nanoparticles immobilized on biodegradable microcapsules containing chitosan-guar gum composite for synthesis of biaryl compounds, Konya J. Eng. Sci. 8 (2020) 113–121. https://doi.org/10.36306/konjes.698694.

[193] R.S. Soumya, V.P. Vineetha, P.L. Reshma, K.G. Raghu, Preparation and Characterization of Selenium Incorporated Guar Gum Nanoparticle and Its Interaction with H9c2 Cells, PLoS One. 8 (2013) e74411. https://doi.org/10.1371/journal.pone.0074411.

[194] S. Lim, S. Gunasekaran, J.Y. Imm, Gelatin-Templated Gold Nanoparticles as Novel Time–Temperature Indicator, J. Food Sci. 77 (2012) N45–N49. https://doi.org/10.1111/J.1750-3841.2012.02872.X.

[195] B.H. Dong, J.P. Hinestroza, Metal nanoparticles on natural cellulose fibers: Electrostatic assembly and in situ synthesis, ACS Appl. Mater. Interfaces. 1 (2009) 797–803. https://doi.org/10.1021/AM800225J/ASSET/IMAGES/MEDIUM/AM-2008-00225J_0001.GIF.

[196] N.N. Thinh, P.T.B. Hanh, L.T.T. Ha, L.N. Anh, T.V. Hoang, V.D. Hoang, L.H. Dang, N. Van Khoi, T.D. Lam, Magnetic chitosan nanoparticles for removal of Cr(VI) from aqueous solution, Mater. Sci. Eng. C. 33 (2013) 1214–1218. https://doi.org/10.1016/J.MSEC.2012.12.013.

[197] C. Dong, W. Chen, C. Liu, Preparation of novel magnetic chitosan nanoparticle and its application for removal of humic acid from aqueous solution, Appl. Surf. Sci. 292 (2014) 1067–1076. https://doi.org/10.1016/J.APSUSC.2013.12.125.

[198] F. Hosseini, S. Sadighian, H. Hosseini-Monfared, N.M. Mahmoodi, Dye removal and kinetics of adsorption by magnetic chitosan nanoparticles, New Pub Balaban. 57

(2016) 24378–24386. https://doi.org/10.1080/19443994.2016.1143879.

[199] H.M.A. Ehmann, D. Breitwieser, S. Winter, C. Gspan, G. Koraimann, U. Maver, M. Sega, S. Köstler, K. Stana-Kleinschek, S. Spirk, V. Ribitsch, Gold nanoparticles in the engineering of antibacterial and anticoagulant surfaces, Carbohydr. Polym. 117 (2015) 34–42. https://doi.org/10.1016/J.CARBPOL.2014.08.116.

[200] S.M. Syame, W.S. Mohamed, R.K. Mahmoud, S.T. Omara, Synthesis of copper-chitosan nanocomposites and their applications in treatment of local pathogenic isolates bacteria, Orient. J. Chem. 33 (2017) 2959–2969. https://doi.org/10.13005/OJC/330632.

[201] T. Kamal, S.B. Khan, A.M. Asiri, Nickel nanoparticles-chitosan composite coated cellulose filter paper: An efficient and easily recoverable dip-catalyst for pollutants degradation, Environ. Pollut. 218 (2016) 625–633. https://doi.org/10.1016/J.ENVPOL.2016.07.046.

[202] S. Chattopadhyay, S.K. Dash, S. Kar Mahapatra, S. Tripathy, T. Ghosh, B. Das, D. Das, P. Pramanik, S. Roy, Chitosan-modified cobalt oxide nanoparticles stimulate TNF-α-mediated apoptosis in human leukemic cells, J. Biol. Inorg. Chem. 19 (2014) 399–414. https://doi.org/10.1007/S00775-013-1085-2/FIGURES/8.

[203] S.K. Tahir, M.S. Yousaf, S. Ahmad, M.K. Shahzad, A.F. Khan, M. Raza, K.A. Majeed, A. Khalid, H. Zaneb, I. Rabbani, H. Rehman, Effects of chromium-loaded chitosan nanoparticles on the intestinal electrophysiological indices and glucose transporters in broilers, Animals. 9 (2019) 819. https://doi.org/10.3390/ani9100819.

[204] P. Abrica-González, J.A. Zamora-Justo, A. Sotelo-López, G.R. Vázquez-Martínez, J.A. Balderas-López, A. Muñoz-Diosdado, M. Ibáñez-Hernández, Gold nanoparticles with chitosan, N-acylated chitosan, and chitosan oligosaccharide as DNA carriers, Nanoscale Res. Lett. 14 (2019) 1–14. https://doi.org/10.1186/S11671-019-3083-Y/FIGURES/11.

[205] A. Sugunan, C. Thanachayanont, J. Dutta, J.G. Hilborn, Heavy-metal ion sensors using chitosan-capped gold nanoparticles, Sci. Technol. Adv. Mater. 6 (2005) 335–340. https://doi.org/10.1016/J.STAM.2005.03.007/XML.

[206] C.O. Mohan, S. Gunasekaran, C.N. Ravishankar, Chitosan-capped gold nanoparticles for indicating temperature abuse in frozen stored products, Npj Sci. Food. 3 (2019) 1–6. https://doi.org/10.1038/s41538-019-0034-z.

[207] M. Lavinia, S.N. Hibaturrahman, H. Harinata, A.A. Wardana, Antimicrobial activity and application of nanocomposite coating from chitosan and ZnO nanoparticle to

inhibit microbial growth on fresh-cut papaya, Food Res. 4 (2020) 307–311. https://doi.org/10.26656/fr.2017.4(2).255.

[208] S.G. Warkar, J. Meena, Synthesis and applications of biopolymer /FeO nanocomposites: A review, J. New Mater. Electrochem. Syst. 25 (2022) 7–16. https://doi.org/10.14447/JNMES.V25I1.A02.

[209] S. Chaudhary, P. Sharma, P. Chauhan, R. Kumar, A. Umar, Functionalized nanomaterials: a new avenue for mitigating environmental problems, Int. J. Environ. Sci. Technol. 16 (2019) 5331–5358. https://doi.org/10.1007/s13762-019-02253-2.

[210] S. Dutta, C.B. Pohrmen, I. Banerjee, A. Trivedi, R. Verma, S. Dubey, Bio-derived metal and metal oxide incorporated biopolymer nanocomposites for dye degradation applications: A review, Octa J. Biosci. 9 (2021) 30–36. https://www.researchgate.net/publication/354340923 (accessed July 21, 2022).

[211] D. Gan, L. Han, M. Wang, W. Xing, T. Xu, H. Zhang, K. Wang, L. Fang, X. Lu, Conductive and Tough Hydrogels Based on Biopolymer Molecular Templates for Controlling in Situ Formation of Polypyrrole Nanorods, ACS Appl. Mater. Interfaces. 10 (2018) 36218–36228. https://doi.org/10.1021/ACSAMI.8B10280/SUPPL_FILE/AM8B10280_SI_001.PDF.

[212] A.L. Daniel-da-Silva, T. Trindade, B.J. Goodfellow, B.F.O. Costa, R.N. Correia, A.M. Gil, In situ synthesis of magnetite nanoparticles in carrageenan gels, Biomacromolecules. 8 (2007) 2350–2357. https://doi.org/10.1021/BM070096Q/SUPPL_FILE/BM070096Q-FILE002.PDF.

[213] Y. Anwar, I. Ullah, M.A. Al-Shaeri, B.O. Aljohny, Ex-situ synthesis of bacterial cellulose-copper oxide nanoparticles for effective chemical and biological properties, Desalin. Water Treat. 197 (2020) 182–190. https://doi.org/10.5004/dwt.2020.25961.

[214] K. Kraśniewska, S. Galus, M. Gniewosz, Biopolymers-Based Materials Containing Silver Nanoparticles as Active Packaging for Food Applications–A Review, Int. J. Mol. Sci. 21 (2020) 698. https://doi.org/10.3390/ijms21030698.

[215] S. Gao, Y. Shi, S. Zhang, K. Jiang, S. Yang, Z. Li, E. Takayama-Muromachi, Biopolymer-Assisted Green Synthesis of FeO Nanoparticles and Their Magnetic Properties, J. Phys. Chem. C. 112 (2008) 10398–10401. https://doi.org/10.1021/JP802500A.

[216] M. Darroudi, M. Bagherpour, H.A. Hosseini, M. Ebrahimi, Biopolymer-assisted green synthesis and characterization of calcium hydroxide nanoparticles, Ceram. Int. 42 (2016) 3816–3819. https://doi.org/10.1016/J.CERAMINT.2015.11.045.

[217] T.C.Y. Leung, C.K. Wong, Y. Xie, Green synthesis of silver nanoparticles using biopolymers, carboxymethylated-curdlan and fucoidan, Mater. Chem. Phys. 121 (2010) 402–405. https://doi.org/10.1016/J.MATCHEMPHYS.2010.02.026.

[218] S. Kanchi, S. Ahmed, Green metal nanoparticles: Synthesis, characterization and their applications, Macabresque Hum. Viol. Hate Genocide, Mass Atrocity Enemy-Making. (2018) 1–694. https://doi.org/10.1002/9781119418900.

[219] S. Pandey, G.K. Goswami, K.K. Nanda, Green synthesis of biopolymer–silver nanoparticle nanocomposite: An optical sensor for ammonia detection, Int. J. Biol. Macromol. 51 (2012) 583–589. https://doi.org/10.1016/J.IJBIOMAC.2012.06.033.

[220] A. Rana, I. Hasan, B.H. Koo, R.A. Khan, Green synthesized CeO_2 nanowires immobilized with alginate-ascorbic acid biopolymer for advance oxidative degradation of crystal violet, Colloids Surfaces A Physicochem. Eng. Asp. 637 (2022) 128225. https://doi.org/10.1016/J.COLSURFA.2021.128225.

[221] B. Hemmati, S. Javanshir, Z. Dolatkhah, Hybrid magnetic Irish moss/Fe_3O_4 as a nano-biocatalyst for synthesis of imidazopyrimidine derivatives, RSC Adv. 6 (2016) 50431–50436. https://doi.org/10.1039/C6RA08504K.

[222] H.L. Ma, Y.F. Xu, X.R. Qi, Y. Maitani, T. Nagai, Superparamagnetic FeO nanoparticles stabilized by alginate: Pharmacokinetics, tissue distribution, and applications in detecting liver cancers, Int. J. Pharm. 354 (2008) 217–226. https://doi.org/10.1016/J.IJPHARM.2007.11.036.

[223] B. Rastegari, H.R. Karbalaei-Heidari, S. Zeinali, H. Sheardown, The enzyme-sensitive release of prodigiosin grafted β-cyclodextrin and chitosan magnetic nanoparticles as an anticancer drug delivery system: Synthesis, characterization and cytotoxicity studies, Colloids Surfaces B Biointerfaces. 158 (2017) 589–601. https://doi.org/10.1016/J.COLSURFB.2017.07.044.

[224] J. Meena, P.S. Jassal, Cresol and it derivative Organic pollutant removal from waste water by adsorption the magneto chitosan nanoparticle, Int. J. Chem. Stud. 5 (2017) 850–854.

[225] I.O. Wulandari, V.T. Mardila, D.J.D.H. Santjojo, A. Sabarudin, Preparation and Characterization of Chitosan-coated Fe_3O_4 Nanoparticles using Ex-Situ Co-Precipitation Method and Tripolyphosphate/Sulphate as Dual Crosslinkers, IOP Conf. Ser. Mater. Sci. Eng. 299 (2018) 012064. https://doi.org/10.1088/1757-899X/299/1/012064.

[226] B. Khedri, K. Shahanipour, S. Fatahian, F. Jafary, Preparation of chitosan-coated

Fe_3O_4 nanoparticles and assessment of their effects on enzymatic antioxidant system as well as high-density lipoprotein/low-density lipoprotein lipoproteins on wistar rat, Biomed. Biotechnol. Res. J. 2 (2018) 68. https://doi.org/10.4103/BBRJ.BBRJ_98_17.

[227] S. Wang, Y. Tan, D. Zhao, G. Liu, Amperometric tyrosinase biosensor based on Fe_3O_4 nanoparticles–chitosan nanocomposite, Biosens. Bioelectron. 23 (2008) 1781–1787. https://doi.org/10.1016/j.bios.2008.02.014.

[228] J. Shin, K.Y. Lee, T. Yeo, W. Choi, Facile One-pot Transformation of FeOs from Fe_2O_3 Nanoparticles to Nanostructured Fe_3O_4@C Core-Shell Composites via Combustion Waves, Sci. Reports 2016 61. 6 (2016) 1–10. https://doi.org/10.1038/srep21792.

[229] T.I. Yang, R.N.C. Brown, L.C. Kempel, P. Kofinas, Magneto-dielectric properties of polymer–Fe_3O_4 nanocomposites, J. Magn. Magn. Mater. 320 (2008) 2714–2720. https://doi.org/10.1016/J.JMMM.2008.06.008.

[230] C. Baker, S.I. Shah, S.K. Hasanain, Magnetic behavior of iron and iron-oxide nanoparticle/polymer composites, J. Magn. Magn. Mater. 280 (2004) 412–418. https://doi.org/10.1016/J.JMMM.2004.03.037.

[231] J.L. Wilson, P. Poddar, N.A. Frey, H. Srikanth, K. Mohomed, J.P. Harmon, S. Kotha, J. Wachsmuth, Synthesis and magnetic properties of polymer nanocomposites with embedded iron nanoparticles, J. Appl. Phys. 95 (2004) 1439. https://doi.org/10.1063/1.1637705.

[232] Z. Zia, A. Hartland, M.R. Mucalo, Use of low-cost biopolymers and biopolymeric composite systems for heavy metal removal from water, Int. J. Environ. Sci. Technol. 17 (2020) 4389–4406. https://doi.org/10.1007/s13762-020-02764-3.

[233] J. Shen, I. Kaur, M.M. Baktash, Z. He, Y. Ni, A combined process of activated carbon adsorption, ion exchange resin treatment and membrane concentration for recovery of dissolved organics in pre-hydrolysis liquor of the kraft-based dissolving pulp production process, Bioresour. Technol. 127 (2013) 59–65. https://doi.org/10.1016/j.biortech.2012.10.031.

[234] E. Liu, X. Zheng, X. Xu, F. Zhang, E. Liu, Y. Wang, C. Li, Y. Yan, Preparation of diethylenetriamine-modified magnetic chitosan nanoparticles for adsorption of rare-earth metal ions, New J. Chem. 41 (2017) 7739–7750. https://doi.org/10.1039/C7NJ02177A.

[235] A.I. Zouboulis, I.A. Katsoyiannis, Arsenic Removal Using FeO Loaded Alginate Beads, Ind. Eng. Chem. Res. 41 (2002) 6149–6155.

https://doi.org/10.1021/IE0203835.

[236] J.H. Min, J.G. Hering, Arsenate sorption by Fe(III)-doped alginate gels, Water Res. 32 (1998) 1544–1552. https://doi.org/10.1016/S0043-1354(97)00349-7.

[237] S.F. Lim, Y.M. Zheng, S.W. Zou, J.P. Chen, Characterization of copper adsorption onto an alginate encapsulated magnetic sorbent by a combined FT-IR, XPS, and mathematical modeling study, Environ. Sci. Technol. 42 (2008) 2551–2556. https://doi.org/10.1021/ES7021889/SUPPL_FILE/REVISED_ES2007-021889_SUPPORTING_INFORMATION.PDF.

[238] A.S.A. Bakr, Y.M. Moustafa, M.M.H. Khalil, M.M. Yehia, E.A. Motawea, Magnetic nanocomposite beads: Synthesis and uptake of Cu(II) ions from aqueous solutions, Can. J. Chem. 93 (2014) 289–296. https://doi.org/10.1139/CJC-2014-0282/ASSET/IMAGES/LARGE/CJC-2014-0282CON.JPEG.

[239] B. Rouhi Broujeni, A. Nilchi, A.H. Hassani, R. Saberi, Preparation and characterization of chitosan/Fe_2O_3 nano composite for the adsorption of thorium (IV) ion from aqueous solution, Water Sci. Technol. 78 (2018) 708–720. https://doi.org/10.2166/WST.2018.343.

[240] Y.-C. Chang, D.-H. Chen, Preparation and adsorption properties of monodisperse chitosan-bound Fe_3O_4 magnetic nanoparticles for removal of Cu(II) ions, J. Colloid Interface Sci. 283 (2005) 446–451. https://doi.org/10.1016/j.jcis.2004.09.010.

[241] G.Z. Kyzas, E.A. Deliyanni, Mercury(II) removal with modified magnetic chitosan adsorbents, Molecules. 18 (2013) 6193–6214. https://doi.org/10.3390/molecules18066193.

[242] B. An, Q. Liang, D. Zhao, Removal of arsenic(V) from spent ion exchange brine using a new class of starch-bridged magnetite nanoparticles, Water Res. 45 (2011) 1961–1972. https://doi.org/10.1016/J.WATRES.2011.01.004.

[243] Y. Wanna, A. Chindaduang, G. Tumcharern, D. Phromyothin, S. Porntheerapat, J. Nukeaw, H. Hofmann, S. Pratontep, Efficiency of SPIONs functionalized with polyethylene glycol bis(amine) for heavy metal removal, J. Magn. Magn. Mater. 414 (2016) 32–37. https://doi.org/10.1016/J.JMMM.2016.04.064.

[244] H. Shi, J. Yang, L. Zhu, Y. Yang, H. Yuan, Y. Yang, X. Liu, Removal of Pb^{2+}, Hg^{2+}, and Cu^{2+} by chain-like Fe_3O_4@SiO_2@Chitosan magnetic nanoparticles, J. Nanosci. Nanotechnol. 16 (2016) 1871–1882. https://doi.org/10.1166/JNN.2016.10712.

[245] J. Meena, P. Singh Jassal, Phenol organic impurity remove from pollutants water by batch adsorption studies with using magneto chitosan nanoparticle, Anveshana's Int. J.

Res. Eng. Appl. Sci. 2 (2017). www.anveshanaindia.com (accessed July 21, 2022).

[246] J.K. Sahoo, A. Kumar, J. Rath, T. Mohanty, P. Dash, H. Sahoo, Guar gum-coated FeO nanocomposite as an efficient adsorbent for Congo red dye, Desalin. Water Treat. 95 (2017) 342–354. https://doi.org/10.5004/dwt.2017.21572.

[247] D. Pathania, S. Kumari, Nanocomposites Based on Biopolymer for Biomedical and Antibacterial Applications, ACS Symp. Ser. 1353 (2020) 375–391. https://doi.org/10.1021/BK-2020-1353.CH015.

Chapter-2

Materials and Methods

2.1 Overview

In the current study, co-precipitation was used to synthesize nanoparticles of the biopolymer nanocomposites carboxymethyl tamarind kernel gum/FeO and carboxymethyl tamarind kernel gum/Zinc oxide, which were then analysed for their structural, thermal, and conduction characteristics using XRD, FESEM, FTIR, and TGA. The preparation and characterization procedures used to create the bionanocomposite are described in detail in this chapter.

2.2 Materials

Carboxymethyl tamarind kernel gum was donated by Hindustan Gum and Chemicals Ltd. Bhiwani, Haryana, India. The powder was then sieved, and a particle size smaller than 40 mm was employed for further utilization. Before usage, this powder was dried in an oven maintained at 45°C for 24 hours. $FeCl_3 \cdot 6H_2O$, $FeSO_4 \cdot 7H_2O$, and ammonia were procured from Central Drug House Pvt. Ltd. New Delhi, India. Every solution used in the analysis was made in double-distilled water (DDW). To determine the antibacterial potential of synthesized nanocomposite against pathogenic bacteria, three bacteria cultures viz. *Pseudomonas aeruginosa, Escherichia coli,* and *Enterococcus faecalis* were provided by the Department of (Botany and Microbiology), Gurukul Kangri (Deemed to be University), Hardwar, Uttarakhand.

2.3 Synthesis of nanocomposites

2.3.1 Carboxymethyl tamarind kernel gum/FeO (CMTKG/FeO) nanocomposites

Carboxymethyl tamarind kernel gum/iron (CMTKG/FeO) nanocomposites were prepared by *in situ* co-precipitation method with some modifications. The co-precipitation approach is preferable to other methods because it is easier to use, speeds up formations, and makes it simple to manage particle size and composition [1]. This is an energy-efficient technique since it may be carried out at low temperatures, and also uses minimal organic solvents [2]. FeO nanoparticles were *in situ* synthesized by co-precipitation of ferrous and ferric salts in which 3.333g of $FeSO_4 \cdot 7H_2O$ and 6.479g of $FeCl_3 \cdot 6H_2O$ were dissolved in 150 mL double-distilled aqueous solution. After stirring for 45 min, chemical precipitation was achieved at

35°C by adding 20 mL of $NH_3 \cdot H_2O$ solution (25% v/v). At the time of reaction mechanisms, pH was maintained at about 10. The reaction system was kept at 60°C for one hour. The aqueous solution of CMTKG was obtained by dissolving 1g CMTKG in 150 mL DDW. This solution was then added dropwise into the obtained magnetic fluid in the flask and was followed by the addition of 2 mL epichlorohydrin while continuously stirring at 75°C for three hours. The residue obtained was washed with DDW to remove the unreacted chemicals and water-soluble impurities. Finally, the residue was washed with alcohol and dried at 50°C in a hot air oven.

2.3.2 Carboxymethyl tamarind kernel gum/zinc oxide (CMTKG/ZnO) nanocomposites

ZnO nanoparticles were created by co-precipitating zinc acetate in alcohol (10 mL), which was subsequently reduced to ZnO nanoparticles by adding 10 mL of 0.05 M NaOH solution. At 60°C, this solution was magnetically agitated continuously until it became homogeneous. A 150 mL aqueous solution in a conical flask containing 1 g of carboxymethyl tamarind kernel gum was added, and the combination was magnetically agitated at 60°C to produce viscous solutions. 150 mg of zinc solutions were added to this, and mixing continued until a 24-hour homogenous solution was obtained. Finally, a CMTKG/ZnO immobilized polymeric precipitate was produced. Following 20-minute centrifugation at 10,000 rpm to remove any remaining debased particles, the mixture was washed with acetone. The precipitate was then dried in the hot air oven at 50°C after being rinsed with C_2H_5OH. The prepared dry powder of biocomposites was put away in desiccators for further use.

2.3.3 Carboxymethyl tamarind kernel gum nanoparticles

In the conical flask, 1g carboxymethyl tamarind kernel gum was added with 150 mL double distilled water. In order to gain viscous solutions, the mixture was magnetically stirred at 40°C. Further, stirring continuously at 75°C for 24 hours and mixing until a clear solution was obtained. To remove any loose debased particles, the mixture was centrifuged at 10,000 rpm for 20 minutes and rinsed with acetone. The precipitate was then washed with C_2H_5OH and dried in a hot air oven at 50 °C. CMTKG was ground into a powder. This was stored in desiccators and cleaned with acetone to remove any loose debased particles before being used with different adsorption methods.

2.4 Characterization

The properties were characterized by Dynamic light scattering, Fourier-transform infrared spectroscopy, X-ray diffraction, Thermal Gravimetric Analysis, and UV-Visible spectroscopy. Furthermore, nanocomposites were explored for their potential applications as sensors for ammonia detection and antibacterial activity.

2.4.1 UV-Visible spectral studies

UV-Visible absorption spectra of an aqueous solution of nanocomposites and aqueous distributions. FeO nanoparticles were worked at room temperature using a Perkin Elmer Lambda 5 spectrophotometer along a 1cm optical path length. Change in Surface Plasmon Resonance (SPR) of nanocomposites in the dispersion was recorded using a UV-Vis spectrophotometer.

2.4.2 Fourier-transform infrared spectroscopy analysis

The infrared spectra (4000–400 cm^{-1}) of samples were analyzed on a Perkin Elmer FT-IR BX2 instrument. The pellets were synthesized by mixing 10 mg of the crystals sample with 200 mg of spectroscopic grade KBr.

2.4.3 X-ray diffraction studies

X-ray diffraction studies of synthesized nanocomposites were carried out using an X-ray diffractometer (P Analytical X'Pert Pro) at the current and voltage of 40 mA using Cu K α radiations (k = 1.5406 nm and λ=1.5406 Å) and Scanning angle 2θ in the range of 0-80^{o}. Nanoparticle size has been also calculated for nanocomposites using Debye –Scherrer equation [3] as follows.

$$D = \frac{K\lambda}{\beta\cos\theta}$$

Here k = 0.9 λ is the wavelength of the source (1.5Å), β is the full-width-at-half-maximum (FWHM), and θ is the direction of the angle.

2.4.4 SEM analysis

The SEM investigations of the products provide information on their morphology and size. The morphological features of nanocomposites were discovered using the FE-SEM (Model: JEOL JSM-6610LV, Hitachi, Japan). ImageJ software was used to determine the average size of Fe nanoparticles statistically.

2.4.5 High Resolution Transmission electron microscopy (HR-TEM) analysis

HR-TEM analysis was conducted by JEOL: JEM 2100 plus model. 5 mg of dry CMTKG nanoparticles were dissolved in 25 mL of C_2H_5OH and sonicated to mix the mixture. A copper grid that had been thoroughly covered with a 10 mL dispersion of nanoparticles (chloroform 1 percent arrangement of formvar in spectroscopic grade) was then dried in vacuum.

2.4.6 Thermal Gravimetric Analysis

Thermal Gravimetric Analysis (TGA) of nanocomposite were performed with 10°C/min of uniform heating rate and inert nitrogen atmosphere (25-900°C) using a Perkin Elmer Differential Thermal Analyser.

2.4.7 Dynamic light scattering

Dynamic light scattering (Zetasizer nano Z.S. Malvern Instruments Ltd) was utilized to detect the size distribution of particles by analysing dynamic fluctuations of light scattering intensity reasons by the Brownian velocity of the particles.

2.4.8 Sensing study for ammonia detection

The sensors studies of ammonia solution were executed by optical measurement. The ammonia sensing nature of CMTKG/FeO nanocomposite was investigated in an aqueous medium using the surface plasmon resonance (SPR). The sensing activity of synthesized nanocomposites was carried out using a 28% aqueous ammonia solution. Different concentration solutions of ammonia (1–100 ppm) were prepared (1 ppm, 10 ppm, 25 ppm, 50 ppm, 75 ppm and 100 ppm) using DDW just before analyzing samples. Ammonia sensing properties were investigated by surface plasma resonance property.

2.4.9 Antibacterial activity

Three antibiotic-resistant isolates of *Pseudomonas aeruginosa*, *Escherichia coli*, and *Enterococcus faecalis* from each bacterial species were chosen for this experiment. Following an agar well diffusion assay, the antibacterial activity was carried out according to the procedure. Measurements were made of the clear zone (in millimetres) surrounding the disc that represented the antibacterial activity. The activity was performed as per protocol following an agar well diffusion assay [4]. For positive control, gentamicin antibiotic was used.

2.4.10 Adsorption studies

The batch approach was used to conduct adsorption tests at room temperature (298–313 K) and a respectable fermentation rate. In a thermostatic water shower shaker for a duration of 10 to 100 minutes, various concentrations of CMTKG/ZnO biocomposite were equilibrated with 10 mL of chromium solution (10 to 50 mg/L). Through centrifugation and the residual convergence of chromium particles in the supernatant fluid, the adsorbent was separated from the solutions. It was looked at by using a UV spectrophotometer. The experiments were conducted at different chromium (VI) concentrations with a good adsorbent percent and variable contact durations for dynamic estimates. The impact of changing pH on adsorption was investigated in the pH range of 0–10. The pH of the liquids was altered by using a weaker HCl or NaOH setup (both 0.01 M). The assessments were administered repeatedly, and average characteristics were noted. The amount of chromium (VI) absorbed per unit mass of adsorbent (qe, mg. g^{-1}) was determined using the following criterion by Eq. (2.1):

$$\%Adsorption = \frac{C0-Ct}{C0} \tag{2.1}$$

The equilibrium was calculated using the formula given in Eq. (2.2):

$$\mathrm{qe} = C0 - Ct \times \frac{v}{w} \tag{2.2}$$

where q_e is the balance limit of chromium (VI) on the adsorbent (mg g^{-1}), C0 is the underlying convergence of chromium (VI) (mg L^{-1}), Ce is the balance grouping of chromium (VI) (mg L^{-1}), V is the volume of chromium (VI) utilized (L) and W is the heaviness of adsorbent (g) utilized.

2.4.11 Antifungal activity determination

Utilizing MTCC2799, which is the minimal concentration of the sample needed to inhibit % of the fungus *Aspersilium flamous*, the antifungal activity of CMTKG/ZnO nanocomposites was assessed. A stronger antifungal impact was assumed to exist in every sample with a lower MTCC-2799 score. The positive control was amphotericin B.

2.4.12 DPPH scavenging activity

The ability of carboxymethyl tamarind kernel gum to scavenge 2,2-diphenyl-2-picrylhydrazyl (DPPH) free radicals was investigated [5,6]. The DMSO was diluted to 1 mg/mL using the CMTKG stock solution. Diluted solutions (1 mL each) were coupled with DPPH (3 mL), as shown in Figure 6.2. The absorbance was measured at 517 nm after 30 minutes in the dark at room temperature, much like the control samples [7].

The % inhibition was calculated using the formula below (Eq. 2.3):

$$\text{Inhibition } \% = \frac{\text{Absorbace of Blank} - \text{Absorbance of sample}}{\text{Absorbance of Blank}} \times 100 \qquad (2.3)$$

Reference

[1]. Lagrow, A. P.; Besenhard, M. O.; Hodzic, A.; Sergides, A.; Bogart, L. K.; Gavriilidis, A.; Thanh, N. T. K. Unravelling the Growth Mechanism of the Co-Precipitation of FeO Nanoparticles with the Aid of Synchrotron X-Ray Diffraction in Solution. *Nanoscale* **2019**, *11* (14), 6620–6628. https://doi.org/10.1039/c9nr00531e.

[2]. Rane, A. V.; Kanny, K.; Abitha, V. K.; Thomas, S. *Methods for Synthesis of Nanoparticles and Fabrication of Nanocomposites*; Elsevier Ltd., 2018. https://doi.org/10.1016/b978-0-08-101975-7.00005-1.

[3].Holzwarth, U.; Gibson, N. The Scherrer Equation versus the "Debye-Scherrer Equation." *Nature Nanotechnology* **2011**, *6* (9), 534. https://doi.org/10.1038/nnano.2011.145.

[4]. Devillers, J.; Steiman, R.; Seigle-Murandi, F. The Usefulness of the Agar-Well Diffusion Method for Assessing Chemical Toxicity to Bacteria and Fungi. *Chemosphere* **1989**, *19* (10–11), 1693–1700. https://doi.org/10.1016/0045-6535(89)90512-2.

[5].Shukla, R. K.; Kishan; Shukla, A.; Singh, R. Evaluation of Nutritive Value, Phytochemical Screening, Total Phenolic Content and in-Vitro Antioxidant Activity of the

Seed of Prunus Domestica L. *Plant Science Today*. 2021, pp 830–835. https://doi.org/10.14719/PST.2021.8.4.1231.

[6].Chandra, H.; Patel, D.; Kumari, P.; Jangwan, J. S.; Yadav, S. Phyto-Mediated Synthesis of Zinc Oxide Nanoparticles of Berberis Aristata: Characterization, Antioxidant Activity and Antibacterial Activity with Special Reference to Urinary Tract Pathogens. *Materials Science and Engineering C* **2019**, *102* (March), 212–220. https://doi.org/10.1016/j.msec.2019.04.035.

[7].Pirsa, S.; Farshchi, E.; Roufegarinejad, L. Antioxidant/Antimicrobial Film Based on Carboxymethyl Cellulose/Gelatin/TiO2–Ag Nano-Composite. *Journal of Polymers and the Environment* **2020**, *28* (12), 3154–3163. https://doi.org/10.1007/s10924-020-01846-0.

Chapter-3

Scope of work

3.1 Rationale of work

Numerous plant-derived materials are gaining relevance in the fields of medicine and biotechnology every day, due to their abundant availability in nature, eco-friendly, renewable, and sustainable extraction facility, as well as their reduced cost. Natural gums generated from plants have lately made a name for themselves as biopolymers thanks to their biosafety, biodegradability, and low cost of manufacturing using renewable natural resources. Natural polysaccharides that come from plants are called plant-derived gums. These macromolecular structures have a wide range of physiological properties because they are made up of several sugar units that are attached to one another.

Among the many polysaccharides generated from plants, tamarind kernel gum is a potential biopolymer. It is made from the endosperm of tamarind seeds and is frequently referred to as tamarind kernel gum. It is widely used as a polymer in a wide range of applications, including those in the chemical engineering, pharmaceutical, cosmetic, food, paper, and textile industries. In recent years, tamarind kernel gum has been investigated and used as an advantageous excipient in a number of dosage forms for better medication delivery. Despite being widely employed in a variety of biomedical applications, such as its large spectrum of uses in pharmaceutical formulations as excipients, tamarind gum has certain potential disadvantages. The native tamarind kernel gum has a foul smell and a dismal appearance. Additionally, it has low water solubility. In particular, tamarind kernel gum frequently shows the presence of water-insoluble components and has a propensity for breaking down quickly in watery environments. To get over these limitations, functional groups—modifications of different functional groups found in polymer structures—such as carboxymethyl have been included into tamarind kernel gum by chemical modification.

In comparison to native gums, carboxymethylated gums often show improved hydrophilicity and clarity of solutions. The native gum's prospective features enhancements increase its solubility in aqueous media. Tamarind kernel gum that has been carboxymethylated is found to be more enzymatically and microbially resistant than natural gum. In aqueous conditions, carboxymethyl tamarind kernel gum has a greater viscosity and a slower rate of degradation.

The increase in biopolymers-based nanocomposites is receiving scientific attention as a result of the current population, climate change, and industrial pursuits. Recently, interest has been drawn to the use of various biopolymers and their nanocomposites in the development of innovative applications from the standpoint of the environment. Since most biopolymers are biodegradable and made from renewable resources, they don't have a detrimental effect on the environment. According to a review of the literature, several metal and metal oxide nanoparticles have drawn a lot of interest by improving the characteristics of the biopolymer matrix. Metallic nanoparticles can give the biopolymers additional electrical conductivity, catalytic activity, and plasmonic features in terms of functionality. Additionally, due to their improved aqueous processability and dispersibility within biopolymer matrices, metal oxide nanoparticles can be potentially used.

Based on the aforementioned information and further research on natural polymer-based functional materials for biomedical applications, carboxymethyl tamarind kernel gum-metal nanocomposites were synthesized in this work. These nanocomposites were investigated using FTIR, XRD, SEM, TEM, TGA, DTA, and DLS. They were used for their biosensing, antimicrobial, antifungal, metal removal, anti-oxidant, and anti-fouling capabilities.

Biocomposite, based on biopolymer- carboxymethyl tamarind kernel gum embedded with iron and zinc oxide nanoparticles has not yet reported in the literature before to the best of my knowledge.

3.2 Research objectives

The primary goal of this research is to fabricate novel formulations of carboxymethyl tamarind kernel gum-metal nanocomposites using the in situ co-precipitation method. These formulations will be used for their antimicrobial, antifungal, metal removal, anti-oxidant, and anti-fouling properties.

Main study objectives are enlisted below:

To prepare and optimize carboxymethyl tamarind kernel gum /FeO nanocomposites, as well as an evaluation of their potential applications for ammonia sensor activity and antimicrobial activity.

To prepare and optimize carboxymethyl tamarind kernel gum/ZnO nanocomposites, characterization of these materials, application of their antifungal properties, and removal of Cr metal from contaminated water.

To prepare and optimize carboxymethyl tamarind kernel gum nanoparticles, characterize them through testing, and use them for their anti-oxidant and anti-fouling properties.

3.3 Plan of work

(i) Literature review

(ii) Defining key objectives

(iii) Formulation of carboxymethyl tamarind kernel gum/ZnO nanocomposites by co-precipitations method (*in situ* generation)

(iv) Formulation of carboxymethyl tamarind kernel gum/FeO nanocomposites by co-precipitations method (*in situ* generation)

(v) Following the preparation of the nanocomposites, synthesized nanocomposites will be subjected to the following characterization techniques:

a) Structural analysis by Fourier-transform infrared spectroscopy (FTIR) spectroscopy and X-ray diffraction (XRD)

b) Surface morphological analysis by Scanning Electron Microscopy (SEM) and Transmission Electron Microscopy (TEM)

c) Thermal analysis by Thermogravimetric Analysis (TGA) and Differential Thermal Analysis (DTA)

d) Dynamic Light Scattering (DLS)

(vi) After preparing nanocomposites, they are subjected to various biological chemical activities, such as antioxidant, antibacterial, antifungal, antifouling, ammonia sensor, and hazardous metal removal from contaminated water.

Chapter-4

Synthesis and characterizations of carboxymethyl tamarind kernel Gum/FeO nanocomposites, its application in liquid ammonia sensing and antimicrobial activity

4.1 Introduction

Metal nanoparticles have been widely employed to develop gas sensors that can detect a wide range of gases, due to their superior electrical and morphological characteristics and high surface-to-volume ratio. Due to its numerous uses in nano-fields including ferrofluids [1–3], magnetocaloric refrigeration [4], biotechnology [5,6], and in vivo bio-medical sector [7], super-paramagnetic FeOs have undergone substantial research in recent years. These materials have a number of potential biomaterial uses in magnetically controlled drug administration [8–10], magnetic resonance imaging [11,12], tissue healing [13,14], gene [15], biosensing [16], immunoassays [17], RNA and DNA purification [18], antioxidant activity, cellular, and genotoxicity [19] and enzyme immobilization [20], agriculture [21] and gas sensing [22]. Numerous sectors, including catalysis [23–25], environmental protection [26,27], clinical diagnostics [28,29], and therapy [30–32], have conducted substantial research on it (Jordan et al., 2003).

Magnetic oxide nanoparticles have various topologies, such as nanotubes [33,34], nanowires [35–37], nanorods [38–41], and nanocomposites [42–44], which have also been synthesized. Several techniques have been proposed for the synthesis of metal nanoparticles, including electrochemical [45], microemulsions [46], flow injection [47], sonochemical method [48], biosynthesis [49], chemical (sol-gel) [50], hydrothermal reverse micelle [51], template method [52], co-precipitation [53], etc.), and mechanical-chemical (laser ablation arc [54], combustion [55], discharge [56], electrodeposition [57], and pyrolysis [58]) methods.

The need for natural polysaccharides in place of synthetic biopolymers in many biomedical fields is becoming more and more popular as a result of the socioeconomic environment of the modern world [59–61]. A common class of natural bio-polysaccharides that are non-toxic, biodegradable, less costly, and readily available in the environment are plant polysaccharides [62]. Plant polysaccharides are increasingly playing a proactive role in enhancing the

performance of drugs in terms of stability, drug release, target specificity, and bioavailability [63,64]. One such derivative of tamarind kernel gum, which is produced from the kernel of *Tamarindus indica*, is carboxymethyl tamarind kernel gum (CMTKG). CMTKG is made up of a β-D-glucan backbone chain with β-D-galactopyranosyl and α-D-xylopyranose side chains connected to glucose [65,66]. This finds applications [67] as antimicrobial activity [68], antioxidant activity, anti-fouling activity, and adsorption for various organic/inorganic impurities from wastewater. CMTKG is hydrophilic and capable of absorbing different aqua solutions. The carboxymethyl group increases viscosity and confers resistance to enzymatic processes on the molecule [69]. Due to their capacity to function as reducing agents, regulate particle development, and stabilize the particles, they are garnering interest as matrix materials for immobilizing nanoparticles and producing biogenic nanomaterials with novel or better features [70].

Semiconducting metal oxide chemical sensors have recently piqued the interest of ecologists, technologists, environmentalists, and others due to environmental pollution and unintentional leaking of harmful gases and liquids [71–73]. Due to its hazardous and contaminating characteristics, ammonia is one of the industrial gases in liquid form that is of interest [74]. Its global output exceeds 100 million tonnes annually because of its many uses, which include the creation of nitrogenous fertilizers and other nitrogenous compounds as well as an industrial refrigerant [75,76]. If severely concentrated, it might cause serious burns to our skin, eyes, throat, or lungs, which could result in lung illness and irreversible blindness [77,78]. Therefore, it is desirable to identify and monitor the presence of ammonia as early as possible in a wide variety of commercial applications.

To analyze the gaseous ammonia concentration, various sensors based on organic and metal-oxide conducting polymer films have been made [79–81]. Although efficient, these sensors are unable to detect the concentration of ammonia in liquid form. The nanoparticles used as sensors often show alteration in the dielectric constant of the surrounding medium by altering the solvent or by complex development at the surface of nanoparticles.

Metal oxide nanostructures have been used in several sensing studies for the detection of different substances, including hydrazine, acetone, ethanol, etc [82,83]. The features of the thin films created by the physisorption and chemisorption procedures are mostly used in the chemical sensing by metal oxide thin films. The present modifications of the manufactured thin films brought on by the chemical elements of the reacting system in an aqueous medium

serve as the basis for chemical detection. In the current study, we attempted to develop well-dispersed CMTKG/FeO nanocomposites by in situ co-precipitation technique and investigated their potential use as sensors for ammonia detection. The potential of the synthesized nanocomposite was also investigated for antibacterial activity against urinary tract isolates such as *Pseudomonas aeruginosa*, *Escherichia coli*, and *Enterococcus faecalis*.

4.2. Experimental

4.2.1 Materials

Carboxymethyl tamarind kernel gum (CMTKG) was donated by Hindustan Gum and Chemicals Ltd. Bhiwani, Haryana, India. The powder was then sieved, and a particle size smaller than 40 mm was employed for further utilization. Ferric Chloride Hexahydrate ($FeCl_3 \cdot 6H_2O$),Epichlorohydrin(C_3H_5ClO) Ferrous Sulphate Heptahydrate ($FeSO_4 \cdot 7H_2O$), and ammonia (NH_3) were procured from Central Drug House Pvt. Ltd. New Delhi, India. Every solution used in the analysis was made in double-distilled water (DDW). To determine the antibacterial potential of synthesized nanocomposite against pathogenic bacteria, three bacteria cultures viz. *Pseudomonas aeruginosa, Escherichia coli,* and *Enterococcus faecalis* were provided by the Department of (Botany and Microbiology), Gurukul Kangri (Deemed to be University), Hardwar, Uttarakhand.

4.2.2 Preparation of carboxymethyl tamarind kernel gum/FeO (CMTKG/FeO) nanocomposites

CMTKG/FeO nanocomposites were prepared by *in situ* co-precipitation method with some modifications. The co-precipitation approach is preferable to other methods because it is easier to use, speeds up formations, and makes it simple to manage particle size and composition [84]. This is an energy-efficient technique since it may be carried out at low temperatures, and also uses minimal organic solvents [85]. FeO nanoparticles were *in situ* synthesized by co-precipitation of ferrous and ferric salts in which 3.333g of $FeSO_4 \cdot 7H_2O$ and 6.479g of $FeCl_3 \cdot 6H_2O$ were dissolved in 150 mL double-distilled aqueous solution. After stirring for 45 min, chemical precipitation was achieved at 35°C by adding 20 mL of ammonia solution (25% v/v). At the time of reaction mechanisms, pH was maintained at about 10. The reaction system was kept at 60°C for one hour. The aqueous solution of CMTKG was obtained by adding 1g CMTKG in 150 mL DDW. This solution was then added dropwise into the obtained FeO fluid in the flask and was followed by the addition of 2 mL epichlorohydrin while continuously stirring (300 rpm) using magnetic stirrer at 75°C for

three hours. The residue obtained was washed with DDW to remove the unreacted chemicals and water-soluble impurities. Finally, the residue was washed with alcohol and dried at 50℃ in a hot air oven for 10 to 20 minutes.

4.2.3 Characterization

The synthesized nanocomposite was characterized by Dynamic light scattering, Fourier-transform infrared spectroscopy, X-ray diffraction, Thermal Gravimetric Analysis, and UV-Visible spectroscopy. Furthermore, nanocomposites were explored for their potential applications as sensors for ammonia detection and antibacterial activity.

4.2.3.1 UV-Visible spectral studies

UV-Visible absorption spectra of an aqueous solution of CMTKG/FeO nanocomposites and aqueous distributions. FeO nanoparticles were subjected to test at room temperature using a Perkin Elmer Lambda 5 spectrophotometer along a 1cm optical path length. Change in Surface Plasmon Resonance (SPR) of nanocomposites in the dispersion was recorded using a UV-Vis spectrophotometer.

4.2.3.2 Fourier-transform infrared spectroscopy analysis

The infrared spectra (4000–400 cm^{-1}) of samples were analysed on a Perkin Elmer FT-IR BX2 instrument. The pellets were prepared by mixing 10 mg of the crystals sample with 200 mg of spectroscopic grade KBr.

4.2.3.3 X-ray diffraction studies

X-ray diffraction studies of prepared CMTKG/FeO nanocomposites were carried out using an X-ray diffractometer (P Analytical X'Pert Pro) at the current and voltage of 40 mA using Cu K α radiations (k = 1.5406 nm and λ=1.5406 Å) and Scanning angle 2θ in the range of 0-80^{o}. Nanoparticle size has been also calculated for FeO nanoparticles using Debye –Scherer equation [86] as follows.

$$D = \frac{K\lambda}{\beta\cos\theta}$$

Here k = 0.9 λ is the wavelength of the source (1.5Å), β is the full-width-at-half-maximum (FWHM), and θ is the direction of the angle.

4.2.3.4 SEM analysis

The SEM investigations of the products provide information on their morphology and size. The morphological features of CMTKG/ FeO nanocomposites were discovered using the FE-SEM (SU8010, Hitachi, Japan). ImageJ software was used to determine the average size of Fe nanoparticles statistically.

4.2.3.5 Thermal Gravimetric Analysis

Thermal Gravimetric Analysis (TGA) of CMTKG and CMTKG/ FeO nanocomposite were performed with 10°C/min of uniform heating rate and inert nitrogen atmosphere (25-900°C) using a Perkin Elmer Differential Thermal Analyzer.

4.2.3.6 Dynamic light scattering

Dynamic light scattering (Zetasizer nano Z.S. Malvern Instruments Ltd) was utilized to detect the size distribution of particles by analyzing dynamic fluctuations of light scattering intensity reasons by the Brownian velocity of the particles. For the purpose of analysis, CMTKG aqueous solution from the co-precipitation method of in situ Fe-O nanoparticles was utilized.

4.2.3.7 Sensing study for ammonia detection

The sensing studies of ammonia solution were executed by optical measurement. The ammonia sensing nature of CMTKG/FeO nanocomposite was investigated in an aqueous medium using the surface plasmon resonance (SPR). The sensing activity of synthesized CMTKG/ FeO nanocomposites was carried out using a 28% aqueous ammonia solution. Different concentration solutions of ammonia (1ppm, 10 pmm, 25 ppm, 50ppm, 75 ppm and 100 ppm) were prepared using DDW just before analyzing samples. Ammonia sensing properties were investigated by surface plasma resonance property.

4.2.3.8 Antibacterial activity

Three antibiotic-resistant isolates of *Pseudomonas aeruginosa*, *Escherichia coli*, and *Enterococcus faecalis* from each bacterial species were chosen for this experiment. Following an agar well diffusion assay, the antibacterial activity was carried out according to the procedure. Measurements were made of the clear inhibition zone (in millimetres) surrounding the disc that represented the antibacterial activity. The activity was performed as per protocol

following an agar well diffusion assay [87]. For positive control, gentamicin antibiotic was used.

4.3. Results and discussions

4.3.1 Evaluation of CMTKG/ FeO nanocomposites

The optical property of FeO nanoparticles is determined by recording the absorbance of the synthesized nanocomposites using a UV-visible spectrophotometer. Figure 4.1 shows the UV-visible absorption spectrum of CMTKG/FeO nanocomposites. The range shows the shifting of the peak positions of the majority-Fe absorption towards a low wavelength of 354 nm, indicating the existence of FeO nanoparticles. Due to their strong Surface Plasmon Resonance (SPR) band transition, CMTKG/ FeO nanocomposites were able to absorb light in the visible spectrum between 200 and 600 nm. Additionally, similar outcomes have been reported by Devi et al. (2019).

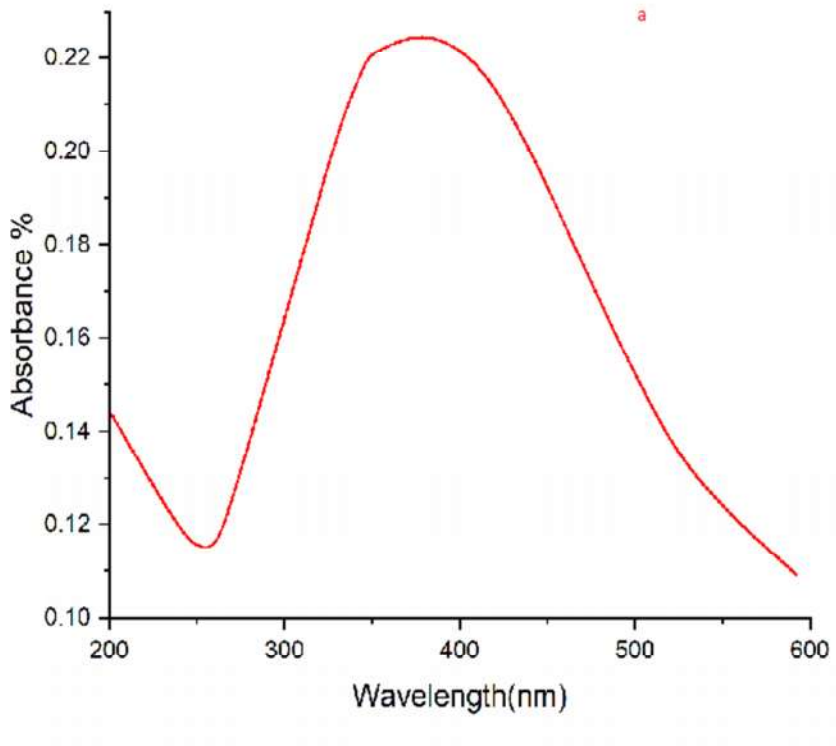

Figure 4.1: UV–Visible absorption spectra CMTKG/FeO nanocomposites

4.3.2 FTIR analysis

FTIR spectra bands of CMTKG and CMTKG/ FeO are shown in Figure 4.2. CMTKG demonstrates a characteristic large absorption peak at 3424 cm^{-1} for -OH stretching vibrations. The absorption at 2926 cm^{-1} correlates to C-H stretching vibrations. The absorption at 1632 cm^{-1} is due to –COO- symmetric vibrations, and at 1408 cm^{-1} and 1112 cm^{-1} because of O-H bending and C-O stretching vibrations, respectively.

CMTKG/FeO showed a broad absorption band at 3329 cm^{-1} and 3421 cm^{-1} correlating –OH stretching vibration, the absorption peak at 1628 cm^{-1} corresponds to –COO- symmetric vibrations. The vibrations observed at 1397 cm^{-1} and 1290 cm^{-1} were due to O-H bending and C-O stretching, respectively, and at 3116 cm^{-1} due to C–H stretching vibrations. The spectrum also has a band at 751 cm^{-1} suggesting Fe-O ions vibrations [30]. All the peaks of CMTKG were found also in CMTKG/FeO nanocomposite with a slight shift. While the presence of a new peak at 715 cm^{-1} confirms the presence of CMTKG – Fe interaction. Besides this, the slight change in the intensity of adsorptions bands between (1112 and 1290) cm^{-1} also confirms the interaction between CMTKG and Fe ions.

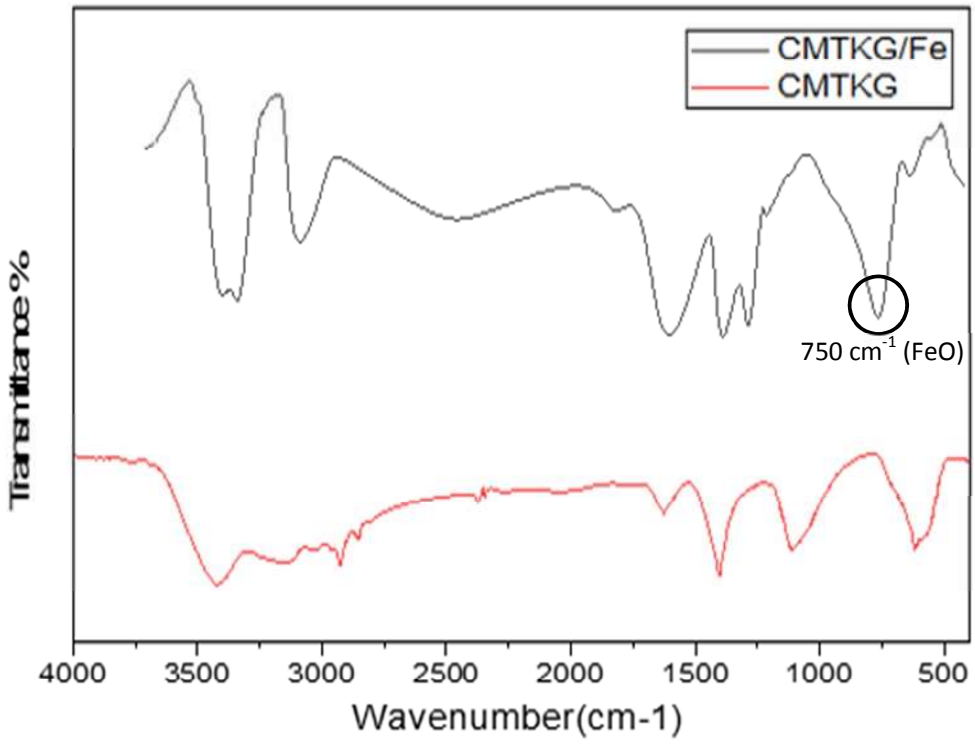

Figure 4.2: FTIR spectra of CMTKG and CMTKG/FeO

4.3.3 XRD Analysis

X-ray patterns of CMTKG and CMTKG/FeO nanocomposite are shown in Figure 4.3. XRD analysis of CMTKG and CMTKG/ FeO have been studied to see the crystalline nature of both nanoparticles. XRD of the CMTKG and CMTKG/FeO show almost similar patterns having sharp peaks. However, CMTKG/FeO shows sharper peaks in comparison to CMTKG. This confirms the interaction of Fe with CMTKG in CMTKG/ FeO nanocomposite. A similar observation has been reported in the literature [88].

The average size of CMTKG/FeO nanocomposite was calculated from Debye Scherrer equation.

$$D = \frac{K\lambda}{\beta\cos\theta}$$

Here k=0.9 λ is the wavelength of source (1.5Å), β is the FWHM, and θ is the direction of the angle. The average size of CMTKG/FeO nanocomposite was found of 42.50 nm.

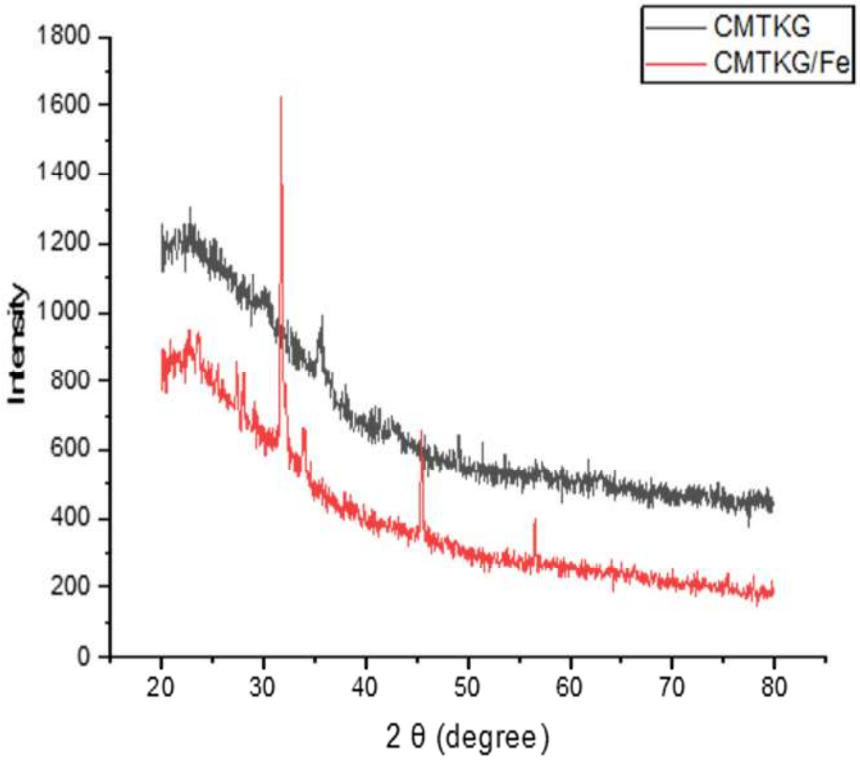

Figure 4.3: X-Ray Diffraction spectra of CMTKG and CMTKG/ FeO nanocomposite

4.3.4 Morphological characterization

SEM micrographs of CMTKG and CMTKG/FeO nanocomposite are shown in Figure 4.4. SEM provides a beneficial report about the particle size and polydispersity profile. The change in the SEM micrographs of the composite before and after the incorporation of Fe_3O_4 indicates the structural changes in the synthesized nanocomposite. The CMTKG and CMTKG/ FeO nanoparticles were shown to have uniform spherical sizes in a disorderly distribution. ImageJ software was used to determine the average size of FeO nanoparticles statistically. The particle size was determined to be 60–90 nm. Identical results were also reported by Ahmad and co-workers (2009) [89].

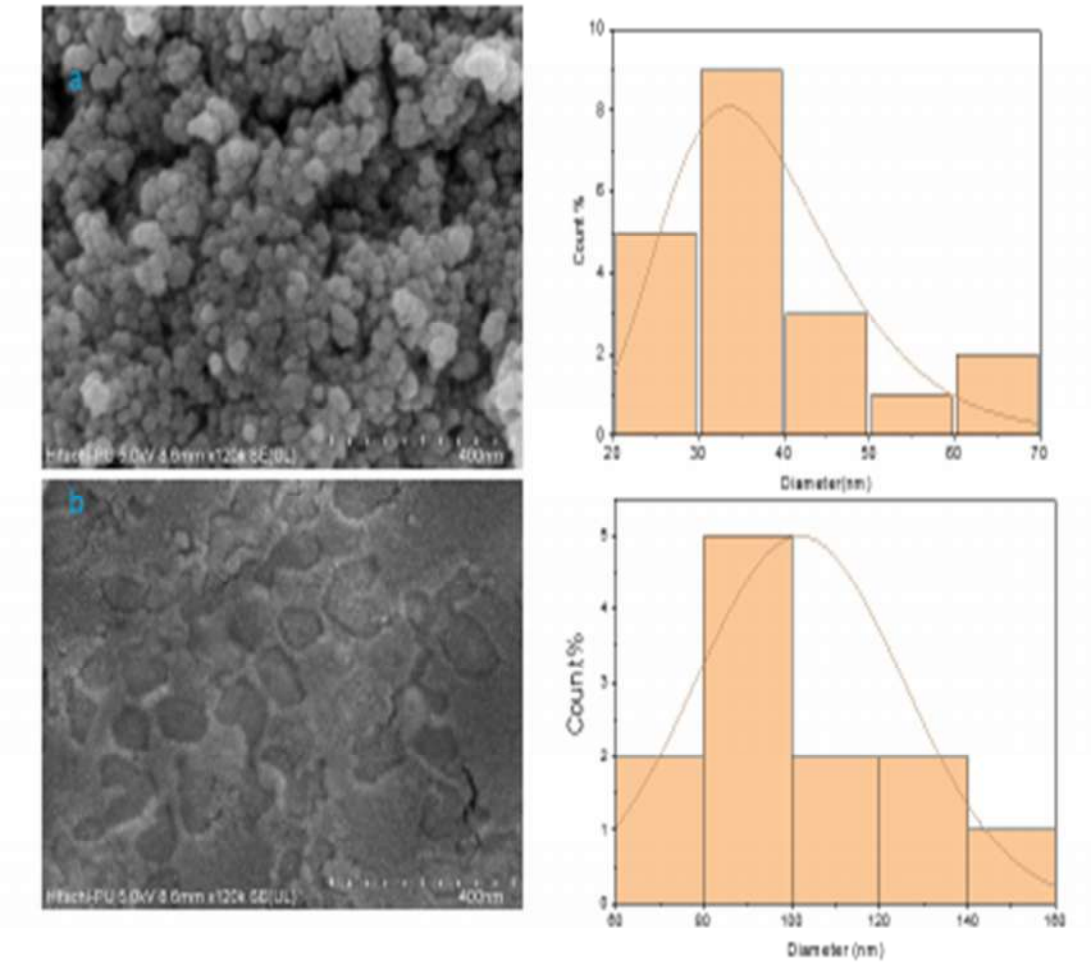

Figure 4.4: SEM micrograph and particle size determination of (a) CMTKG and (b) CMTKG/ FeO nanocomposite

4.3.5 Thermo gravimetric analysis

The thermic co-tension of synthesized CMTKG/ FeO nanocomposite is found to be more than CMTKG. Hence, to confirm this property, a comparison of the thermal analysis was conducted. The thermogram of CMTKG and CMTKG/ FeO weight loss was analyzed in three distinguished stages, as shown in Figure 4.5. The weight reduction of 5.76%, at the beginning stage (32–160°C) is characteristic of the expulsions of moisture from the biopolymer. The second stage of weight loss (190–420°C) could be because of the biopolymer backbone reductions, and dissolutions of carboxymethyl and hydroxyl functional groups of CMTKG with 30.60% weight loss. This was pursued by the 3rd stage of degradation (653–725°C) with 3.96% weight loss. The weight decrease was reported in three positions for CMTKG/FeO nanocomposite as well. The 1st region (190–340°C) was due to the reduction of refuse cross-linker. The weight loss of 24.45% for the 2^{nd} region (390–580°C) is the characteristic of biopolymers' degradation. The 3rd stage (675–860 °C) was found with 4.30% of weight loss. However, CMTKG/FeO nanocomposite showed higher mass % until they touched 400°C in comparison to the CMTKG. Similarly, at 900°C, the CMTKG/ FeO nanocomposite recorded greater than 35% of residual mass compared to CMTKG which showed 20% of the residual mass. As a result, it was determined that the thermal stability of CMTKG/FeO nanocomposite was significantly higher than that of the CMTKG. The same findings were also reported by Khushbu and the team (2019) [90].

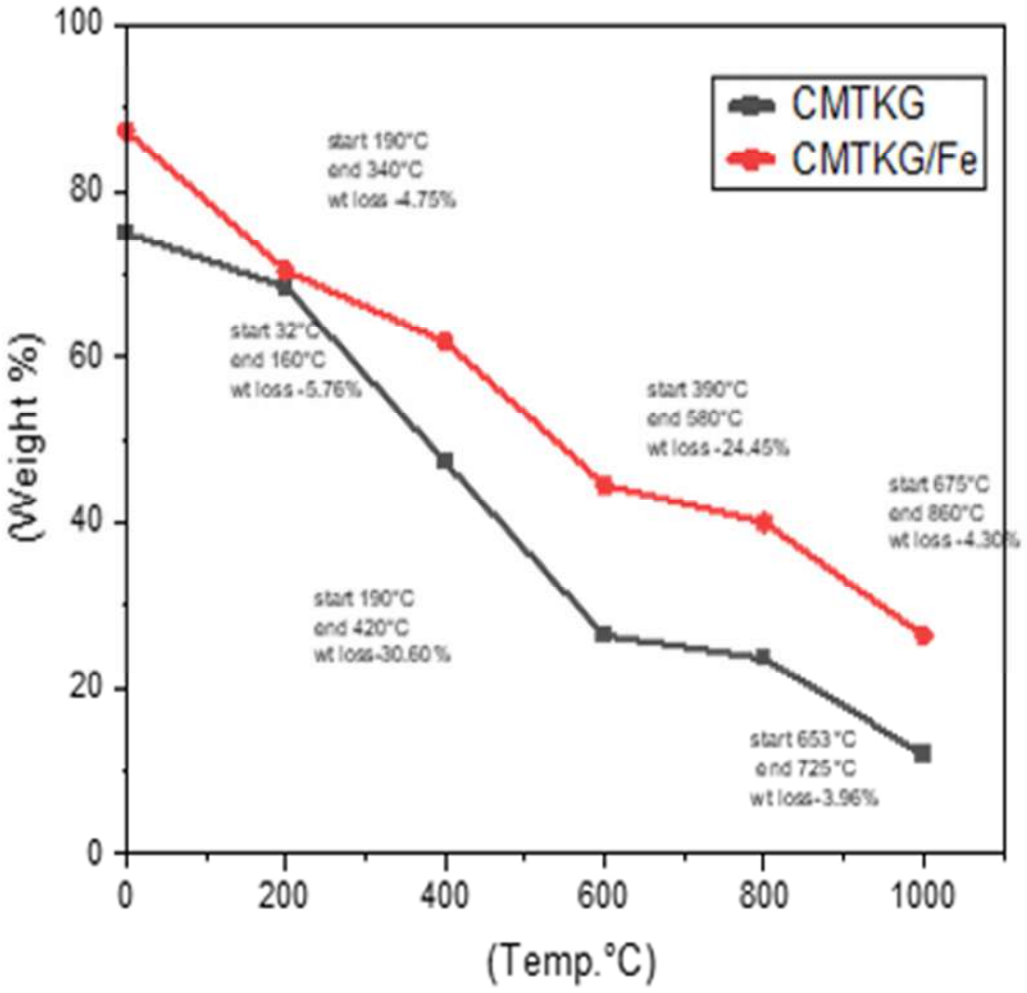

Figure 4.5: Thermal gravimetric analysis of CMTKG and CMTKG/FeO nanocomposite

4.3.6 Dynamic light scattering analysis

The DLS technique was employed to study the particle size of synthesized Fe-O nanoparticles. The size dissemination of the green synthesized Fe-O nanoparticles is presented in Figure 4.6. Findings evidently acknowledge that most of the particles show size dissemination from ~60 to ~90 nm with the highest size dissemination at about 75 nm [91].

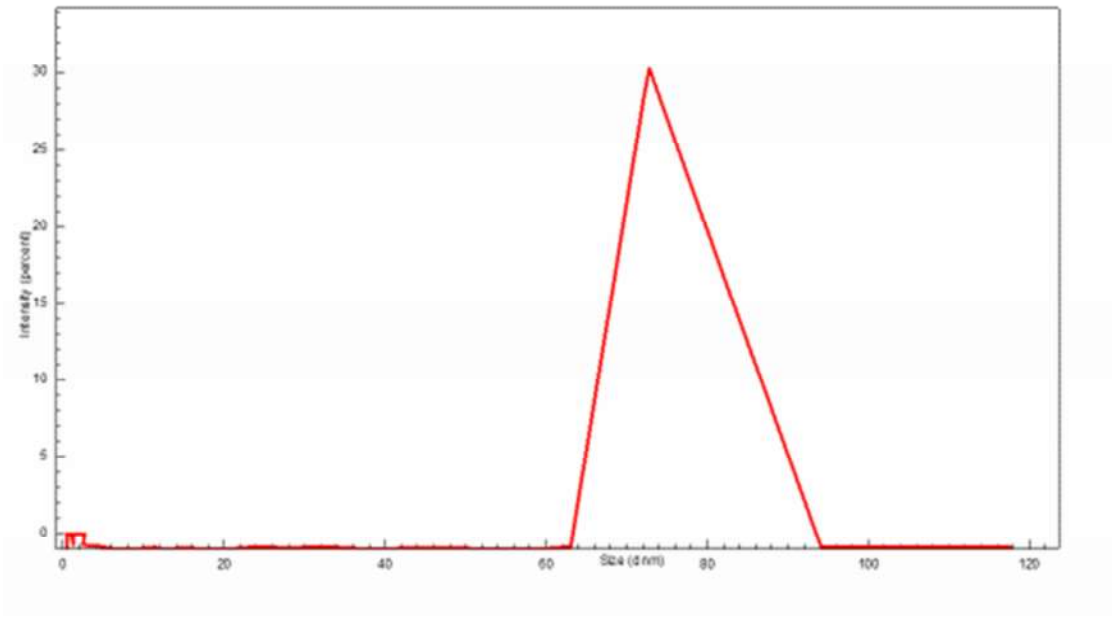

Figure 4.6: DLS analysis of Fe-O nanoparticles

4.3.7 Potential applications of developed CMTKG/FeO nanocomposite

4.3.7.1 Ammonia sensing performance

The sensing ability of CMTKG/ FeO nanocomposite in numerous ammonia concentrations at room temperature is depicted in Figure 4.7. The changes in absorbance spectra for the various concentration of ammonia were monitored using a UV-Vis spectrophotometer and the same was observed to increase from 1 to 100 ppm of ammonia concentration. For each measurement, fresh CMTKG/FeO nanocomposite colloidal solutions were combined with various ammonia solutions. The results revealed the shift of Surface Plasmon Resonance peak intensity from 313 nm to 331 nm with the subsequent rise in ammonia concentration. This spectral shift may be attributed to the changes in inter particles range and shifts in the dielectric constant of the medium [92]. The complex that forms on the surface of the nanocomposites may be the cause of the change in absorption intensity that occurs after adding them to the ammonia solution.

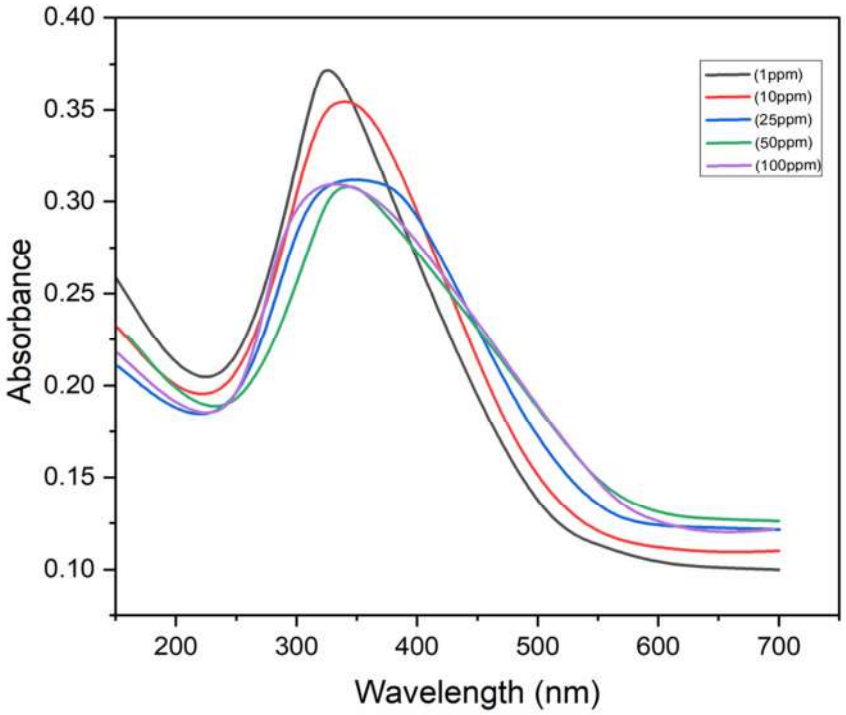

Figure 4.7: Spectral absorbance of CMTKG/FeO nanocomposite as a function of numerous ammonia concentrations

4.3.7.2 Antibacterial activity

In the present investigation, CMTKG/FeO nanocomposites were evaluated for the exploration of their antimicrobial activity against 3 pathogenic bacteria viz. *Escherichia coli, Pseudomonas aeruginosa,* and *Enterococcus faecalis*. The polysaccharide nanocomposite containing in situ produced FeO nanoparticles and CMTKG as a reducing and capping agent demonstrated antibacterial efficacy against *Enterococcus faecalis* with a zone of inhibition of 12.4 ±0.5 mm, as shown in Table 4.1. The inspection showed no significant differences in antibacterial activity against *Escherichia coli* and *Pseudomonas aeruginosa* (Figure 4.8).

Table 4.1: Antibacterial activity of nanocomposite against pathogenic bacteria

Test organism	Zone of inhibition in mm		
	Nanocomposite	**Gentamicin (30µg)**	**DMSO**
Enterococcus faecalis(A)	12.4 ± 0.5	NA	NG
Escherichia coli(B)	NA	15.2 ± 0.4	NG
Pseudomonas aeruginosa(C)	NA	9.0 ± 0.1	NG
NA: No Activity **NG:** No Growth			

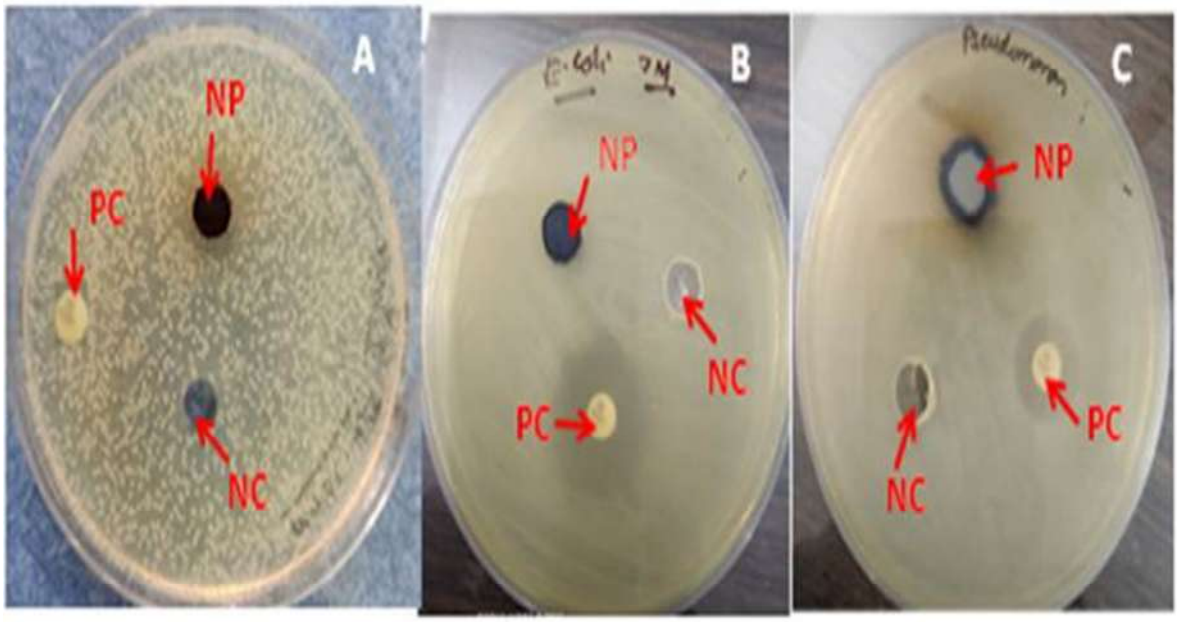

Figure 4.8: Antibacterial activity of CMTKG/FeO nanocomposites (NP: Nanocomposites, PC: Positive Control, NC: Negative Control)

4.4 Conclusion

Nanocomposite polysaccharides with in situ generated FeO nanoparticles were prepared using $Fe_2O_3.7H_2O$ and $FeCl_3 \cdot 6H_2O$ solutions as the source and CMTKG as the reducing and capping agent by co-precipitations method. The scanning electron microscopy, X-ray spectral analysis, and DLS analysis indicated the generation of spherical CMTKG/FeO

nanocomposites in the average size in the range of 40-90 nm. The thermal stability of CMTKG/ FeO nanocomposites was found significantly higher than that of the CMTKG.

These nanocomposites exhibited excellent antibacterial activity against both *Enterococcus faecalis* and hence can be considered for applications in antibacterial textiles for personal and hospital uses. The sensor properties of the synthesized nanocomposite solution across rising ammonia concentrations in the range of 1–100 ppm by observing the changes in SPR situations and magnitude with a UV-Visible Spectrophotometer have been notified. Eventually, CMTKG/FeO nanocomposites show promising ammonia sensing properties. This research expands the potential uses of CMTKG/FeO nanocomposites on a broad scale.

References

[1] R.Y. Hong, T.T. Pan, H.Z. Li, Microwave synthesis of magnetic Fe3O4 nanoparticles used as a precursor of nanocomposites and ferrofluids, Journal of Magnetism and Magnetic Materials. 303 (2006) 60–68. https://doi.org/10.1016/j.jmmm.2005.10.230.

[2] K. Theis-Bröhl, A. Saini, M. Wolff, J.A. Dura, B.B. Maranville, J.A. Borchers, Self-assembly of magnetic nanoparticles in ferrofluids on different templates investigated by neutron reflectometry, Nanomaterials. 10 (2020) 1–15. https://doi.org/10.3390/nano10061231.

[3] K. Theis-Bröhl, A. Saini, M. Wolff, J.A. Dura, B.B. Maranville, J.A. Borchers, Self-assembly of magnetic nanoparticles in ferrofluids on different templates investigated by neutron reflectometry, Nanomaterials. 10 (2020) 1–15. https://doi.org/10.3390/nano10061231.

[4] M.A. Hamad, H.R. Alamri, M.E. Harb, Environmentally Friendly Energy Harvesting Using Magnetocaloric Solid-State Nanoparticles as Magnetic Refrigerator, J. Low Temp. Phys. 204 (2021) 57–63. https://doi.org/10.1007/s10909-021-02595-7.

[5] L. Bidondo, F. Festari, T. Freire, C. Giacomini, Immobilized peptide□N□glycosidase F onto magnetic nanoparticles: A biotechnological tool for protein deglycosylation under native conditions, Biotechnol. Appl. Biochem. 69 (2022) 209–220. https://doi.org/10.1002/bab.2099.

[6] S.A.H. Martínez, E.M. Melchor-Martínez, J.A.R. Hernández, R. Parra-Saldívar, H.M.N. Iqbal, Magnetic nanomaterials assisted nanobiocatalysis systems and their applications in biofuels production, Fuel. 312 (2022) 122927. https://doi.org/10.1016/j.fuel.2021.122927.

[7] M. Gisbert-Garzarán, M. Vallet-Regí, Nanoparticles for Bio-Medical Applications, Nanomaterials. 12 (2022) 1189. https://doi.org/10.3390/nano12071189.

[8] A.R. Timerbaev, Analytical methodology for developing nanomaterials designed for magnetically-guided delivery of platinum anticancer drugs, Talanta. 243 (2022) 123371. https://doi.org/10.1016/J.TALANTA.2022.123371.

[9] D. Stanicki, T. Vangijzegem, I. Ternad, S. Laurent, An update on the applications and characteristics of magnetic FeO nanoparticles for drug delivery, Expert Opin. Drug Deliv. 19 (2022) 321–335. https://doi.org/10.1080/17425247.2022.2047020.

[10] M. Yuan, E.A. Bancroft, J. Chen, R. Srinivasan, Y. Wang, Magnetic Fields and Magnetically Stimulated Gold-Coated Superparamagnetic FeO Nanoparticles Differentially Modulate L-Type Voltage-Gated Calcium Channel Activity in Midbrain Neurons, ACS Appl. Nano Mater. 5 (2022) 205–215. https://doi.org/10.1021/ACSANM.1C02665/SUPPL_FILE/AN1C02665_SI_002.PDF

[11] L. Wang, S.-M. Lai, C.-Z. Li, H.-P. Yu, P. Venkatesan, P.-S. Lai, D-Alpha-Tocopheryl Poly(ethylene Glycol 1000) Succinate-Coated Manganese-Zinc Ferrite Nanomaterials for a Dual-Mode Magnetic Resonance Imaging Contrast Agent and Hyperthermia Treatments, Pharmaceutics. 14 (2022) 1000. https://doi.org/10.3390/pharmaceutics14051000.

[12] C. Lu, X. Xu, T. Zhang, Z. Wang, Y. Chai, Facile synthesis of superparamagnetic nickel-doped FeO nanoparticles as high-performance T 1 contrast agents for magnetic resonance imaging, J. Mater. Chem. B. 10 (2022) 1623–1633. https://doi.org/10.1039/D1TB02572D.

[13] A. Dasari, J. Xue, S. Deb, Magnetic Nanoparticles in Bone Tissue Engineering, Nanomaterials. 12 (2022) 757. https://doi.org/10.3390/nano12050757.

[14] R. Daya, C. Xu, N.-Y.T. Nguyen, H.H. Liu, Angiogenic Hyaluronic Acid Hydrogels with Curcumin-Coated Magnetic Nanoparticles for Tissue Repair, ACS Appl. Mater. Interfaces. 14 (2022) 11051–11067. https://doi.org/10.1021/acsami.1c19889.

[15] D. Kami, S. Takeda, Y. Itakura, S. Gojo, M. Watanabe, M. Toyoda, Application of Magnetic Nanoparticles to Gene Delivery, Int. J. Mol. Sci. 12 (2011) 3705–3722. https://doi.org/10.3390/ijms12063705.

[16] L. Gloag, M. Mehdipour, D. Chen, R.D. Tilley, J.J. Gooding, Advances in the Application of Magnetic Nanoparticles for Sensing, Adv. Mater. 31 (2019) 1904385. https://doi.org/10.1002/adma.201904385.

[17] M. Pastucha, Z. Farka, K. Lacina, Z. Mikušová, P. Skládal, Magnetic nanoparticles for smart electrochemical immunoassays: a review on recent developments, Microchim. Acta. 186 (2019) 312. https://doi.org/10.1007/s00604-019-3410-0.

[18] I. Perçin, V. Karakoç, S. Akgöl, E. Aksöz, A. Denizli, Poly(hydroxyethyl methacrylate) based magnetic nanoparticles for plasmid DNA purification from Escherichia coli lysate, Mater. Sci. Eng. C. 32 (2012) 1133–1140. https://doi.org/10.1016/j.msec.2012.02.031.

[19] G. Kaur, V. Dogra, R. Kumar, S. Kumar, K. Singh, Fabrication of FeO nanocolloids using metallosurfactant-based microemulsions: antioxidant activity, cellular, and genotoxicity toward Vitis vinifera, J. Biomol. Struct. Dyn. 37 (2019) 892–909. https://doi.org/10.1080/07391102.2018.1442251.

[20] M. Bilal, Y. Zhao, T. Rasheed, H.M.N. Iqbal, Magnetic nanoparticles as versatile carriers for enzymes immobilization: A review, Int. J. Biol. Macromol. 120 (2018) 2530–2544. https://doi.org/10.1016/j.ijbiomac.2018.09.025.

[21] D.K. Verma, R. Malik, J. Meena, R. Rameshwari, Synthesis, characterization and applications of chitosan based metallic nanoparticles: A review, J. Appl. Nat. Sci. 13 (2021) 544–551. https://doi.org/10.31018/jans.v13i2.2635.

[22] S.K. Basha, K.V. Lakshmi, V.S. Kumari, Ammonia sensor and antibacterial activities of green zinc oxide nanoparticles, Sens. Bio-Sensing Res. 10 (2016) 34–40. https://doi.org/10.1016/j.sbsr.2016.08.007.

[23] J.M. Walker, J.M. Zaleski, A simple route to diverse noble metal-decorated FeO nanoparticles for catalysis, Nanoscale. 8 (2016) 1535–1544. https://doi.org/10.1039/C5NR06700F.

[24] P. Kumar, V. Tomar, D. Kumar, R.K. Joshi, M. Nemiwal, Magnetically active FeO nanoparticles for catalysis of organic transformations: A review, Tetrahedron. 106–107 (2022) 132641. https://doi.org/10.1016/j.tet.2022.132641.

[25] P.C. Naha, Y. Liu, G. Hwang, Y. Huang, S. Gubara, V. Jonnakuti, A. Simon-Soro, D. Kim, L. Gao, H. Koo, D.P. Cormode, Dextran-Coated FeO Nanoparticles as Biomimetic Catalysts for Localized and pH-Activated Biofilm Disruption, ACS Nano. 13 (2019) 4960–4971. https://doi.org/10.1021/acsnano.8b08702.

[26] K. Tharani, A. Jegatha Christy, S. Sagadevan, L.C. Nehru, Photocatalytic and antibacterial performance of FeO nanoparticles formed by the combustion method, Chemical Physics Letters. 771 (2021) 138524. https://doi.org/10.1016/j.cplett.2021.138524.

[27] K.Q. Jabbar, A.A. Barzinjy, S.M. Hamad, FeO nanoparticles: Preparation methods, functions, adsorption and coagulation/flocculation in wastewater treatment, Environ.

Nanotechnology, Monit. Manag. 17 (2022) 100661. https://doi.org/10.1016/j.enmm.2022.100661.

[28] N. Lamichhane, M.E. Sharifabad, B. Hodgson, T. Mercer, T. Sen, Superparamagnetic FeO nanoparticles (SPIONs) as therapeutic and diagnostic agents, in: Nanoparticle Ther., Elsevier, 2022: pp. 455–497. https://doi.org/10.1016/B978-0-12-820757-4.00003-X.

[29] A. Singh, M.M. Amiji, Application of nanotechnology in medical diagnosis and imaging, Curr. Opin. Biotechnol. 74 (2022) 241–246. https://doi.org/10.1016/j.copbio.2021.12.011.

[30] M.G. Montiel Schneider, M.J. Martín, J. Otarola, E. Vakarelska, V. Simeonov, V. Lassalle, M. Nedyalkova, Biomedical Applications of FeO Nanoparticles: Current Insights Progress and Perspectives, Pharmaceutics. 14 (2022) 204. https://doi.org/10.3390/pharmaceutics14010204.

[31] H. Hosseinkazemi, S. Samani, A. O'Neill, M. Soezi, M. Moghoofei, M.H. Azhdari, F. Aavani, A. Nazbar, S.H. Keshel, M. Doroudian, Applications of FeO Nanoparticles against Breast Cancer, J. Nanomater. 2022 (2022) 1–12. https://doi.org/10.1155/2022/6493458.

[32] C. Chircov, R.-E. Ştefan, G. Dolete, A. Andrei, A.M. Holban, O.-C. Oprea, B.S. Vasile, I.A. Neacşu, B. Tihăuan, Dextran-Coated FeO Nanoparticles Loaded with Curcumin for Antimicrobial Therapies, Pharmaceutics. 14 (2022) 1057. https://doi.org/10.3390/pharmaceutics14051057.

[33] L.-L. Gu, C. Wang, S.-Y. Qiu, P.-J. Zuo, K.-X. Wang, Y.-C. Zhang, J. Gao, Y. Xie, X.-D. Zhu, Cobalt-FeO nanoparticles anchored on carbon nanotube paper to accelerate polysulfide conversion for lithium-sulfur batteries, J. Alloys Compd. 909 (2022) 164805. https://doi.org/10.1016/j.jallcom.2022.164805.

[34] S. Bao, M. Tu, H. Huang, C. Wang, Y. Chen, B. Sun, B. Xu, Heterogeneous FeO nanoparticles anchored on carbon nanotubes for high-performance lithium-ion storage and fenton-like oxidation, J. Colloid Interface Sci. 601 (2021) 283–293. https://doi.org/10.1016/j.jcis.2021.05.137.

[35] A.I. Martínez-Banderas, A. Aires, M. Quintanilla, J.A. Holguín-Lerma, C. Lozano-Pedraza, F.J. Teran, J.A. Moreno, J.E. Perez, B.S. Ooi, T. Ravasi, J.S. Merzaban, A.L. Cortajarena, J. Kosel, Iron-Based Core–Shell Nanowires for Combinatorial Drug Delivery and Photothermal and Magnetic Therapy, ACS Appl. Mater. Interfaces. 11 (2019) 43976–43988. https://doi.org/10.1021/acsami.9b17512.

[36] A.B.A. Nana, T. Marimuthu, P.P.D. Kondiah, Y.E. Choonara, L.C. Du Toit, V. Pillay, Multifunctional Magnetic Nanowires: Design, Fabrication, and Future Prospects as Cancer Therapeutics, Cancers (Basel). 11 (2019) 1956. https://doi.org/10.3390/cancers11121956.

[37] D. Wang, B. Zhu, X. He, Z. Zhu, G. Hutchins, P. Xu, W.-N. Wang, FeO nanowire-based filter for inactivation of airborne bacteria, Environ. Sci. Nano. 5 (2018) 1096–1106. https://doi.org/10.1039/C8EN00133B.

[38] S. Qasim, A. Zafar, M.S. Saif, Z. Ali, M. Nazar, M. Waqas, A.U. Haq, T. Tariq, S.G. Hassan, F. Iqbal, X.-G. Shu, M. Hasan, Green synthesis of FeO nanorods using Withania coagulans extract improved photocatalytic degradation and antimicrobial activity, J. Photochem. Photobiol. B Biol. 204 (2020) 111784. https://doi.org/10.1016/j.jphotobiol.2020.111784.

[39] A. Nikitin, M. Khramtsov, A. Garanina, P. Mogilnikov, N. Sviridenkova, I. Shchetinin, A. Savchenko, M. Abakumov, A. Majouga, Synthesis of FeO nanorods for enhanced magnetic hyperthermia, J. Magn. Magn. Mater. 469 (2019) 443–449. https://doi.org/10.1016/j.jmmm.2018.09.014.

[40] S.O. Aisida, N. Madubuonu, M.H. Alnasir, I. Ahmad, S. Botha, M. Maaza, F.I. Ezema, Biogenic synthesis of FeO nanorods using Moringa oleifera leaf extract for antibacterial applications, Appl. Nanosci. 10 (2020) 305–315. https://doi.org/10.1007/s13204-019-01099-x.

[41] S. Jain, A. Panigrahi, T.K. Sarma, Counter Anion-Directed Growth of FeO Nanorods in a Polyol Medium with Efficient Peroxidase-Mimicking Activity for Degradation of Dyes in Contaminated Water, ACS Omega. 4 (2019) 13153–13164. https://doi.org/10.1021/acsomega.9b01201.

[42] E.N. Zare, T. Abdollahi, A. Motahari, Effect of functionalization of FeO nanoparticles on the physical properties of poly (aniline-co-pyrrole) based nanocomposites: Experimental and theoretical studies, Arab. J. Chem. 13 (2020) 2331–2339. https://doi.org/10.1016/j.arabjc.2018.04.016.

[43] N.H. Abdullah, K. Shameli, E.C. Abdullah, L.C. Abdullah, Solid matrices for fabrication of magnetic FeO nanocomposites: Synthesis, properties, and application for the adsorption of heavy metal ions and dyes, Compos. Part B Eng. 162 (2019) 538–568. https://doi.org/10.1016/j.compositesb.2018.12.075.

[44] A. Maleki, R. Taheri-Ledari, J. Rahimi, M. Soroushnejad, Z. Hajizadeh, Facile Peptide Bond Formation: Effective Interplay between Isothiazolone Rings and Silanol Groups at

Silver/FeO Nanocomposite Surfaces, ACS Omega. 4 (2019) 10629–10639. https://doi.org/10.1021/acsomega.9b00986.

[45] M. Aliahmad, A. Rahdar, F. Sadeghfar, S. Bagheri, M.R. Hajinezhad, Synthesis and Biochemical effects of magnetite nanoparticle by surfactant-free electrochemical method in an aqueous system:the current density effect, Nanomedicine Res. J. 1 (2016) 39–46. https://doi.org/10.7508/NMRJ.2016.01.006.

[46] A.B. Chin, I.I. Yaacob, Synthesis and characterization of magnetic FeO nanoparticles via w/o microemulsion and Massart's procedure, J. Mater. Process. Technol. 191 (2007) 235–237. https://doi.org/10.1016/j.jmatprotec.2007.03.011.

[47] G. Salazar-Alvarez, M. Muhammed, A.A. Zagorodni, Novel flow injection synthesis of FeO nanoparticles with narrow size distribution, Chemical Engineering Science. 61 (2006) 4625–4633. https://doi.org/10.1016/j.ces.2006.02.032.

[48] E.H. Kim, H.S. Lee, B.K. Kwak, B.K. Kim, Synthesis of ferrofluid with magnetic nanoparticles by sonochemical method for MRI contrast agent, Journal of Magnetism and Magnetic Materials. 289 (2005) 328–330. https://doi.org/10.1016/j.jmmm.2004.11.093.

[49] K.B. Narayanan, N. Sakthivel, Biological synthesis of metal nanoparticles by microbes, Advances in Colloid and Interface Science. 156 (2010) 1–13. https://doi.org/10.1016/j.cis.2010.02.001.

[50] M.S. Chambers, D.S. Keeble, D. Fletcher, J.A. Hriljac, Z. Schnepp, Evolution of the Local Structure in the Sol-Gel Synthesis of Fe3C Nanostructures, Inorganic Chemistry. 60 (2021) 7062–7069. https://doi.org/10.1021/acs.inorgchem.0c03692.

[51] Z. Shen, A. Wu, X. Chen, FeO Nanoparticle Based Contrast Agents for Magnetic Resonance Imaging, Molecular Pharmaceutics. 14 (2017) 1352–1364. https://doi.org/10.1021/acs.molpharmaceut.6b00839.

[52] S. Zhu, D. Zhang, Z. Chen, Y. Zhang, Controlled synthesis of core/shell magnetic FeO/carbon systems via a self-template method, Journal of Materials Chemistry. 19 (2009) 7710–7715. https://doi.org/10.1039/b912057b.

[53] M.O. Besenhard, A.P. LaGrow, A. Hodzic, M. Kriechbaum, L. Panariello, G. Bais, K. Loizou, S. Damilos, M. Margarida Cruz, N.T.K. Thanh, A. Gavriilidis, Co-precipitation synthesis of stable FeO nanoparticles with NaOH: New insights and continuous production via flow chemistry, Chemical Engineering Journal. 399 (2020) 125740. https://doi.org/10.1016/j.cej.2020.125740.

[54] R.A. Ismail, G.M. Sulaiman, S.A. Abdulrahman, T.R. Marzoog, Antibacterial activity of magnetic FeO nanoparticles synthesized by laser ablation in liquid, Materials Science and Engineering C. 53 (2015) 286–297. https://doi.org/10.1016/j.msec.2015.04.047.

[55] K. Tharani, A. Jegatha Christy, S. Sagadevan, L.C. Nehru, Photocatalytic and antibacterial performance of FeO nanoparticles formed by the combustion method, Chemical Physics Letters. 771 (2021) 138524. https://doi.org/10.1016/j.cplett.2021.138524.

[56] Lagrow, A. P.; Besenhard, M. O.; Hodzic, A.; Sergides, A.; Bogart, L. K.; Gavriilidis, A.; Thanh, N. T. K. Unravelling the Growth Mechanism of the Co-Precipitation of FeO Nanoparticles with the Aid of Synchrotron X-Ray Diffraction in Solution. *Nanoscale* **2019**, *11* (14), 6620–6628. https://doi.org/10.1039/c9nr00531e.

[57] P. Singh, K.R. Singh, R. Verma, J. Singh, R.P. Singh, Efficient electro-optical characteristics of bioinspired FeO nanoparticles synthesized by Terminalia chebula dried seed extract, Mater. Lett. 307 (2022) 131053. https://doi.org/10.1016/j.matlet.2021.131053.

[58] A. Badawi, M.G. Althobaiti, S.S. Alharthi, A.N. Alharbi, A.A. Alkathiri, S.E. Alomairy, Effect of zinc doping on the structure and optical properties of FeO nanostructured films prepared by spray pyrolysis technique, Appl. Phys. A. 128 (2022) 123. https://doi.org/10.1007/s00339-021-05154-9.

[59] A. Koyyada, P. Orsu, Natural gum polysaccharides as efficient tissue engineering and drug delivery biopolymers, Journal of Drug Delivery Science and Technology. 63 (2021) 102431. https://doi.org/10.1016/j.jddst.2021.102431.

[60] M.C. Biswas, B. Jony, P.K. Nandy, R.A. Chowdhury, S. Halder, D. Kumar, S. Ramakrishna, M. Hassan, M.A. Ahsan, M.E. Hoque, M.A. Imam, Recent Advancement of Biopolymers and Their Potential Biomedical Applications, Journal of Polymers and the Environment. 30 (2022) 51–74. https://doi.org/10.1007/s10924-021-02199-y.

[61] M.S.B. Reddy, D. Ponnamma, R. Choudhary, K.K. Sadasivuni, A comparative review of natural and synthetic biopolymer composite scaffolds, Polymers. 13 (2021). https://doi.org/10.3390/polym13071105.

[62] G. Huang, F. Chen, W. Yang, H. Huang, Preparation, deproteinization and comparison of bioactive polysaccharides, Trends in Food Science and Technology. 109 (2021) 564–568. https://doi.org/10.1016/j.tifs.2021.01.038

[63] A.K. Nayak, M.S. Hasnain, A.K. Dhara, D. Pal, Plant Polysaccharides in Pharmaceutical Applications, in: 2021: pp. 93–125. https://doi.org/10.1007/978-3-030-54027-2_3.

[64] O.P.N. Yarley, A.B. Kojo, C. Zhou, X. Yu, A. Gideon, H.H. Kwadwo, O. Richard, Reviews on mechanisms of in vitro antioxidant, antibacterial and anticancer activities of

water-soluble plant polysaccharides, International Journal of Biological Macromolecules. 183 (2021) 2262–2271. https://doi.org/10.1016/j.ijbiomac.2021.05.181.

[65] K. Mali, S. Dhawale, R. Dias, V. Ghorpade, Delivery of drugs using tamarind gum and modified tamarind gum: A review, Bulletin of Faculty of Pharmacy, Cairo University. 57 (2019) 1–24. https://doi.org/10.21608/bfpc.2019.47260.

[66] A.K. Shukla, R.S. Bishnoi, M. Kumar, V. Fenin, C.P. Jain, Applications of Tamarind seeds Polysaccharide-based copolymers in Controlled Drug Delivery: An overview, Asian J. Pharm. Pharmacol. 4 (2018) 23–30. https://doi.org/10.31024/ajpp.2018.4.1.5.

[67] Khushbu, S.G. Warkar, Potential applications and various aspects of polyfunctional macromolecule- carboxymethyl tamarind kernel gum, European Polymer Journal. 140 (2020) 110042. https://doi.org/10.1016/j.eurpolymj.2020.110042.

[68] S. Agarwal, M. Hoque, N. Bandara, K. Pal, P. Sarkar, Synthesis and characterization of tamarind kernel powder-based antimicrobial edible films loaded with geraniol, Food Packaging and Shelf Life. 26 (2020) 100562. https://doi.org/10.1016/j.fpsl.2020.100562.

[69] P. Goyal, V. Kumar, P. Sharma, Carboxymethylation of Tamarind kernel powder, Carbohydrate Polymers. 69 (2007) 251–255. https://doi.org/10.1016/j.carbpol.2006.10.001.

[70] A.K. Nayak, D. Pal, Functionalization of Tamarind Gum for Drug Delivery, 2018. https://doi.org/10.1007/978-3-319-66417-0_2

[71] D. Singh Rana, N. Thakur, D. Singh, P. Sonia, Molybdenum and tungsten disulfide based nanocomposites as chemical sensor: A review, Mater. Today Proc. 62 (2022) 2755–2761. https://doi.org/10.1016/j.matpr.2022.01.147.

[72] S.N. Nangare, A.G. Patil, S.M. Chandankar, P.O. Patil, Nanostructured metal–organic framework-based luminescent sensor for chemical sensing: current challenges and future prospects, J. Nanostructure Chem. (2022). https://doi.org/10.1007/s40097-022-00479-0.

[73] Y. Wang, X. Yang, L. Pang, P. Geng, F. Mi, C. Hu, F. Peng, M. Guan, Application progress of magnetic molecularly imprinted polymers chemical sensors in the detection of biomarkers, Analyst. 147 (2022) 571–586. https://doi.org/10.1039/D1AN01112J.

[74] J.J. Renard, S.E. Calidonna, M. V. Henley, Fate of ammonia in the atmosphere - A review for applicability to hazardous releases, Journal of Hazardous Materials. 108 (2004) 29–60. https://doi.org/10.1016/j.jhazmat.2004.01.015

[75] A.I. Amhamed, S. Shuibul Qarnain, S. Hewlett, A. Sodiq, Y. Abdellatif, R.J. Isaifan, O.F. Alrebei, Ammonia Production Plants—A Review, Fuels. 3 (2022) 408–435. https://doi.org/10.3390/fuels3030026.

[76] J. Brightling, Ammonia and the fertiliser industry: The development of ammonia at Billingham, Johnson Matthey Technology Review. 62 (2018) 32–47. https://doi.org/10.1595/205651318X696341.

[77] M.P. Diana, W.S. Roekmijati, W.U. Suyud, Why it is often underestimated: Historical Study of Ammonia Gas Exposure Impacts towards Human Health, E3S Web of Conferences. 73 (2018). https://doi.org/10.1051/e3sconf/20187306003.

[78] J. Meulenbelt, Ammonia, Medicine. 40 (2012) 94–95. https://doi.org/10.1016/j.mpmed.2011.11.006.

[79] D. Zhang, J. Liu, C. Jiang, A. Liu, B. Xia, Quantitative detection of formaldehyde and ammonia gas via metal oxide-modified graphene-based sensor array combining with neural network model, Sensors and Actuators, B: Chemical. 240 (2017) 55–65. https://doi.org/10.1016/j.snb.2016.08.085.

[80] Q. Zhong, H. Xu, H. Ding, L. Bai, Z. Mu, Z. Xie, Y. Zhao, Z. Gu, Preparation of conducting polymer inverse opals and its application as ammonia sensor, Colloids and Surfaces A: Physicochemical and Engineering Aspects. 433 (2013) 59–63. https://doi.org/10.1016/j.colsurfa.2013.04.053.

[81] M.O. Diniz, A.F. Golin, M.C. Santos, R.F. Bianchi, E.M. Guerra, Improving performance of polymer-based ammonia gas sensor using POMA/V2O5 hybrid films, Organic Electronics. 67 (2019) 215–221. https://doi.org/10.1016/j.orgel.2019.01.039.

[82] T. Li, W. Yin, S. Gao, Y. Sun, P. Xu, S. Wu, H. Kong, G. Yang, G. Wei, The Combination of Two-Dimensional Nanomaterials with Metal Oxide Nanoparticles for Gas Sensors: A Review, Nanomaterials. 12 (2022) 982. https://doi.org/10.3390/nano12060982.

[83] K.G. Krishna, S. Parne, N. Pothukanuri, V. Kathirvelu, S. Gandi, D. Joshi, Nanostructured metal oxide semiconductor-based gas sensors: A comprehensive review, Sensors Actuators A Phys. 341 (2022) 113578. https://doi.org/10.1016/j.sna.2022.113578.

[84] A.P. Lagrow, M.O. Besenhard, A. Hodzic, A. Sergides, L.K. Bogart, A. Gavriilidis, N.T.K. Thanh, Unravelling the growth mechanism of the co-precipitation of FeO nanoparticles with the aid of synchrotron X-Ray diffraction in solution, Nanoscale. 11 (2019) 6620–6628. https://doi.org/10.1039/c9nr00531e.

[85] A.V. Rane, K. Kanny, V.K. Abitha, S. Thomas, Methods for Synthesis of Nanoparticles and Fabrication of Nanocomposites, Elsevier Ltd., 2018. https://doi.org/10.1016/b978-0-08-101975-7.00005-1.

[86] U. Holzwarth, N. Gibson, The Scherrer equation versus the “Debye-Scherrer equation,” Nature Nanotechnology. 6 (2011) 534. https://doi.org/10.1038/nnano.2011.145.

[87] J. Devillers, R. Steiman, F. Seigle-Murandi, The usefulness of the agar-well diffusion method for assessing chemical toxicity to bacteria and fungi, Chemosphere. 19 (1989) 1693–1700. https://doi.org/10.1016/0045-6535(89)90512-2

[88] V. Singh, P. Kumar, Carboxymethyl tamarind gum–silica nanohybrids for effective immobilization of amylase, J. Mol. Catal. B Enzym. 70 (2011) 67–73. https://doi.org/10.1016/j.molcatb.2011.02.006.

[89] S. Ahmad, U. Riaz, A. Kaushik, J. Alam, Soft Template Synthesis of Super Paramagnetic Fe_3O_4 Nanoparticles a Novel Technique, J. Inorg. Organomet. Polym. Mater. 19 (2009) 355–360. https://doi.org/10.1007/s10904-009-9276-6.

[90] Khushbu, S.G. Warkar, A. Kumar, Synthesis and assessment of carboxymethyl tamarind kernel gum based novel superabsorbent hydrogels for agricultural applications, Polymer. 182 (2019) 121823. https://doi.org/10.1016/j.polymer.2019.121823.

[91] H.S. Devi, M.A. Boda, M.A. Shah, S. Parveen, A.H. Wani, Green synthesis of FeO nanoparticles using Platanus orientalis leaf extract for antifungal activity, Green Processing and Synthesis. 8 (2019) 38–45. https://doi.org/10.1515/gps-2017-0145.

[92] S.T. Dubas, V. Pimpan, Green synthesis of silver nanoparticles for ammonia sensing, Talanta. 76 (2008) 29–33. https://doi.org/10.1016/j.talanta.2008.01.062

Chapter-5

Synthesis and characterization of carboxymethyl tamarind kernel gum/ZnO nanocomposites and its application in chromium metal removal and antifungal activity

5.1 Introduction

Water contamination has become a deliberate environmental concern globally in recent years. This is due to the existence of several pollutants that infiltrate aquatic systems as a result of the uncontrolled and rapid increase in the world's population, industry, agricultural fertilizers, urbanization, and the widespread use of chemicals [1,2]. Chromium is regarded as one of those heavy metals that pollutes both land and water and is mostly released through factories that produce textiles, leather tanning, electroplating, and metal extraction [3]. Chromium exists in two oxidation states in hydrated situations: one is trivalent Chromium (III) and the other is hexavalent Chromium (VI) [4]. After entering the water, Cr undergoes a number of changes, including oxidation, reduction, sorption, desorption, precipitation, and dissolution. Cr (III) solubility is pH-dependent, whereas Cr (VI) is quite soluble at all pH levels. The most hazardous form of chromium is hexavalent, which is typically coupled with oxygen to generate the oxoanions CrO_4^{2-} and Cr_2O^{2-}. Trivalent chromium is less poisonous, less mobile, and has a significant association with soil organic matter [5–7]. In addition to being a potent epithelium irritant, Cr (VI) is also considered to be a human carcinogen [8]. Similar poisoning by Cr (VI) occurs in a variety of plants [9], aquatic creatures [10], microbes [11], and other species. Hence, it is vital to remove chromium from water because of the rising usage of effluent water for irrigation and the excessive chromium build up in various soil profiles.

Along similar lines, the sole approach focused on the reduction and adsorption of toxic Cr (III) to more dangerous Cr (VI) has been used by researchers [12,13]. Co-precipitation [14,15], chemical reduction [16], coagulation [17,18], ion exchange [19–21], and adsorption [22,23] have all been used to remove chromium from polluted water. However, the majority of these methods were reportedly found to be expensive. Conversely, adsorption methods are a good alternative because they are safe for the environment, effective, and non-toxic [24].

There has been a lot of interest in the development of new, affordable nanomaterial for applications such as pollution monitoring and environmental remediation. Recent research suggests that the use of nanoparticles, nanofiltration, or other products originating from the development of nanotechnology may be able to resolve or considerably improve many of the problems relating to water quality [25–28].

The synthesis of ZnO nanoparticles has been intensively developed due to their distinct chemical and physical properties [29]. They have piqued the interest of researchers due to their novel applications such as adsorptions [30], sensor activity [31], heat treatment [32], antimicrobial activity [33], anti-fungus [34], wound healing [35], ultra-violet filtering [36], and excessive catalytic and photochemical activity [37, 38].

Nearly all analysts concur that it is indeed crucial to produce new-material in an aqueous medium by employing a green method with the assistance of covering, salting, or hydrolytic experts. This is due to the fact that it is simple to conduct and has no effect on the environment. Therefore, it is imperative to cap the ZnO nanoparticles (NPs) with biopolymer in order to increase their affordability, stability, flexibility, and sustainability. Biopolymers are natural, non-toxic, renewable, and sustainable polymer alternatives, and are widely used in agriculture, environment, medicine, and industry [39–45]. Chitin, chitosan, cellulose, tamarind kernel gum, starch, and pectin are some of the biopolymers that have potential applications in the biomedical and pharmaceutical industries [46]. Biopolymers like alginate, chitosan, and starch are good choices for matrix polymers because their chains have a lot of hydroxyl groups, which are excellent at interacting with complex particles and provide a suitable environment for the growth of nanoparticles [47]. Many biopolymers, such as chitosan and cellulose, are not water soluble and have been discovered to degrade in natural solutions. Biopolymer has also been shown to be bio and muco-adhesive, biocompatible, biodegradable, and non-aggravating in biomedical applications such as drug delivery, bio nano-reactors, nano-filtration, biosensors, and antibacterial activity [48,49].

Tamarind seed kernel polysaccharide, a derivative of glycosaminoglycan, is produced by extracting the seeds of *Tamarindus indica*, a plant in the fabaceae family. It is composed of galactoxyloglucan polysaccharide (55-65%), a monomer of galactose, glucose, and xylose with a molar ratio of 3:2:1 [50,51]. Carboxymethyl tamarind kernel gum (CMTKG) is the carboxylate form of tamarind kernel gum. CMTKG in-corporate backbone chain of β-D-glucan having side chains of β-D-galactopyranosyl and α-D-xylopyranose related to glucose

systems [52]. Objectively speaking to other semi-synthetic polysaccharide derivatives, CMTKG is less expensive. Given that the structure shares a hydrophilic backbone with cellulose, it could be the best solution from the perspective of biopolymers [53].

Various research on the antifungal and antibacterial activity of ZnO NPs has shown that they are effective antimicrobial agents. However, research on nanoparticles' antifungal effectiveness against filamentous fungus is scarce [54]. On blending ZnO nanoparticles in a CMTKG phase, the amount of padding, particle dissipation, relations padding/ matrix, and other parameters can be affected. Processing conditions may further complicate ZnO antifungal activity [34]. Biocomposites may demonstrate excellent stability, maximum accessibility, and even fascinating augmentation caused by nanoparticle–matrix interaction.

In light of the aforementioned information, we aimed to fabricate well-dispersed CMTKG/ZnO nanocomposites using the in situ co-precipitation process in this chapter and looked into their possible application in the removal of chromium from water. The potential of the synthesized nanocomposite was also investigated for antifungal activity against isolates of *Aspersilium flamous*.

5.2. Experimental

5.2.1 Materials

Hindustan Gum and Chemicals Ltd. in Bhiwani, Haryana, India supplied the carboxymethyl tamarind kernel gum. The powder was subsequently sieved, and for future use, particles of a size less than 40 mm were used. This powder was dried for 24 hours before use in an oven that was monitored at 110°C. Zinc acetate, potassium dichromate, acetone, and absolute alcohol were procured from Central Drug House Pvt. Ltd. India. Every solution used in the analysis was made in double-distilled water (DDW). To determine the antifungal potential of synthesized nanocomposite isolates of *Aspersilium flamous* were provided by the Department of (Botany and Microbiology), Gurukul Kangri (Deemed to be University), Haridwar, Uttarakhand.

5.2.2 Preparation of Cr (VI) solution

$K_2Cr_2O_7$ was dissolved in de-ionized water that had been attenuated to the necessary concentrations (10–80 mg L^{-1}) in order to prepare solutions of Chromium (VI) (100 mg L^{-1}).

5.2.3 Synthesis of CMTKG/ZnO nanocomposites

ZnO nanoparticles were created by co-precipitating zinc acetate in alcohol (10 mL), which was subsequently reduced to ZnO nanoparticles by adding 10 mL of 0.05 M NaOH solution. At 60°C, this solution was magnetically agitated continuously until it became homogeneous. A 150 mL aqueous solution in a conical flask containing 1 g of carboxymethyl tamarind kernel gum was added, and the combination was magnetically agitated at 60°C to produce viscous solutions. 150 mg of zinc solutions were added to this, and mixing continued until a 24-hour homogenous solution was obtained. Finally, a CMTKG/ZnO immobilized polymeric precipitate was produced. Following 20-minute centrifugation at 10,000 rpm to remove any remaining debased particles, the mixture was washed with acetone. The precipitate was then dried in the hot air oven at 50°C after being rinsed with C_2H_5OH. The prepared dry powder of biocomposites was put away in desiccators for further use.

5.2.4 Characterization

5.2.4.1 Dynamic light scattering (DLS) analysis

Zetasizer nano Z.S. Malvern Instruments Ltd. available at Delhi Technological University, New Delhi was utilized to detect the size distribution of particles. In this analysis, the dynamic discrepancy of light scattering intensity reasons by the Brownian velocity of the nanoparticles was measured.

5.2.4.2 Fourier transform infrared (FTIR) analysis

Using a Perkin Elmer FT-IR BX2 instrument, the infrared spectra (4000–400 cm^{-1}) of the samples were examined. 200 mg of spectroscopic grade KBr and 10 mg of the crystal sample were blended to produce the pellets.

5.2.4.3 Field emission scanning electron microscopy (FE-SEM) analysis

Surface morphological analysis of CMTKG/ZnO nanocomposite was analyzed by Scanning Electron Microscope (Model: JEOL JSM-6610LV). SEM provides extremely useful information about molecule size and polydispersity profile. Moreover, objects' size and shape are described in depth by the SEM investigation.

5.2.4.4 High resolution transmission electron microscope (HR-TEM) analysis

For the HR-TEM test, 5 mg of dried CMTKG/ZnO nanocomposites were dispersed in 25 mL of C_2H_5OH using an ultrasonicator. A permanently coated copper grid was administered with a 10 mL dispersion of nanocomposites.

5.2.4.5 X-ray diffraction (XRD) analysis

X-ray diffraction studies of synthesized CMTKG/ZnO nanocomposites were carried out using an X-ray diffractometer (P Analytical X'Pert Pro). The analysis was done at the current and voltage of 40 mA using Cu K α radiations (k = 1.5406 nm and λ=1.5406 Å) and scanning angle 2θ in the range of 0-80^o. The crystal particle size was determined using Debye–Scherrer equation [55], as follows (Eq. (5.1));

$$D = \frac{K\lambda}{\beta\cos\theta} \qquad (5.1)$$

Here k is 0.9, λ is the wavelength of source (1.5 Å), β is the FWHM and θ is the diffractions of angle.

5.2.4.6 Adsorption studies

The batch approach was used to conduct adsorption tests at room temperature (298–313 K). In a thermostatic water bath shaker for a duration of 10 to 100 minutes, various concentrations of CMTKG/ZnO biocomposite were equilibrated with 10 mL of chromium solution (10 to 50 mg/L). Through centrifugation and the residual convergence of chromium particles in the supernatant fluid, the adsorbent was separated from the solutions. It was looked at by using a UV spectrophotometer. The experiments were conducted at different chromium (VI) concentrations with a good adsorbent % and variable contact durations for dynamic estimates. The impact of changing pH on adsorption was investigated in the pH range of 0–10. The pH of the liquids was altered by using a weaker HCl or NaOH setup (both 0.01 M). The assessments were administered repeatedly, and average characteristics were noted. The amount of chromium (VI) particle absorbed per unit mass of adsorbent (qe, mg. g^{-1}) was determined using the following criterion by Eq. (5.2):

$$\%Adsorption = \frac{C0-Ct}{C0} \qquad (5.2)$$

The equilibrium was calculated using the formula given in Eq. (5.3):

$$\text{qe} = C0 - Ct \times \frac{v}{w} \qquad (5.3)$$

Where, qe is the equilibrium absorption capacity of chromium (VI) (mg g−1), $C0$ is the initial concentration of chromium (VI) (mg L^{-1}), Ce is the concentration of chromium (VI) (mg L^{-1}) at time t, v is the volume of chromium (VI) utilized (L) and w is the weight of adsorbent (g) utilized.

5.2.4.7 Antifungal activity determination

Utilizing MTCC2799, which is the minimal concentration of the sample needed to inhibit % of the fungus *Aspersilium flamous*, the antifungal activity of CMTKG/ZnO nanocomposite was assessed. A stronger antifungal impact was assumed to exist in every sample with a lower MTCC-2799 score. The positive control was amphotericin B.

The standard culture of *Aspergillus flavus* MTCC 2799 was used to test the antifungal activity of a sample of CMTKG/ZnO nanocomposite using the poisoned food method. Specifically, different concentrations of nanocomposites (1000 ppm, 2000 ppm, and 3000 ppm) were prepared by adding the appropriate amount into cooled molten Potato Dextrose Agar (PDA) media except the control plate (i.e. without nanocomposite), and after solidifying, 6 mm well was created accordingly with the help of sterile cork borer. Each well received 100 µl of spore suspension of *Aspergillus flavus* MTCC2799. Petri plates used for the test and control were incubated at 28 °C for 5 days while the fungus growth was continuously observed. Following incubation, the percentage of inhibition was estimated using the following formula:

$$\text{Inhibition of mycelial growth (\%)} = \frac{Ac - At}{Ac} \times 100$$

where Ac is the mean diameter of the colony in the control sample, and At is the mean diameter of the colony in the treated sample.

5.3 Results and discussion

5.3.1 Synthesis of CMTKG/ZnO nanocomposites

It is presumed that the ZnO NPs are attached to the CMTKG biopolymer matrix through H-bonding between the hydroxyl and ZnO NPs, as proposed in Scheme S1.

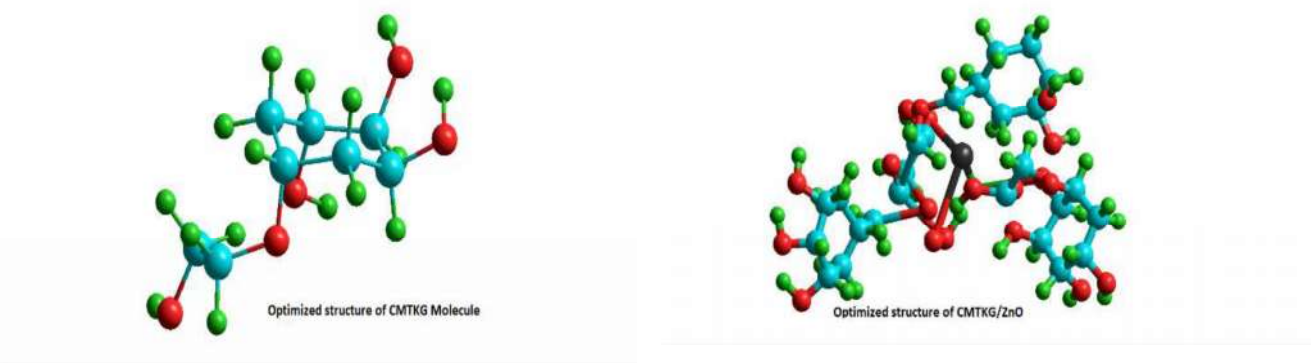

Scheme 1: Schematic presentations of structures of (a) CMTKG (b) CMTKG/ZnO biocomposite

5.3.2 Particle size determination by DLS

Using the dynamics light approach, the particle size of synthesized CMTKG-ZnO nanocomposites was measured. Figure 5.1 shows the size distribution of the CMTKG-ZnO nanocomposites generated by the green process. As a result, the bulk of the particles had sizes between 56 and 76 nm, with the biggest size distributions occurring around 66 nm [56].

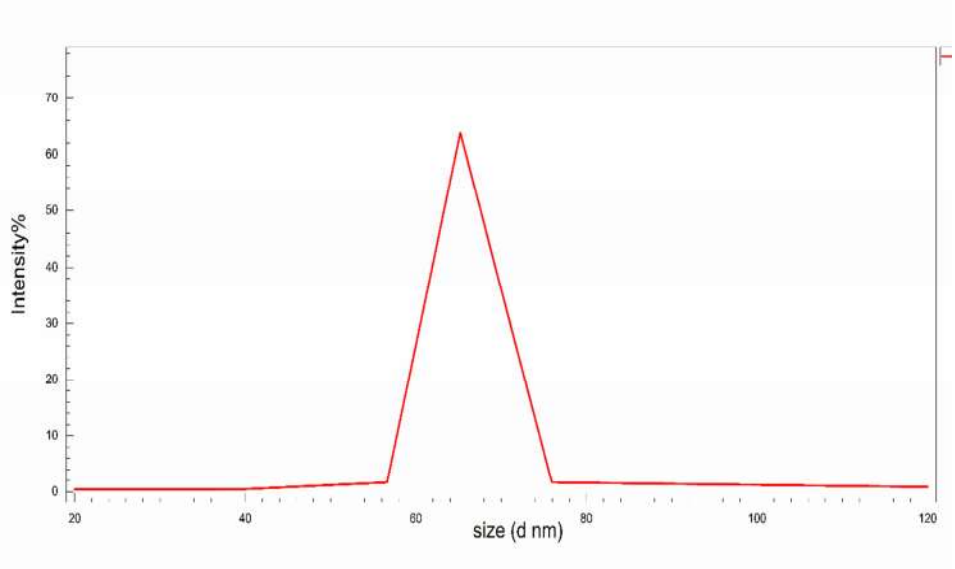

Figure 5.1: DLS analysis of CMTKG-ZnO nanocomposites

5.3.3 Fourier transform infrared (FTIR)

The FTIR spectra of CMTKG and CMTKG-ZnO nanocomposites are shown in Figure 5.2. The typical adsorption band for C-OH stretching vibrations is shown by CMTKG at 3406

cm^{-1}. At (1710 and 1600) cm^{-1}, respectively, COO- absorptions are attributed to symmetric and asymmetric absorption bands [52]. The band at 2825 cm^{-1} is formed by the C-H stretching of the -CH_2 groups, whereas the -COO- are assigned to symmetric and asymmetric vibrations at 1720 and 1645 cm^{-1} in the spectra of CMTKG/ZnO. Around 1110 cm^{-1} and 1290 cm^{-1} in the adsorption bands, stretching vibrations C-O may be seen [10]. The distinctive peak at 480 cm^{-1} with a band at 3427 cm^{-1} due to the adsorption bands between (1110 and 1241) cm^{-1} suggests an interaction between CMTKG and ZnO, which confirms the transparent framing of CMTKG-ZnO nanocomposites [49].

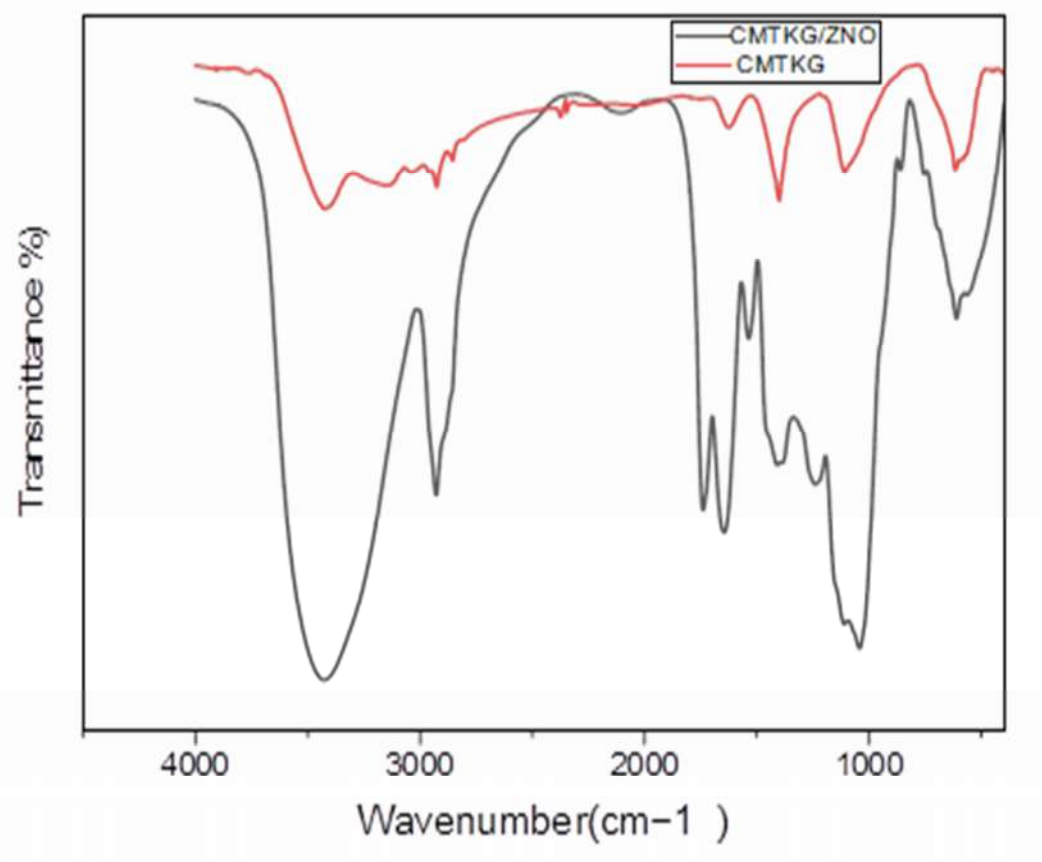

Figure 5.2: FTIR of CMTKG and CMTKG/ZnO nanocomposites

5.3.4 XRD

Figure 5.3 illustrates the XRD spectra of CMTKG and CMTKG/ZnO nanocomposite. There are no crystallinity model peaks in the XRD spectra of pure CMTKG in a CMTKG/ZnO. Nanocomposites showed two unique peaks at 2Θ = 28° and 35° and revealed evidence of the inclusion of ZnO nanoparticles in the nanocomposites. It was discovered that the

nanocomposites had an average size of 31.69 nm. A similar observation was also reported by Singh et al. (2017) [38].

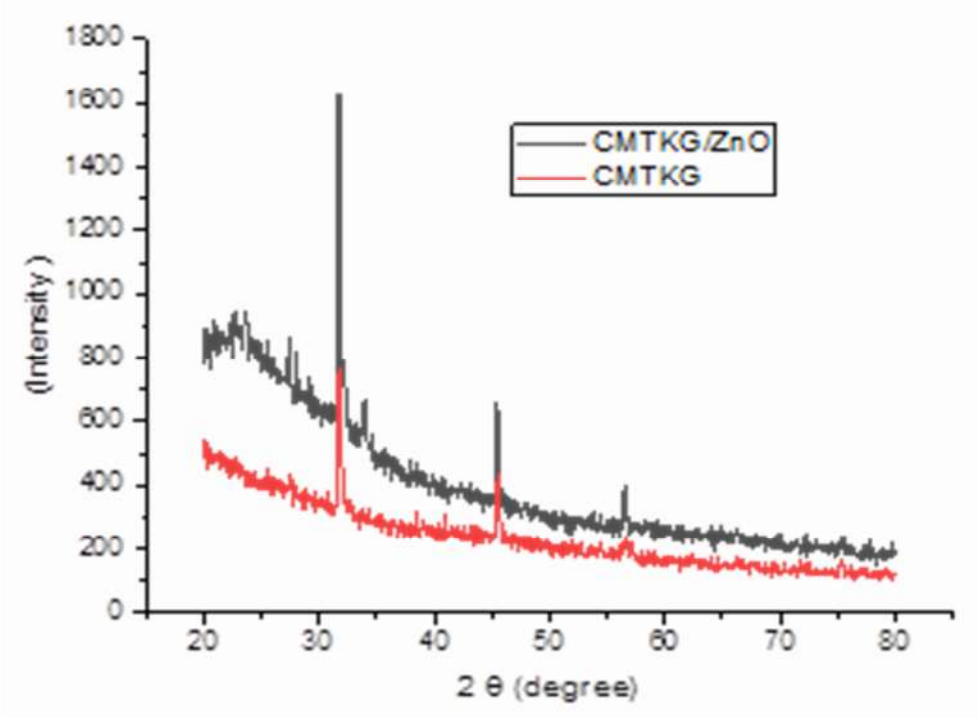

Figure 5.3: XRD of CMTKG and CMTKG/ZnO nanocomposites

5.3.5 Field Emission-Scanning Electron Microscopy (FE-SEM)

Figure 5.4 shows SEM micrographs of CMTKG and CMTKG/ZnO nanocomposites at various magnifications. Figure 5.4 (a) shows the homogeneous morphology of the CMTKG sample surface. ZnO particle shape and size are shown in Figure 5.4 (b). ZnO particles were rectangular in shape with an average cross-section area of 120 nm × 220 nm and 10 to 15 nm thickness. SEM image (Figure 5.4 (b)) also shows the intercalation and exploration of nanoparticle layers. A similar conclusion was also brought to light by Azeez and the team [29].

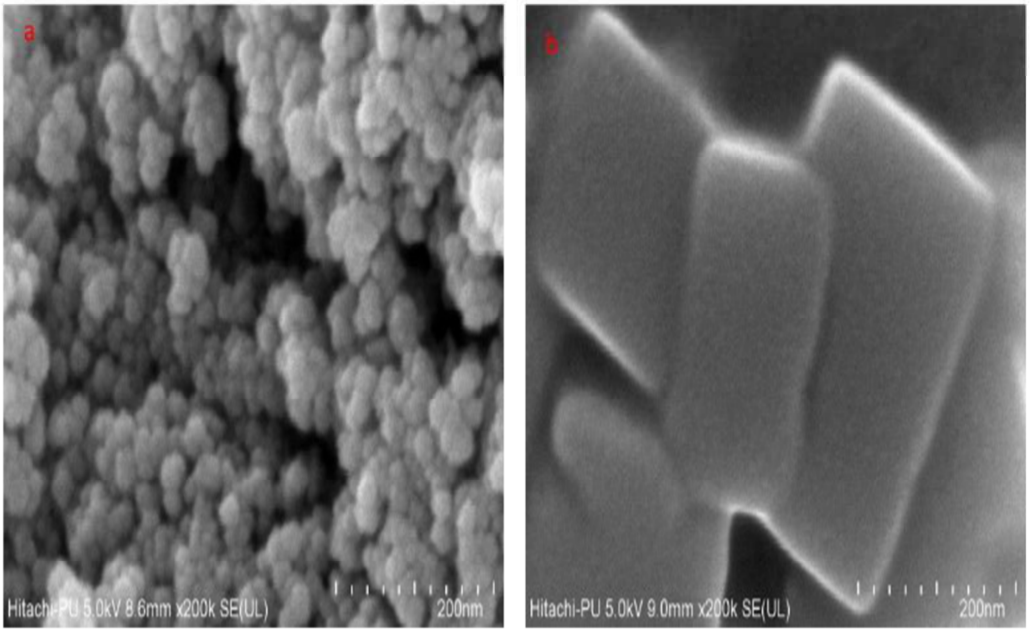

Figure 5.4: Scanning micrograph of (a) CMTKG and (b) CMTKG/ZnO nanocomposites

5.3.6 High Resolution-Transmission Electron Microscopy (HR-TEM)

The existence of organized pores in the black spots in the TEM images of the CMTKG/ZnO nanocomposite (Figure 5.5) indicated that the spots were caused by ZnO nanoparticles. The picture demonstrates the even dispersion of ZnO nanoparticles. Additionally, a range of particle sizes between 40 and 90 nm was discovered. The CMTKG/ZnO nanocomposites exhibit homogeneous spherical size in a disordered distribution. A comparable finding was also reported by Pal and coworkers [57].

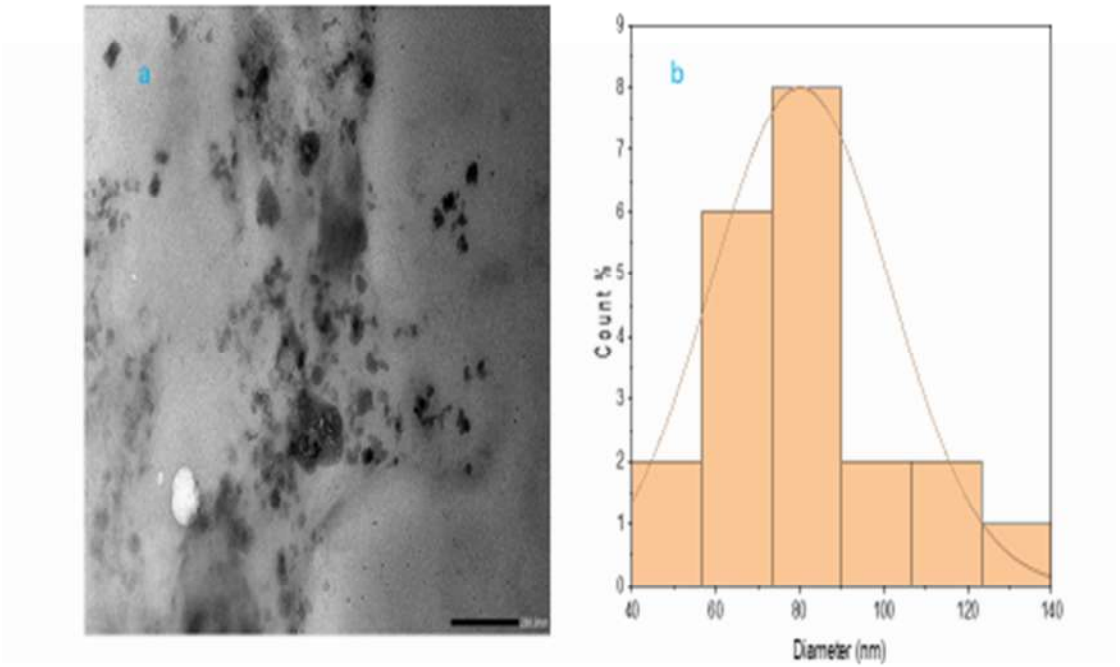

Figure 5.5: HR-TEM and particle size distribution of CMTKG/ZnO nanocomposites

5.3.7 Adsorption studies

5.3.7.1 Effect of contact time

Under the constant adsorbent dosage of the 2 mg/L CMTKG/ZnO biocomposite and the Cr (VI) concentration of 30 mg/L, the impact of varying the contact duration on the Chromium (VI) excretion percent and qe were investigated, as shown in Figure 5.6. (a). The qe and percent elimination rose as the contact duration grew from 10 to 80 minutes, reaching equilibrium within the optimum contact period of 80 minutes. 95.50 percent is the largest removal percentage that has been noted. The rapid rise in percent adsorption and adsorption efficiency at the beginning is due to the concentration gradient between Chromium in solution and in adsorbent and also attributed to the available vacant sites. Chromium (VI) particles may reach the strong phase of the adsorbent's outer layer over time, increasing the return rate of the particles and raising the amount of adsorption [58].

5.3.7.2 Effect of adsorbent dose

Effects of adsorbent dose on chromium removal are shown in Figure 5.6 (b). These experiments were performed at a constant contact time of 80 minutes, at constant initial Chromium (VI) concentration in feed (30 mg/L), and with varying adsorbent amounts from 0.01 mg/L to 3.0 mg/L. The percentage of removal increases with an increase in the adsorbent portion, and balance was obtained at 2.0 g/L. However, values of qe decreased with increasing adsorbent concentration. qe is defined as the removal of Chromium (VI) ions per unit weight of adsorbent (Equation (2)). Thus, qe represents the efficiency of the adsorbent in a particular experiment. Therefore, these results indicate that although the percent removal of chromium increases with increasing adsorbent concentration but the efficiency of adsorbent decreases with increasing its concentration. The maximum percent extraction of Chromium (IV) (93.40%) was found with a 3 mg/L CMTKG/ZnO adsorbent concentration At 2.0 g/L, the highest evacuation percentage recorded was 93.40 %. No significant increase in the percentage of evacuation was noted after that. As shown in Figure 5.6 (b), a larger chance of the adsorption stage may be associated with an increase in the expulsion percentage of adsorbate particles with an increase in the adsorbent portion. Greater availability of adsorption sites and sorptive surface area may be the cause of the increase in the percentage of adsorbate ions removed with an increase in adsorbent dosage.

5.3.7.3 Effect of pH

The effects of feed pH on the adsorption capability of adsorbent (CMTKG/ZnO nanocomposite) are shown in Figure 5.6.(c). The CMTKG/ZnO nanocomposite's adsorption capacity was affected by pH in the range of 2 to 10 at constant contact time (80 minutes), constant adsorbent dose (2 mg/L), and constant initial concentration of Chromium (VI) in feed (30 mg/L). The adsorption process is significantly influenced by pH. The results showed that Chromium (VI) % removal, and the adsorbent efficiency (qe) both increased with increasing pH values in the acidic region, with the maximum of adsorption taking place at 7.0 pH, as shown in Figure 5.6. (c). Further both % removal and adsorbent efficiency (qe) reduced with increasing pH values in the basic region.

These results confirm that the performance of synthesized CMTKG/ZnO nanocomposite adsorbent for Chromium (VI) extraction strongly depends on the feed pH, and maximum extraction is achieved at 7 pH. At lower pH conditions, less interaction of Cr (VI) with adsorbent was noted and the H^+ compete with Cr (VI) hence observing less adsorption. It has

been hypothesized that at low pH levels, species are primarily adsorbed in their molecular form, but at higher pH levels, species are primarily adsorbed in their ionized form. These findings support the electrostatic attraction of the anionic Cr (VI) species since the Cr (VI) species that developed under these circumstances are most likely to be $HCrO4^-$ and $Cr2O7^{2-}$ anions. However, if pH rises, the efficacy of Cr (VI) adsorption and removal decreased concurrently as the concentration of the hydroxyl (OH-) ion rose and electrostatically competed with anionic Cr (VI) species.

5.3.7.4 Effect of initial Cr (VI) concentration

The percent removal increases as the initial Chromium (VI) ion concentration rises, reaching equilibrium at 30 mg/L. At a fixed contact duration (80 minutes) and adsorbent dosage (2 mg/L), the impact of various initial Chromium (VI) ion concentrations (18 mg/L to 32 mg/L) on the amount of adsorbent was calculated. Results show that *q*e of Chromium was increased with increasing its initial concentration, which suggests that adsorbent particles were not saturated with chromium ions and more chromium can be removed with the same amount of adsorbent. On the other hand, values of percent extraction decreased with increasing initial Chromium (VI) concentration in the feed. Figure 5.6 (d) displays that the highest quantity that could be adsorbed under these circumstances is 93.20 % at 18 mg/L initial Chromium (VI) concentration in the feed. This was expected given the initial Cr (VI) concentrations, which served as the primary impetus to overcome the barriers to the mass transfer of Cr (VI) between the bulk and reactive sites.

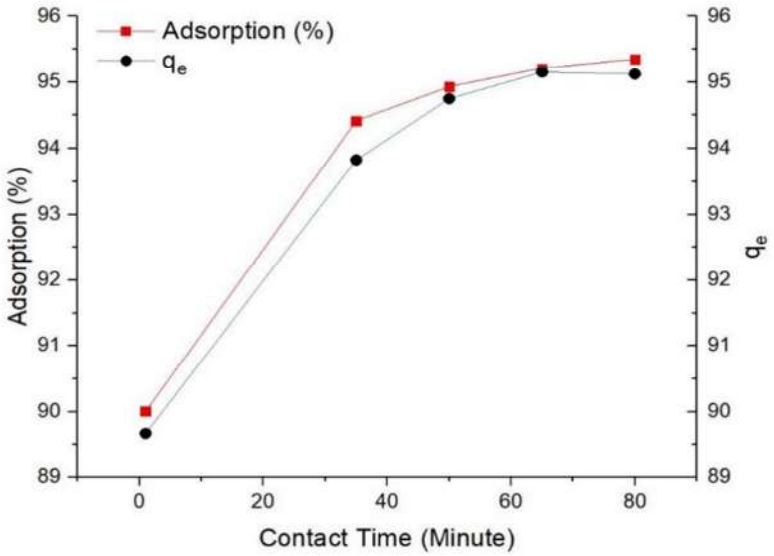

(a)

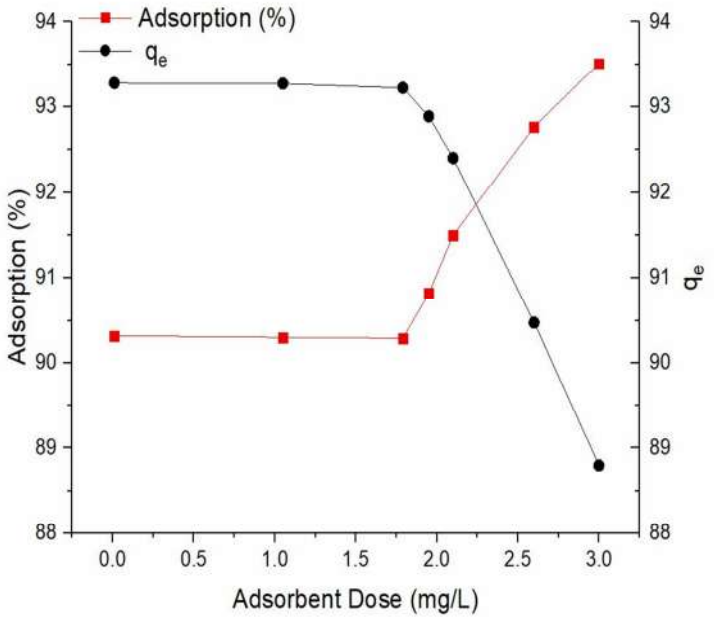
Adsorption (%)
q_e
Adsorption (%)
q_e
Adsorbent Dose (mg/L)

(b)

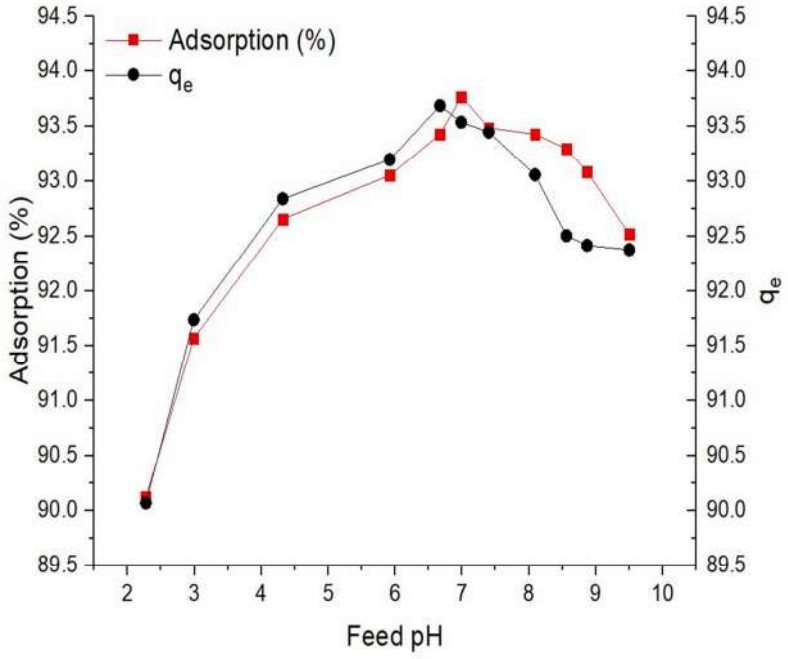
Adsorption (%)
q_e
Adsorption (%)
q_e
Feed pH

(c)

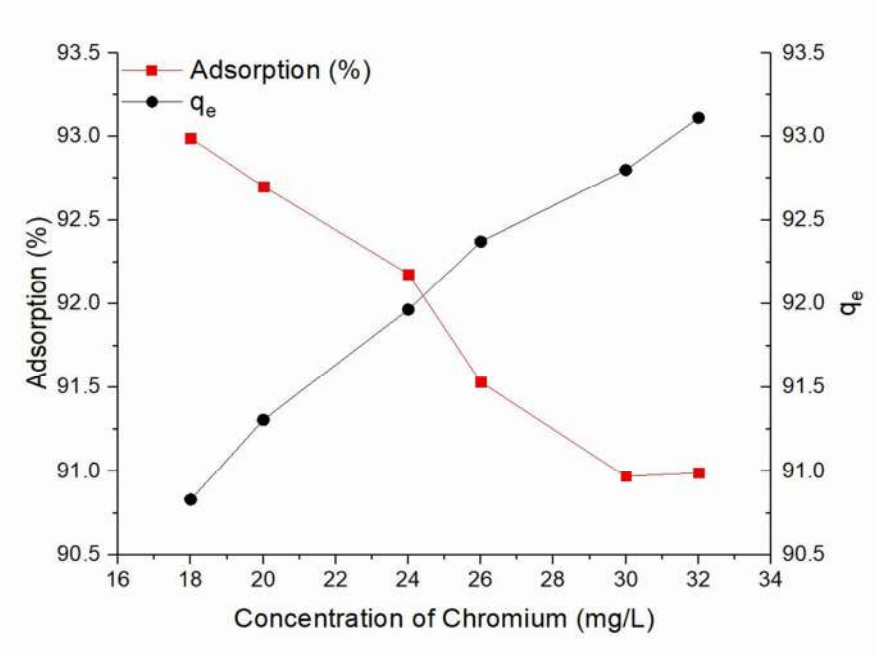

(d)

Figure 5.6: (a) Effect of Contact time; (b) Effect of adsorbent dose of nanocomposite; (c) Effect of pH; (d) Effect of initial concentration of Chromium

Table 5.1 displays, the performance of the synthesized adsorbent (CMTKG/ZnO nanocomposite) compared with previously reported adsorbents. The performance of the CMTKG/ZnO adsorbent was found far better than the other traditional adsorbents reported in the literature for removal Chromium (VI) extraction, which depicts the novelty of the present study for the chromium removal from wastewater with prepared CMTKG/ZnO nanocomposites.

Table 5.1: Comparison studies of various bio-composite for removal of chromium (VI) ions

Adsorbent	Percent Extraction	Reference
CMTKG/ZnO nanocomposite	**95.5**	**Present Study**
Guargum/ZnO biocomposite	55.56	[29]
Activated carbon	3.46	[59]
Polypyrrole/Graphene Oxide	9.56	[60]
Activated carbon/magnetite	57.37	[61]
Mycelian/ carboxymethylcellulose	32.20	[62]
Poly-(methyl acrylate)/guar gum	29.67	[63]

5.3.8 Antifungal activity of CMTKG/ZnO nanocomposites

The antifungal activity of CMTKG/ZnO nanocomposites is presented in Table 5.2. The antifungal activity of CMTKG/ZnO nanocomposites was determined against *A. flavus* MTCC2799. The different concentration (in ppm) was evaluated against the radial growth of *A. flavus* MTCC 2799. The result shows the highest concentration i.e., 3000 ppm was the most effective concentration which inhibit the 50% radial growth of tested fungi followed by 2000 ppm (Figure 5.7). However lower concentration i.e., 1000 ppm only inhibited 26.0 % of radial growth. As a consequence, it was shown that CMTKG/ZnO nanocomposites have substantial antifungal activity. The antifungal activity of Zinc oxide nanoparticle due to the production of Reactive Oxygen Species (ROS) which result in Oxidative stress.

Table 5.2: Percentage radial growth against *Aspersilium flamous* (MTCC-2799) at 1000, 2000, and 3000 ppm

Concentration	Growth area (mm)	Average area growth (mm)	% Inhibition growth
Control	56.00, 54.00	55.00	00.00
1000 ppm	40.00, 41.00	40.50	26.36
2000 ppm	34.00, 37.00	35.50	35.45
3000 ppm	27.00, 28.00	27.50	50.00

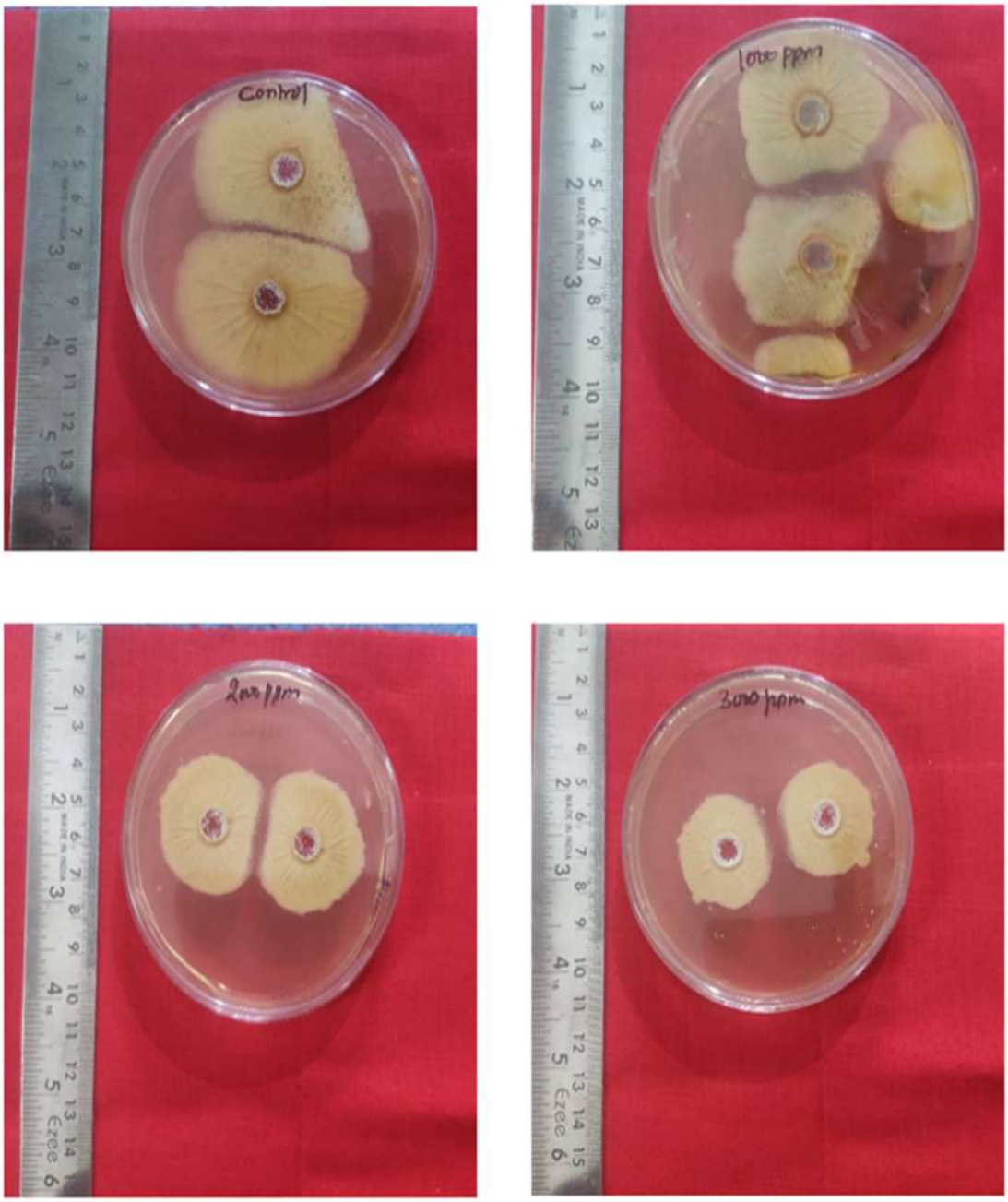

Figure 5.7: Antifungal activity of CMTKG/ZnO nanocomposites against *Aspersilium flamous* (MTCC-2799) at 1000, 2000, and 3000 ppm

5.4 Conclusion

Using an in-situ co-precipitation technique, ZnO nanoparticles consolidated CMTKG to create a new nanocomposite. SEM, HR-TEM, X-ray spectrum analysis, and DLS analysis all showed that rectangular CMTKG/ZnO nanocomposites with average sizes between 31 and 90

nm were produced. It is also presumed that the ZnO nanoparticles are attached to the carboxymethyl tamarind kernel gum biopolymer matrix through H-bonding between the hydroxyl and ZnO nanoparticles, as shown in Figure 5.8. The maximal adsorption capacity of chromium metal has been attained by a successful adsorption procedure. High evacuation productivity, contact time (80 minutes), adsorbent component (2.0 g/L), and adsorptions based on starting chromium concentrations were all confirmed (93.40 %). Subsequently, it was discovered that employing CMTKG/ZnO nanocomposite as the major adsorbent, this technique demonstrated promising, rapid, and efficient removal of chromium (VI) in comparison to earlier reported methods We discovered that the antifungal activity of CMTKG/ZnO nanocomposites has been considerably enhanced.

References

1. C. Yan, Z. Qu, J. Wang, L. Cao, Q. Han, Microalgal bioremediation of heavy metal pollution in water: Recent advances, challenges, and prospects, Chemosphere. 286 (2022) 131870. https://doi.org/10.1016/j.chemosphere.2021.131870.
2. Q. Xu, F. Zhao, B. Wu, X. Fang, J. Chen, T. Yang, X. Chai, L. Yuan, Assessment of Heavy Metal Pollution in Suburban River Sediment of Nantong (China) and Preliminary Exploration of Solidification/Stabilization Scheme, Water. 14 (2022) 2247. https://doi.org/10.3390/w14142247.
3. Jun, R.; Ling, T.; Guanghua, Z. Effects of Chromium on Seed Germination, Root Elongation and Coleoptile Growth in Six Pulses. *Int. J. Environ. Sci. Technol.* 2009, *6* (4), 571–578. https://doi.org/10.1007/BF03326097.
4. Fellenz, N.; Perez-Alonso, F. J.; Martin, P. P.; García-Fierro, J. L.; Bengoa, J. F.; Marchetti, S. G.; Rojas, S. Chromium (VI) Removal from Water by Means of Adsorption-Reduction at the Surface of Amino-Functionalized MCM-41 Sorbents. *Microporous Mesoporous Mater.* 2017, *239*, 138–146. https://doi.org/10.1016/j.micromeso.2016.10.012.
5. Gokila, S.; Gomathi, T.; Sudha, P. N.; Anil, S. Removal of the Heavy Metal Ion Chromiuim(VI) Using Chitosan and Alginate Nanocomposites. *Int. J. Biol. Macromol.* 2017, *104*, 1459–1468. https://doi.org/10.1016/j.ijbiomac.2017.05.117.
6. Zhitkovich, A. Chromium in Drinking Water: Sources, Metabolism, and Cancer Risks. *Chem. Res. Toxicol.* 2011, *24* (10), 1617–1629. https://doi.org/10.1021/tx200251t.
7. Megharaj, M.; Avudainayagam, S.; Naidu, R. Toxicity of Hexavalent Chromium and Its Reduction by Bacteria Isolated from Soil Contaminated with Tannery Waste. *Curr. Microbiol.* 2003, *47* (1), 51–54. https://doi.org/10.1007/s00284-002-3889-0.

8. Oliveira, H. Chromium as an Environmental Pollutant: Insights on Induced Plant Toxicity. *J. Bot.* 2012, *2012*, 1–8. https://doi.org/10.1155/2012/375843.
9. Shanker, A. K.; Cervantes, C.; Loza-Tavera, H.; Avudainayagam, S. Chromium Toxicity in Plants. *Environ. Int.* 2005, *31* (5), 739–753. https://doi.org/10.1016/j.envint.2005.02.003.
10. Velma, V.; Vutukuru, S. S.; Tchounwou, P. B. Ecotoxicology of Hexavalent Chromium in Freshwater Fish: A Critical Review. *Rev. Environ. Health* 2009, *24* (2), 129–145. https://doi.org/10.1515/REVEH.2009.24.2.129.
11. F.L. Petrilli, S. De Flora, Toxicity and Mutagenicity of Hexavalent Chromium on Salmonella typhimurium, Appl. Environ. Microbiol. 33 (1977) 805–809. https://doi.org/10.1128/aem.33.4.805-809.1977.
12. Zhao, G.; Huang, X.; Tang, Z.; Huang, Q.; Niu, F.; Wang, X. Polymer-Based Nanocomposites for Heavy Metal Ions Removal from Aqueous Solution: A Review. *Polym. Chem.* 2018, *9* (26), 3562–3582. https://doi.org/10.1039/c8py00484f.
13. Khan, T. A.; Nazir, M.; Ali, I.; Kumar, A. Removal of Chromium(VI) from Aqueous Solution Using Guar Gum–Nano Zinc Oxide Biocomposite Adsorbent. *Arab. J. Chem.* 2017, *10*, S2388–S2398. https://doi.org/10.1016/j.arabjc.2013.08.019.
14. M. Shi, Y. Zhang, W. Hong, J. Liu, H. Zhu, X. Liu, Y. Geng, Z. Cai, S. Lin, C. Ni, Mechanism of simultaneous lead and chromium removal from contaminated wastewater by a schwertmannite-like mineral, Environ. Sci. Pollut. Res. (2022). https://doi.org/10.1007/s11356-022-21312-9.
15. Z. Fang, W. Liu, T. Yao, G. Zhou, S. Wei, L. Qin, Experimental study of chromium (III) coprecipitation with calcium carbonate, Geochim. Cosmochim. Acta. 322 (2022) 94–108. https://doi.org/10.1016/j.gca.2022.01.019.
16. Cheng, Q.; Wang, C.; Doudrick, K.; Chan, C. K. Hexavalent Chromium Removal Using Metal Oxide Photocatalysts. *Appl. Catal. B Environ.* 2015, *176–177*, 740–748. https://doi.org/10.1016/j.apcatb.2015.04.047.
17. Mahringer, D.; Zerelli, S. S.; Dippon, U.; Ruhl, A. S. Pilot Scale Hexavalent Chromium Removal with Reduction, Coagulation, Filtration and Biological Iron Oxidation. *Sep. Purif. Technol.* 2020, *253* (July), 117478. https://doi.org/10.1016/j.seppur.2020.117478.
18. Martín-Domínguez, A.; Rivera-Huerta, M. L.; Pérez-Castrejón, S.; Garrido-Hoyos, S. E.; Villegas-Mendoza, I. E.; Gelover-Santiago, S. L.; Drogui, P.; Buelna, G. Chromium Removal from Drinking Water by Redox-Assisted Coagulation: Chemical versus Electrocoagulation. *Sep. Purif. Technol.* 2018, *200*, 266–272. https://doi.org/10.1016/j.seppur.2018.02.014.
19. Wang, H.; Song, X.; Zhang, H.; Tan, P.; Kong, F. Removal of Hexavalent Chromium in Dual-Chamber Microbial Fuel Cells Separated by Different Ion Exchange Membranes. *J. Hazard. Mater.* 2020, *384*, 121459. https://doi.org/10.1016/j.jhazmat.2019.121459.

20. Peng, H.; Guo, J. Removal of Chromium from Wastewater by Membrane Filtration, Chemical Precipitation, Ion Exchange, Adsorption Electrocoagulation, Electrochemical Reduction, Electrodialysis, Electrodeionization, Photocatalysis and Nanotechnology: A Review. *Environ. Chem. Lett.* 2020, *18* (6), 2055–2068. https://doi.org/10.1007/s10311-020-01058-x.
21. Xie, Y.; Lin, J.; Liang, J.; Li, M.; Fu, Y.; Wang, H.; Tu, S.; Li, J. Hypercrosslinked Mesoporous Poly(Ionic Liquid)s with High Density of Ion Pairs: Efficient Adsorbents for Cr(VI) Removal via Ion-Exchange. *Chem. Eng. J.* 2019, *378* (April), 122107. https://doi.org/10.1016/j.cej.2019.122107.
22. L. Zhou, T. Chi, Y. Zhou, J. Lv, H. Chen, S. Sun, X. Zhu, H. Wu, X. Hu, Efficient removal of hexavalent chromium through adsorption-reduction-adsorption pathway by iron-clay biochar composite prepared from Populus nigra, Sep. Purif. Technol. 285 (2022) 120386. https://doi.org/10.1016/j.seppur.2021.120386.
23. F. Chen, S. Guo, Y. Wang, L. Ma, B. Li, Z. Song, L. Huang, W. Zhang, Concurrent adsorption and reduction of chromium(VI) to chromium(III) using nitrogen-doped porous carbon adsorbent derived from loofah sponge, Front. Environ. Sci. Eng. 16 (2022) 57. https://doi.org/10.1007/s11783-021-1491-6.
24. S.G. Warkar, J. Meena, Synthesis and applications of biopolymer/FeO nanocomposites: A review, J. New Mater. Electrochem. Syst. 25 (2022) 7–16. https://doi.org/10.14447/JNMES.V25I1.A02.
25. L. Fei, M. Bilal, S.A. Qamar, H.M. Imran, A. Riasat, M. Jahangeer, M. Ghafoor, N. Ali, H.M.N. Iqbal, Nano-remediation technologies for the sustainable mitigation of persistent organic pollutants, Environ. Res. 211 (2022) 113060. https://doi.org/10.1016/j.envres.2022.113060.
26. C. An, C. Sun, N. Li, B. Huang, J. Jiang, Y. Shen, C. Wang, X. Zhao, B. Cui, C. Wang, X. Li, S. Zhan, F. Gao, Z. Zeng, H. Cui, Y. Wang, Nanomaterials and nanotechnology for the delivery of agrochemicals: strategies towards sustainable agriculture, J. Nanobiotechnology. 20 (2022) 11. https://doi.org/10.1186/s12951-021-01214-7.
27. Khan, S.; Naushad, M.; Al-Gheethi, A.; Iqbal, J. Engineered Nanoparticles for Removal of Pollutants from Wastewater: Current Status and Future Prospects of Nanotechnology for Remediation Strategies. *J. Environ. Chem. Eng.* 2021, *9* (5), 106160. https://doi.org/10.1016/j.jece.2021.106160.
28. Yadav, N.; Garg, V. K.; Chhillar, A. K.; Rana, J. S. Detection and Remediation of Pollutants to Maintain Ecosustainability Employing Nanotechnology: A Review. *Chemosphere* 2021, *280* (May), 130792. https://doi.org/10.1016/j.chemosphere.2021.130792.

29. H.H. Azeez, A.A. Barzinjy, S.M. Hamad, Structure, synthesis and applications of ZnO nanoparticles: A review, Jordan J. Phys. 13 (2020) 123–135. https://doi.org/10.47011/13.2.4.
30. Prasad, K.; K. Jha, A. ZnO Nanoparticles: Synthesis and Adsorption Study. *Nat. Sci.* 2009, *01* (02), 129–135. https://doi.org/10.4236/ns.2009.12016.
31. Ma, Q.; Lin, Z. H.; Yang, N.; Li, Y.; Su, X. G. A Novel Carboxymethyl Chitosan-Quantum Dot-Based Intracellular Probe for Zn2+ Ion Sensing in Prostate Cancer Cells. *Acta Biomater.* 2014, *10* (2), 868–874. https://doi.org/10.1016/j.actbio.2013.10.039.
32. P. Kumar, Nisha, P. Sarkar, S. Singh, B.C.K. Mishra, R.S. Katiyar, The influence of post-growth heat treatment on the optical properties of pulsed laser deposited ZnO thin films, Appl. Phys. A. 128 (2022) 372. https://doi.org/10.1007/s00339-022-05511-2.
33. U. Rajamanickam, S. Viswanathan, P. Muthusamy, Biosynthesis of Zinc Nanoparticles Using Actinomycetes for Antibacterial Food Packaging, Int. Conf. Nutr. Food Sci. 39 (2012) 195–199.
34. Akpomie, K. G.; Ghosh, S.; Gryzenhout, M.; Conradie, J. One-Pot Synthesis of Zinc Oxide Nanoparticles via Chemical Precipitation for Bromophenol Blue Adsorption and the Antifungal Activity against Filamentous Fungi. *Sci. Rep.* 2021, *11* (1), 1–17. https://doi.org/10.1038/s41598-021-87819-2.
35. M. Hasanin, E.M. Swielam, N.A. Atwa, M.M. Agwa, Novel design of bandages using cotton pads, doped with chitosan, glycogen and ZnO nanoparticles, having enhanced antimicrobial and wounds healing effects, Int. J. Biol. Macromol. 197 (2022) 121–130. https://doi.org/10.1016/j.ijbiomac.2021.12.106.
36. N. Serpone, D. Dondi, A. Albini, Inorganic and organic UV filters: Their role and efficacy in sunscreens and suncare products, Inorganica Chim. Acta. 360 (2007) 794–802. https://doi.org/10.1016/j.ica.2005.12.057.
37. Marcì, G.; Augugliaro, V.; López-Muñoz, M. J.; Martín, C.; Palmisano, L.; Rives, V.; Schiavello, M.; Tilley, R. J. D.; Venezia, A. M. Preparation Characterization and Photocatalytic Activity of Polycrystalline ZnO/TiO2 Systems. 2. Surface, Bulk Characterization, and 4-Nitrophenol Photodegradation in Liquid-Solid Regime. *J. Phys. Chem. B* 2001, *105* (5), 1033–1040. https://doi.org/10.1021/jp003173j.
38. S. Singh, M. Joshi, P. Panthari, B. Malhotra, A.C. Kharkwal, H. Kharkwal, Citrulline rich structurally stable zinc oxide nanostructures for superior photo catalytic and optoelectronic applications: A green synthesis approach, Nano-Structures & Nano-

Objects. 11 (2017) 1–6. https://doi.org/10.1016/j.nanoso.2017.05.006.

39. Díez-Pascual, A. M. Synthesis and Applications of Biopolymer Composites. *Int. J. Mol. Sci.* 2019, *20* (9). https://doi.org/10.3390/ijms20092321.
40. J. Baranwal, B. Barse, A. Fais, G.L. Delogu, A. Kumar, Biopolymer: A Sustainable Material for Food and Medical Applications, Polymers (Basel). 14 (2022) 983. https://doi.org/10.3390/polym14050983.
41. S.E. Harding, M.P. Deacon, I. Fiebrig, S.S.B. Davis, M.P. Deacon, I. Fiebrig, S.S.B. Davis, Biopolymer Mucoadhesives, Biotechnol. Genet. Eng. Rev. 16 (1999) 41–86. https://doi.org/10.1080/02648725.1999.10647971.
42. M.S.B. Reddy, D. Ponnamma, R. Choudhary, K.K. Sadasivuni, A Comparative Review of Natural and Synthetic Biopolymer Composite Scaffolds, Polymers (Basel). 13 (2021) 1105. https://doi.org/10.3390/polym13071105.
43. B. Aaliya, K. Valiyapeediyekkal Sunooj, M. Lackner, Biopolymer composites: a review, Int. J. Biobased Plast. 3 (2021) 40–84. https://doi.org/10.1080/24759651.2021.1881214.
44. J. Puiggalí, R. Katsarava, Bionanocomposites, in: Clay-Polymer Nanocomposites, Elsevier, 2017: pp. 239–272. https://doi.org/10.1016/B978-0-323-46153-5.00007-0.
45. Darder, M.; Aranda, P.; Ruiz-Hitzky, E. Bionanocomposites: A New Concept of Ecological, Bioinspired, and Functional Hybrid Materials. *Adv. Mater.* 2007, *19* (10), 1309–1319. https://doi.org/10.1002/adma.200602328.
46. Meena, J. R.; Vishwavidyalaya, G. K. Synthesis and Applications of Biopolymer / FeO Nanocomposites : A Review. 2022, No. May. https://doi.org/10.14447/jnmes.v25i1.a02.
47. C. Wang, X. Gao, Z. Chen, Y. Chen, H. Chen, Preparation, Characterization and Application of Polysaccharide-Based Metallic Nanoparticles: A Review, Polymers (Basel). 9 (2017) 689. https://doi.org/10.3390/polym9120689.
48. J. Meena, S.K. Verma, R. Rameshwari, D.K. Verma, Polyaniline/carboxymethyl guar gum nanocomposites: as biodegradable, conductive film, RASAYAN J. Chem. 15 (2022) 1021–1027. https://doi.org/10.31788/RJC.2022.1526820.
49. Khushbu; Warkar, S. G.; Kumar, A. Synthesis and Assessment of Carboxymethyl Tamarind Kernel Gum Based Novel Superabsorbent Hydrogels for Agricultural Applications. *Polymer (Guildf).* 2019, *182* (September), 121823. https://doi.org/10.1016/j.polymer.2019.121823.
50. Pandit, A. P.; Waychal, P. D.; Sayare, A. S.; Patole, V. C. Carboxymethyl Tamarind Seed Kernel Polysaccharide Formulated into Pellets to Target at Colon. *Indian J. Pharm. Educ. Res.* 2018, *52* (3), 363–373. https://doi.org/10.5530/ijper.52.3.42.
51. Singh, V.; Kumar, P. Carboxymethyl Tamarind Gum-Silica Nanohybrids for Effective

Immobilization of Amylase. *J. Mol. Catal. B Enzym.* 2011, *70* (1–2), 67–73. https://doi.org/10.1016/j.molcatb.2011.02.006.

52. Goyal, P.; Kumar, V.; Sharma, P. Carboxymethylation of Tamarind Kernel Powder. *Carbohydr. Polym.* 2007, *69* (2), 251–255. https://doi.org/10.1016/j.carbpol.2006.10.001.
53. S.C. Dhawale, R.J. Dias, V.D. Havaldar, P.R. Kavitake, K.K. Mali, Interpenetrating networks of carboxymethyl tamarind gum and chitosan for sustained delivery of aceclofenac, Marmara Pharm. J. 21 (2017) 771–782. https://doi.org/10.12991/mpj.2017.20.
54. B. Lallo da Silva, M.P. Abuçafy, E. Berbel Manaia, J.A. Oshiro Junior, B.G. Chiari-Andréo, R.C.R. Pietro, L.A. Chiavacci, Relationship Between Structure And Antimicrobial Activity Of Zinc Oxide Nanoparticles: An Overview, Int. J. Nanomedicine. Volume 14 (2019) 9395–9410. https://doi.org/10.2147/IJN.S216204.
55. Holzwarth, U.; Gibson, N. The Scherrer Equation versus the 'Debye-Scherrer Equation' *Nat. Publ. Gr.* 2011, *6* (9), 534.
56. Jain, D.; Shivani; Bhojiya, A. A.; Singh, H.; Daima, H. K.; Singh, M.; Mohanty, S. R.; Stephen, B. J.; Singh, A. Microbial Fabrication of Zinc Oxide Nanoparticles and Evaluation of Their Antimicrobial and Photocatalytic Properties. *Front. Chem.* 2020, *8*. https://doi.org/10.3389/fchem.2020.00778.
57. Pal, S.; Ghorai, S.; Das, C.; Samrat, S.; Ghosh, A.; Panda, A. B. Carboxymethyl Tamarind-g-Poly(Acrylamide)/Silica: A High Performance Hybrid Nanocomposite for Adsorption of Methylene Blue Dye. *Ind. Eng. Chem. Res.* 2012, *51* (48), 15546–15556. https://doi.org/10.1021/ie301134a.
58. Shen, Y. F.; Tang, J.; Nie, Z. H.; Wang, Y. D.; Ren, Y.; Zuo, L. Preparation and Application of Magnetic Fe3O4 Nanoparticles for Wastewater Purification. *Sep. Purif. Technol.* 2009, *68* (3), 312–319. https://doi.org/10.1016/j.seppur.2009.05.020.
59. Selvi, K.; Pattabhi, S.; Kadirvelu, K. Removal of Cr(VI) from Aqueous Solution by Adsorption onto Activated Carbon. *Bioresour. Technol.* 2001, *80* (1), 87–89. https://doi.org/10.1016/S0960-8524(01)00068-2.
60. Li, S.; Lu, X.; Xue, Y.; Lei, J.; Zheng, T.; Wang, C. Fabrication of Polypyrrole/Graphene Oxide Composite Nanosheets and Their Applications for Cr(VI) Removal in Aqueous Solution. *PLoS One* 2012, *7* (8). https://doi.org/10.1371/journal.pone.0043328.
61. Nethaji, S.; Sivasamy, A.; Mandal, A. B. Preparation and Characterization of Corn Cob Activated Carbon Coated with Nano-Sized Magnetite Particles for the Removal of Cr(VI). *Bioresour. Technol.* 2013, *134*, 94–100. https://doi.org/10.1016/j.biortech.2013.02.012.
62. Arica, M. Y.; Bayramoğlu, G. Cr(VI) Biosorption from Aqueous Solutions Using Free and Immobilized Biomass of Lentinus Sajor-Caju: Preparation and Kinetic Characterization.

Colloids Surfaces A Physicochem. Eng. Asp. 2005, *253* (1–3), 203–211. https://doi.org/10.1016/j.colsurfa.2004.11.012.

63. Singh, V.; Pandey, S.; Singh, S. K.; Sanghi, R. Removal of Cadmium from Aqueous Solutions by Adsorption Using Poly(Acrylamide) Modified Guar Gum-Silica Nanocomposites. *Sep. Purif. Technol.* 2009, *67* (3), 251–261. https://doi.org/10.1016/j.seppur.2009.02.023.

Chapter-6

Synthesis and characterization of carboxymethyl tamarind kernel gum nanoparticles and their application in antioxidant activity

6.1 Introduction

When compared to petroleum-based polymers, biopolymers are eco-friendly and naturally abundant polymer alternatives that are extensively used in the pharmaceutical, medical, agricultural, food packaging, biological activity, and environmental industries due to their particularly renewable, sustainable, and nontoxic properties [1–5]. Green synthesis, electrodeposition, combustion, in situ, ex-situ, wet method, hydrothermal, and nano-precipitation have all been used to create biopolymer nanoparticles [6,7]. Natural biopolymer nanoparticles are increasingly being used in applications such as pollution control [8,9], agricultural applications [10], adsorption [11–14], medication delivery [15–17], antibacterial activity [18,19], antioxidant activity [20], anti-cancer activity [21], and catalytic activity [22,23]. Tamarind kernel polymer (TKP) is produced from the seeds of the Tamarindus indica tree. The seeds contain xyloglucans, which are widely used as food thickeners and gelling agents. In the United States, it has primarily been used as a wet end additive in the paper industry, replacing starches and galactomannans [24]. Tamarind is a tropical evergreen tree native to India and other parts of the world. India is currently the world's largest tamarind producer [25]. An anionic water-soluble polymer that is generated from TKP and undergoes a chemical process to become cold water soluble is called carboxymethyl tamarind kernel gum (CMTKG). The polysaccharide chain is added with carboxymethyl groups (-CH2-COOH) so that the molecule may be hydrated in cold water [26]. TKP's derivatization with carboxymethyl groups expose the hydration-containing polysaccharide network, which increases viscosity and prolongs the product's shelf life [27].

CMTKG is composed of D-xylose, D-galactose, and D-glucose in a 1:2:3 molar ratio [28]. This polysaccharide is composed of a carboxymethylated chain of glucopyranosyl units linked by β-D-(1 → 4) and a side chain containing a single xylopyranosyl unit that is further connected to each subsequent second, third, and fourth D-glucopyranosyl unit by α-D-(1 → 6) linkage. While a β-D-(1 → 2) linkage connects one xylopyranosyl unit to one of the D-galactopyranosyl units [29]. It is biodegradable and non-toxic. CMTKG has been used to

create pellets, films, hydrogel and other products. CMTKG nanoparticles is expected to have a wide range of applications, including antioxidant, antibacterial, antifungal, anti-fouling, organic/inorganic impurity removal, drug delivery, medical field, anticatalyst activity, and so on [27,30].

The current study's goals are to synthesize the CMTKG nanoparticles and investigate its antioxidant activity. By using the nano-precipitation approach, CMTKG nanoparticles were synthesized. In this work, the structural, morphological, and antioxidant properties of the optimised CMTKG nanoparticle formulation were assessed.

6.2 Experimental

6.2.1 Reagents and chemicals

Hindustan Gum and Chemicals Ltd. in Bhiwani, Haryana, India supplied the carboxymethyl tamarind kernel gum. It was used without purification. Acetone, and ethanol were procured from Central Drug House Pvt. Ltd. New Delhi, India. Every solution used in the analysis was made in double-distilled water (DDW).

6.2.2 Preparation of carboxymethyl tamarind kernel nanoparticles

One gram of carboxymethyl tamarind kernel gum and 150 millilitres of DDW were homogenized in the conical flask. The mixture was magnetically agitated at 40°C to produce viscous solutions. After that, it was continually stirred for 24 hours at 75°C in order to produce a clear solution. The mixture was centrifuged at 10,000 rpm for 20 minutes and then washed with acetone to get rid of any loose debased particles. Following a C_2H_5OH wash, the precipitate was dried in a hot air oven at 50°C. The CMTKG was reduced to a powder. Before being used again, this was kept in desiccators and cleaned with acetone to get rid of any loose debased particles. A visual illustration of the creation of carboxymethyl tamarind kernel gum nanoparticles is shown in Figure 6.1. In order to conduct further testing, a modest amount of these nanoparticles was suspended in the adequate volume of DDW.

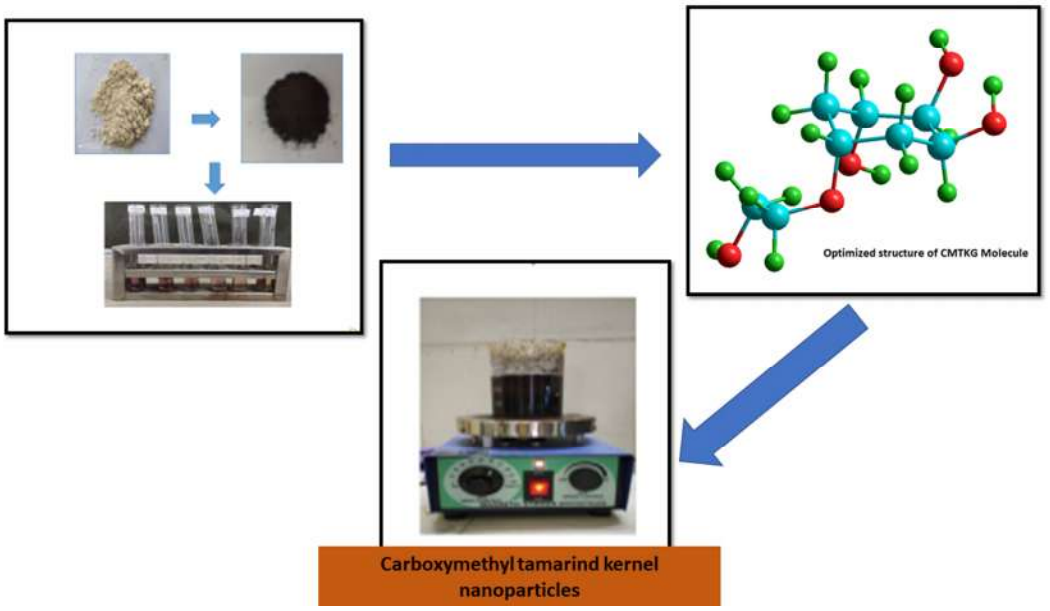

Figure 6.1: Diagrammatic presentation of carboxymethyl tamarind kernel gum nanoparticles synthesis

6.2.3 Characterization

6.2.3.1 Fourier transform infrared (FTIR) analysis

On a Perkin Elmer FT-IR BX2 instrument, infrared spectrum analysis (4000–400 cm^{-1}) had been investigated. The pellets were made by combining 10 mg of the test sample and 200 mg of KBr Spectroscopic grade.

6.2.3.2 Field emission Scamming Electron Microscopy (FE-SEM) Analysis

Surface morphological analysis of CMTKG nanoparticles was done by Scanning Electron Microscope (Model: JEOL JSM-6610LV).

6.2.3.3 High Resolution Transmission Electron Microscopy (HR-TEM)

HR-TEM analysis was conducted by JEOL: JEM 2100 plus model. 5 mg of dry CMTKG nanoparticles were dissolved in 25 mL of C_2H_5OH and sonicated to mix the mixture. A copper grid that had been thoroughly covered with a 10 mL dispersion of nanoparticles (chloroform 1 percent arrangement of formvar in spectroscopic grade) was then dried in vacuum.

6.2.3.4 X-ray diffraction (XRD) analysis

X-ray diffraction studies of synthesized CMTKG nanoparticles were carried out using an X-ray diffractometer (P Analytical X'Pert Pro). The analysis was conducted at the current and voltage of 40 mA using Cu K α radiations (k = 1.5406 nm and λ=1.5406 Å) and Scanning angle 2θ in the range of 0-80^{o}. The following Debye-Scherrer [31] equation (6.1) was used to estimate the nanoparticle size of CMTKG nanoparticles.

$$D = \frac{K\lambda}{\beta\cos\theta} \qquad (6.1)$$

The wavelength of a source 1.5 the (FWHM), and the angle direction are all represented by k = 0.9.

6.2.3.5 Thermal gravimetric analysis (TGA)

TGA of CMTKG nanoparticle were performed with 10°C/min uniform heating rate and inert nitrogen atmosphere (25-900°C) using a Perkin Elmer Differential Thermal Analyser.

6.2.4 DPPH scavenging activity

The ability of carboxymethyl tamarind kernel gum to scavenge 2,2-dyphenyl-2-picrylhydrazyl (DPPH) free radicals was investigated [32,33]. The DMSO was diluted to 1 mg/mL using the CMTKG stock solution. Diluted solutions (1 mL each) were coupled with DPPH (3 mL), as shown in Figure 6.2. The absorbance was measured at 517 nm after 30 minutes in the dark at room temperature, much like the control samples [34].

The % inhibition was calculated using the formula below (Eq. 6.2):

$$\text{Inhibition } \% = \frac{\text{Absorbace of Blank} - \text{Absorbance of sample}}{\text{Absorbance of Blank}} \times 100 \qquad (6.2)$$

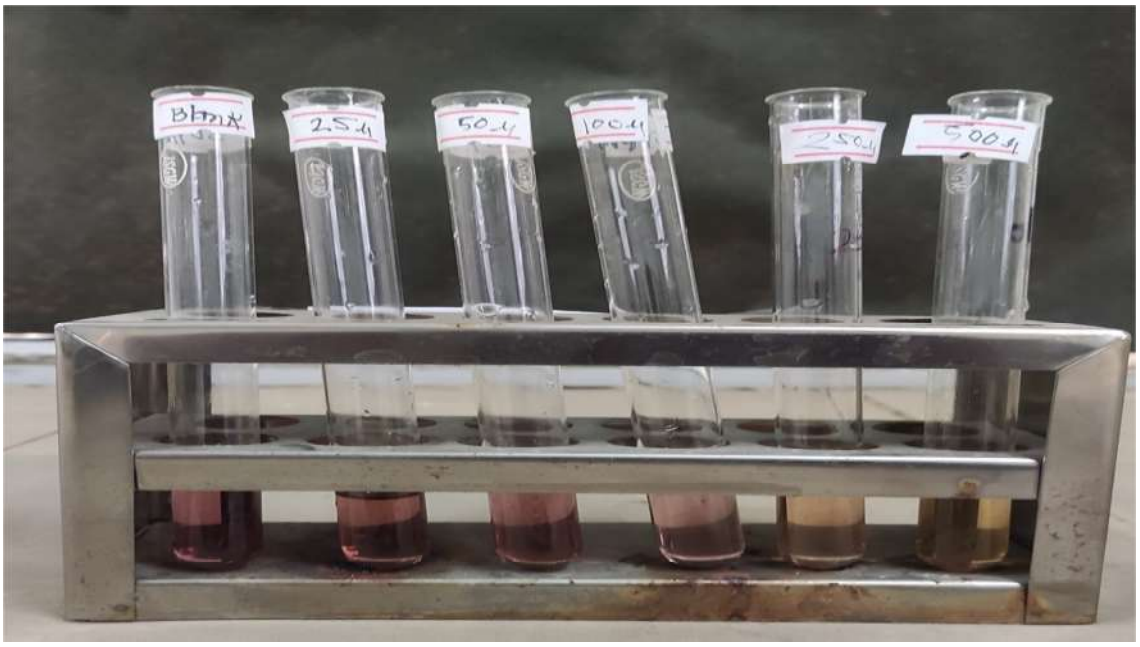

Figure 6.2: Solutions prepared for the analysis of antioxidant activity of CMTKG nanoparticles

6.3 Results and discussions

6.3.1 FTIR

CMTKG nanoparticles' FTIR spectral band is shown in Figure 6.3. The -OH stretching vibrations exhibit a significant absorption peak at 3430 cm-1 in CMTKG. C-H stretching vibrations were associated with the absorption at 2925 cm-1. At 1630 cm-1, COO-symmetric vibrations absorb energy, whereas linked O-H bending and C-O stretching vibrations absorb energy at 1410 cm-1 and 1114 cm-1, respectively [35].

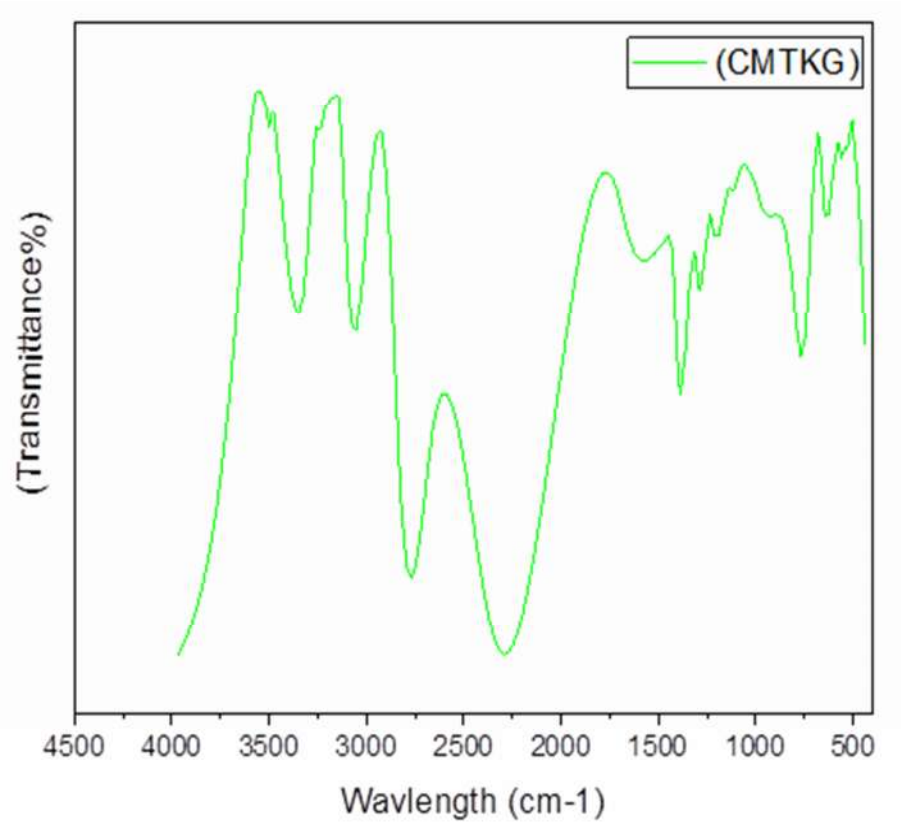

Figure 6.3: FTIR of CMTKG nanoparticles

6.3.2 FE-SEM Microgram

Figure 6.4 shows SEM micrographs and particle size distribution of CMTKG nanoparticles. It is shown that CMTKG is uniformly decorated, and is completely fabricated of almost spherical aggregates on the surface with varying diameters. Additionally, a range of particle sizes between 30 and 40 nm was discovered.

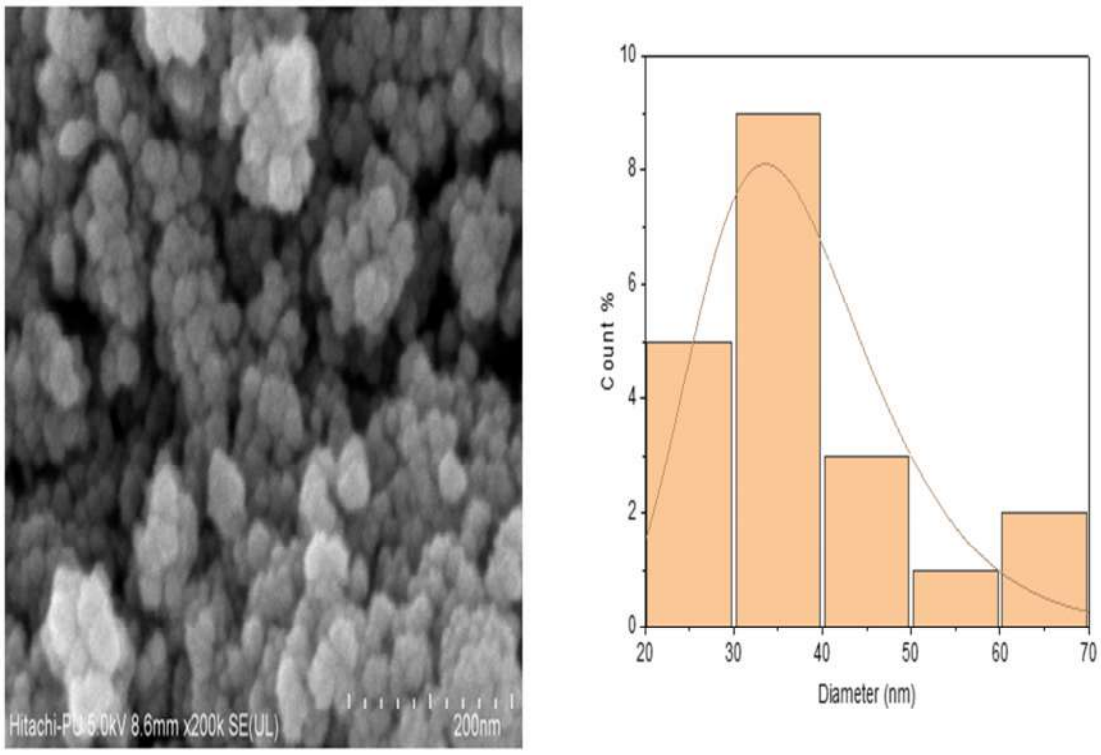

Figure 6.4: SEM micrographs and particle size distribution of CMTKG nanoparticles

6.3.3 HR-TEM

HR-TEM images were used to determine the form, size, and lattice spacing of the CMTKG nanoparticle, as shown in Figure 6.5. The TEM images show fine spherical nanoparticles of 20-50 nm, as well as a few larger particles and clusters in the size range 50–70 nm. These clusters could be caused by drying-induced aggregation during TEM grid preparation [36].

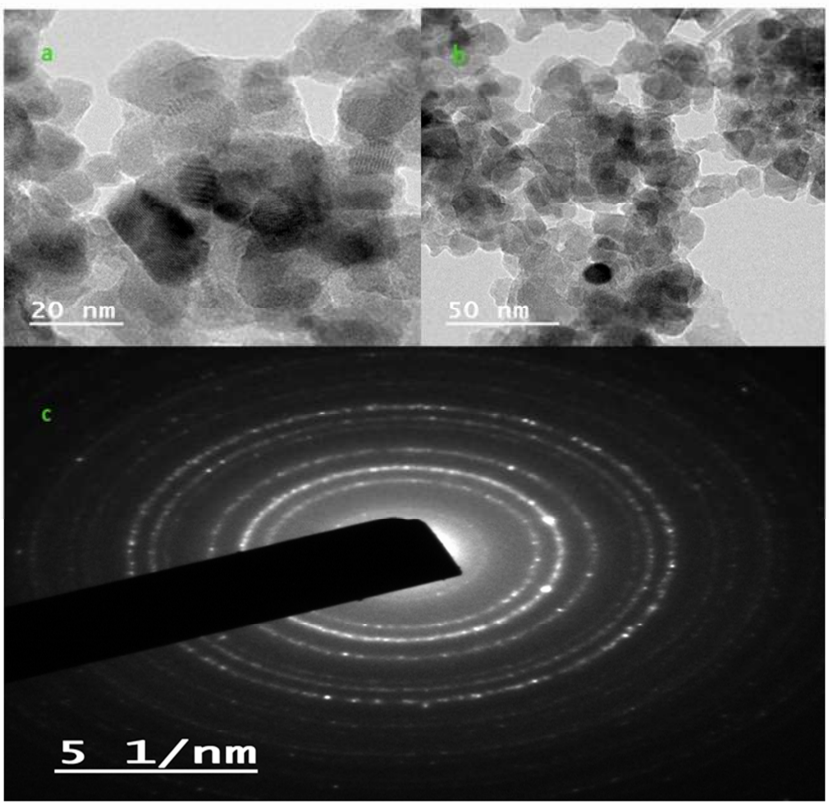

Figure 6.5: High Resolution Transmission electron microscopy of CMTKG nanoparticles

6.3.4 XRD

XRD analysis has been used to study nanoparticles in CMTKG in order to identify their crystalline structure. The X-ray patterns of CMTKG nanoparticles are depicted in Figure 6.6; these findings correlate with the development of nanostructures since they display essentially similar patterns with distinct peaks. The average size of CMTKG nanoparticles was found to be 42.50 nm. A similar finding has been made in the literature [35].

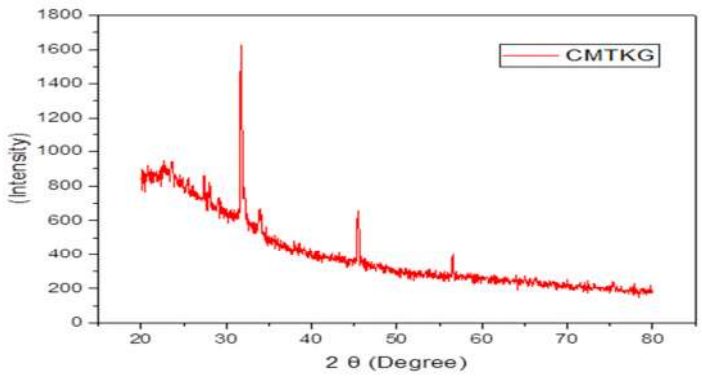

Figure 6.6: X ray diffraction of CMTKG nanoparticles

6.3.5 TGA

Figure 6.7 illustrates the weight variations in CMTKG nanoparticles that were observed as the temperature is raised. At three distinct points, the weight reduction was examined. At the initial stage (32-160°C), the weight dropped by 5.75 %, which is characteristic of wet expulsions from the biopolymer. The dissolution of the CMTKG's carboxymethyl and hydroxyl groups, as well as decrease in the biopolymer backbone, may be accountable for the second stage of weight loss (190–420°C). The third stage of deterioration (653-725°C) occurred with a weight loss of 3.96 % [7].

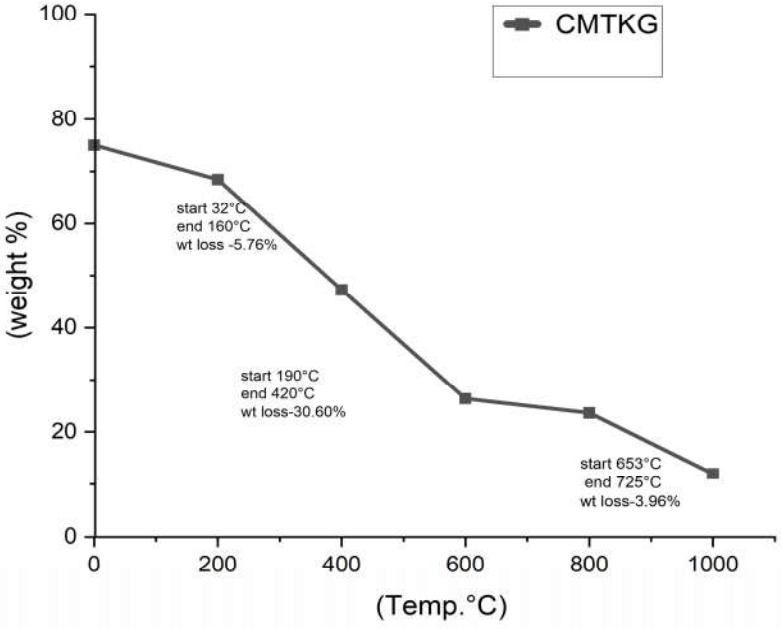

Figure 6.7: Thermo-gravimetric analysis of CMTKG nanoparticles

6.3.6 Antioxidant activity of CMTKG nanoparticles

At room temperature, the efficiency of CMTKG nanoparticles and a conventional anti - oxidant to scavenge free DPPH was investigated with CMTKG nanoparticle concentrations ranging from 25 µg/mL to 500 µg/mL (Table 6.1). With increasing CMTKG nanoparticle concentrations in DMSO, a dose response scavenging effect was seen (Figure 6.8). CMTKG nanoparticles at a concentration of 500 µg/mL were reported to have the greatest value [36,37].

Table 6.1: Antioxidant activity of CMTKG nanoparticles

CMTKG solution	Absorbance (nm)	Colours
Blank CMTKG solution	0.485	Pink
25 µg/mL	0.432	Light pink
50 µg/mL	0.401	Very light pink
100 µg/mL	0.387	Brown
250 µg/mL	0.292	Light brown
500 µg/mL	0.231	Very brown

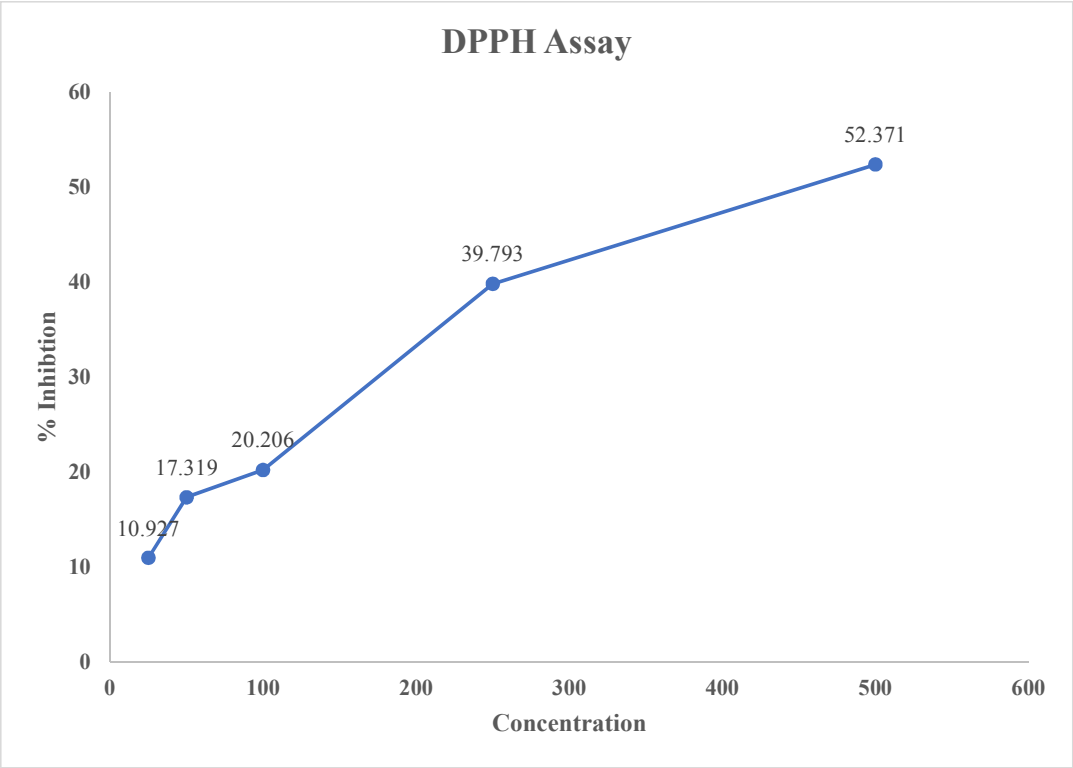

Figure 6.8: Antioxidant activity of CMTKG nanoparticles

6.4 Conclusion

The nano-precipitation approach was employed to successfully generate CMTKG nanoparticles in study Chapter-6. FTIR, SEM, TEM, TDA, and XRD investigations were used to characterize the physical, structural, and morphological features of CMTKG nanoparticles, such as size, shape, and dispersity. CMTKG nanoparticles ranged in size from 20 to 50 nm with average size of 42.50 nm as calculated from Debye-Scherrer equation. The nanoparticles were found to be spherical in shape, with diameters ranging from 20 to 50 nm, as well as scattered huge nanoparticles and clusters of 50 nm, as revealed by TEM. The antioxidant capabilities of the produced CMTKG nanoparticles composites were demonstrated by a radical scavenging model system. All of the outcomes were perfectly matched, just as they had been in the literature. CMTKG nanoparticles created in this manner could be employed as antioxidants. CMTKG nanoparticles are bioactive, biocompatible, and possess antibacterial properties, and hence can be exploited as a bio-polymeric material in tissue engineering, biomedical, and therapeutic applications, according to the findings of this study

References

[1] C. Zhao, J. Li, B. He, L. Zhao, Fabrication of hydrophobic biocomposite by combining cellulosic fibers with polyhydroxyalkanoate, Cellulose. 24 (2017) 2265–2274. https://doi.org/10.1007/s10570-017-1235-8.

[2] S. Gupta, S. Sharma, A. Kumar Nadda, M. Saad Bala Husain, A. Gupta, Biopolymers from waste biomass and its applications in the cosmetic industry: A review, Mater. Today Proc. (2022). https://doi.org/10.1016/j.matpr.2022.06.422.

[3] S. Kumar, I.B. Basumatary, A. Mukherjee, J. Dutta, An Overview of Natural Biopolymers in Food Packaging, in: Biopolym. Food Packag., Wiley, 2022: pp. 1–28. https://doi.org/10.1002/9781119702313.ch1.

[4] R. Agrawal, A. Kumar, S. Singh, K. Sharma, Recent advances and future perspectives of lignin biopolymers, J. Polym. Res. 29 (2022) 222. https://doi.org/10.1007/s10965-022-03068-5.

[5] A. Srivastava, A.K. Srivasatva, A. Singh, P. Singh, S. Verma, M. Vats, S. Sagadevan, Biopolymers as renewable polymeric materials for sustainable development - an overview, Polimery. 67 (2022) 185–196. https://doi.org/10.14314/polimery.2022.5.1.

[6] D.K. Verma, R. Malik, J. Meena, R. Rameshwari, Synthesis, characterization and applications of chitosan based metallic nanoparticles: A review, J. Appl. Nat. Sci. 13 (2021) 544–551. https://doi.org/10.31018/jans.v13i2.2635.

[7] S.G. Warkar, J. Meena, Synthesis and applications of biopolymer/FeO nanocomposites: A review, J. New Mater. Electrochem. Syst. 25 (2022) 7–16. https://doi.org/10.14447/JNMES.V25I1.A02.

[8] S. Palit, C.M. Hussain, Biopolymers, Nanocomposites, and Environmental Protection: A Far-Reaching Review, in: Bio-Based Mater. Food Packag., Springer Singapore, Singapore, 2018: pp. 217–236. https://doi.org/10.1007/978-981-13-1909-9_10.

[9] H. Souzandeh, Y. Wang, A.N. Netravali, W.-H. Zhong, Towards Sustainable and Multifunctional Air-Filters: A Review on Biopolymer-Based Filtration Materials, Polym. Rev. 59 (2019) 651–686. https://doi.org/10.1080/15583724.2019.1599391.

[10] Khushbu, S.G. Warkar, A. Kumar, Synthesis and assessment of carboxymethyl tamarind kernel gum based novel superabsorbent hydrogels for agricultural applications, Polymer (Guildf). 182 (2019) 121823. https://doi.org/10.1016/j.polymer.2019.121823.

[11] P.R. Yaashikaa, P. Senthil Kumar, S. Karishma, Review on biopolymers and composites – Evolving material as adsorbents in removal of environmental pollutants, Environ. Res. 212 (2022) 113114. https://doi.org/10.1016/j.envres.2022.113114.

[12] N. Molaei, O. Bashir Wani, E.R. Bobicki, A comparative study of biopolymer adsorption on model anisotropic clay surfaces using quartz crystal microbalance with dissipation (QCM-D), J. Colloid Interface Sci. 615 (2022) 543–553. https://doi.org/10.1016/j.jcis.2022.01.180.

[13] F. Yang, P. Yang, Biopolymer□Based Membrane Adsorber for Removing Contaminants from Aqueous Solution: Progress and Prospects, Macromol. Rapid Commun. 43 (2022) 2100669. https://doi.org/10.1002/marc.202100669.

[14] A. Tursi, V. Gallizzi, F. Olivito, V. Algieri, A. De Nino, L. Maiuolo, A. Beneduci, Selective and efficient mercury(II) removal from water by adsorption with a cellulose citrate biopolymer, J. Hazard. Mater. Lett. 3 (2022) 100060. https://doi.org/10.1016/j.hazl.2022.100060.

[15] S. Dragojevic, L. Turner, D. Raucher, Circumventing Doxorubicin Resistance Using Elastin-like Polypeptide Biopolymer-Mediated Drug Delivery, Int. J. Mol. Sci. 23 (2022) 2301. https://doi.org/10.3390/ijms23042301.

[16] Kirti, S.S. Khora, Alginate: A Promising Biopolymer in Drug Delivery System, in: Mar. Biomater., Springer Nature Singapore, Singapore, 2022: pp. 61–95. https://doi.org/10.1007/978-981-16-4787-1_3.

[17] J. Jeevanandam, S. Pan, J. Rodrigues, M.A. Elkodous, M.K. Danquah, Medical applications of biopolymer nanofibers, Biomater. Sci. 10 (2022) 4107–4118. https://doi.org/10.1039/D2BM00701K.

[18] C.A. Marangon, M.Á. Vigilato Rodrigues, M.R. Vicente Bertolo, V. da C. Amaro Martins, A.M. Guzzi Plepis, M. Nitschke, The effects of ionic strength and <scp>pH</scp> on antibacterial activity of hybrid biosurfactant□biopolymer nanoparticles, J. Appl. Polym. Sci. 139 (2022) 51437. https://doi.org/10.1002/app.51437.

[19] H. Anbari, A. Maghsoudi, M. Hosseinpour, F. Yazdian, Acceleration of antibacterial activity of curcumin loaded biopolymers against methicillin□resistant Staphylococcus aureus : Synthesis, optimization, and evaluation, Eng. Life Sci. 22 (2022) 58–69. https://doi.org/10.1002/elsc.202100050.

[20] V. vel, N.I. Ilaya, D.S.C. Chandru, D.R.B. Benz, Bioactive N and O Donor Atom of Bidentate Schiff Base Ligands from Chitosan Biopolymer and its Ruthenium(Iii) Complexes an Enhanced Antioxidant Activity, SSRN Electron. J. (2022). https://doi.org/10.2139/ssrn.4112833.

[21] A. Jha, M. Kumar, B. Mishra, Marine Biopolymer-Based Anticancer Drug Delivery Systems, in: Mar. Biomater., Springer Nature Singapore, Singapore, 2022: pp. 351–401. https://doi.org/10.1007/978-981-16-4787-1_11.

[22] N. Seyedi, M. Zahedifar, Preparation and characterization of new palladium complex immobilized on (chitosan)/PoPD biopolymer and its catalytic application in Suzuki cross□coupling reaction, Appl. Organomet. Chem. 36 (2022). https://doi.org/10.1002/aoc.6487.

[23] A. Nasiri, M.A. Khalilzadeh, D. Zareyee, Biosynthesis and characterization of

magnetic starch-silver nanocomposite: catalytic activity in eco-friendly media, J. Coord. Chem. 75 (2022) 256–279. https://doi.org/10.1080/00958972.2022.2038369.

[24] S. Pal, G. Sen, S. Mishra, R.K. Dey, U. Jha, Carboxymethyl tamarind: Synthesis, characterization and its application as novel drug-delivery agent, J. Appl. Polym. Sci. 110 (2008) 392–400. https://doi.org/10.1002/app.28455.

[25] A.P. Pandit, P.D. Waychal, A.S. Sayare, V.C. Patole, Carboxymethyl tamarind seed kernel polysaccharide formulated into pellets to target at colon, Indian J. Pharm. Educ. Res. 52 (2018) 363–373. https://doi.org/10.5530/ijper.52.3.42.

[26] J. Meena, S.K. Verma, R. Rameshwari, D.K. Verma, Polyaniline/carboxymethyl guar gum nanocomposites: as biodegradable, conductive film, RASAYAN J. Chem. 15 (2022) 1021–1027. https://doi.org/10.31788/RJC.2022.1526820.

[27] H. Kaur, M. Ahuja, S. Kumar, N. Dilbaghi, Carboxymethyl tamarind kernel polysaccharide nanoparticles for ophthalmic drug delivery, Int. J. Biol. Macromol. 50 (2012) 833–839. https://doi.org/10.1016/j.ijbiomac.2011.11.017.

[28] K. Mali, S. Dhawale, R. Dias, V. Ghorpade, Delivery of drugs using tamarind gum and modified tamarind gum: A review, Bull. Fac. Pharmacy, Cairo Univ. 57 (2019) 1–24. https://doi.org/10.21608/BFPC.2019.47260.

[29] Khushbu, S.G. Warkar, Potential applications and various aspects of polyfunctional macromolecule- carboxymethyl tamarind kernel gum, Eur. Polym. J. 140 (2020) 110042. https://doi.org/10.1016/j.eurpolymj.2020.110042.

[30] H.R. Badwaik, L. Kumari, S. Maiti, K. Sakure, Ajazuddin, K.T. Nakhate, V. Tiwari, T.K. Giri, A review on challenges and issues with carboxymethylation of natural gums: The widely used excipients for conventional and novel dosage forms, Int. J. Biol. Macromol. 209 (2022) 2197–2212. https://doi.org/10.1016/j.ijbiomac.2022.04.201.

[31] U. Holzwarth, N. Gibson, The Scherrer equation versus the “Debye-Scherrer equation,” Nat. Nanotechnol. 6 (2011) 534–534. https://doi.org/10.1038/nnano.2011.145.

[32] R.K. Shukla, Kishan, A. Shukla, R. Singh, Evaluation of nutritive value, phytochemical screening, total phenolic content and in-vitro antioxidant activity of the

seed of Prunus domestica L., Plant Sci. Today. 8 (2021). https://doi.org/10.14719/pst.2021.8.4.1231.

[33] H. Chandra, D. Patel, P. Kumari, J.S. Jangwan, S. Yadav, Phyto-mediated synthesis of zinc oxide nanoparticles of Berberis aristata: Characterization, antioxidant activity and antibacterial activity with special reference to urinary tract pathogens, Mater. Sci. Eng. C. 102 (2019) 212–220. https://doi.org/10.1016/j.msec.2019.04.035.

[34] S. Pirsa, E. Farshchi, L. Roufegarinejad, Antioxidant/Antimicrobial Film Based on Carboxymethyl Cellulose/Gelatin/TiO_2–Ag Nano-Composite, J. Polym. Environ. 28 (2020) 3154–3163. https://doi.org/10.1007/s10924-020-01846-0.

[35] A.P. Gupta, D.K. Verma, Preparation and characterization of carboxymethyl guar gum nanoparticles, Int. J. Biol. Macromol. 68 (2014) 247–250. https://doi.org/10.1016/j.ijbiomac.2014.05.012.

[36] J. Meena, P. Singh Jassal, Phenol organic impurity remove from pollutants water by batch adsorption studies with using magneto chitosan nanoparticle, Anveshana's Int. J. Res. Eng. Appl. Sci. 2 (2017).

[37] J. Meena, P.S. Jassal, Cresol and it derivative Organic pollutant removal from waste water by adsorption the magneto chitosan nanoparticle, Int. J. Chem. Stud. 5 (2017) 850–854.

Chapter 7

Conclusion and future prospectus

7.1 Conclusion

Chapter 1 discusses introduction of Biopolymer interspersed with metal oxide nanoparticles leading to form nanocomposites. In recent years, several new biopolymer-based nanocomposites dispersed with metal/metallic oxide nanocomposites were created (BMNCs). When compared to metal oxide nanoparticles, nanocomposites have distinct characteristics, such as sorption, energy, volume, size, and shape, which expand the application of the simple metal nanoparticle. BMNCs were prepared by incorporating metal oxide nanoparticles of Pt, Pd, Cu, Co, Zn, Ti, Mn, Fe, etc. in variety of biopolymers such as chitosan, alginate, cellulose, starch, PAA, pectin, tamarind kernel gum, etc. The variety of biopolymers-based nanocomposites, their synthesis and applications have been reported. Chapter 1 also throws light on various processing techniques for synthesizing biopolymer-based nanocomposites and on their applications such as organic/inorganic impurity removal, antibacterial activity, anti-oxidant activity, anticancer activity, electrochemical biosensor activity, and biomedical applications. Extensive Literature survey on the synthesis and applications of tamarind kernel gum and its derivative carboxymethyl tamarind kernel gum (CMTKG) has also been reported.

The experimental techniques used to conduct the research are covered in study Chapter 2 of the thesis. This chapter also includes information on the materials used, approved by the research, and the descriptions and parameters of several characterization techniques used to achieve the objectives of the research effort.

Chapter 3 of this study describes the purpose and parameters of the research that was done for this thesis.

In study **chapter 4**, utilising solutions of $Fe_2O_3.7H_2O$ and $FeCl_36H_2O$ as the source and CMTKG as the reducing and capping agent by in situ co-precipitations method, nanocomposite polysaccharides with in situ created CMTKG/FeO nanocomposites were prepared. The scanning electron microscopy and X-ray spectral analysis indicated the generation of spherical CMTKG/FeO nanoparticles in the average size in the range of 40-90

nm. These nanocomposites exhibited excellent antibacterial activity against both *Gram-positive bacteria* and hence can be considered for applications in antibacterial textiles for personal and hospital uses. The sensor properties of the synthesized nanocomposite solution across raising ammonia concentration in the range of (1–100) ppm by observing the changes in SPR situations and magnitude with a U.V.–Visible Spectrophotometer has been notified

In study chapter 5, a novel CMTKG/ZnO nanocomposite was created using an in-situ method. FTIR and XRD characterizations indicated the presence of ZnO nanoparticles which did not affect the chemical structure of CMTKG. However, chemical interaction between polymeric matrix and nanoparticle was found in FTIR spectra. SEM and TEM images confirms the homogeneous distribution of the ZnO nanoparticles in polymeric matrix with average particle size of 31 and 90 nm. The prepared nano-composite was then analyzed as adsorbent for Chromium (VI) removal. Contact time 80 minutes, adsorbent loading 2 mg/L, initial Chromium (VI) concentration 30 mg/L and feed pH 7 was found as optimum operating parameters for maximizing percent extraction of Chromium (VI) ions (95.5%) from waste water. Prepared composite was then examined as Antifungal material. A. flavus MTCC 2799 growth was successfully prepared by CMTKG/ZnO nano-composites.

The nano-precipitation approach was employed to successfully generate CMTKG nanoparticles in study **Chapter-6**. FTIR, SEM, TEM, TDA, and XRD investigations were used to characterize the physical, structural, and morphological features of CMTKG nanoparticles, such as size, shape, and dispersity. CMTKG NPs ranged in size from 40 to 60 nm. The nanoparticles were found to be spherical in shape, with diameters ranging from 20 to 50 nm, as well as scattered huge nanoparticles and clusters of 50 nm, as revealed by TEM. The antioxidant capabilities of the produced CMTKG nanoparticles composites were demonstrated by a radical scavenging model system. All of the outcomes were perfectly matched, just as they had been in the literature. CMTKG nanoparticles created in this manner could be employed as antioxidants. CMTKG nanoparticles exhibit good bioactive, biocompatible, and antibacterial properties, and hence can be exploited as a bio-polymeric material in tissue engineering, biomedical, and therapeutic applications, according to the findings of this study

7.2 Future prospects

The potential in this field concerns the development of carboxymethyl tamarind kernel gum/ Fe/ZnO nanocomposites with clay, metal oxides, and metal oxide modified clay, which can be used in sensors, pharmaceutical, biomedical, and textile industries, as well as the decontamination of organic/inorganic impurities from wastewater. The scientific community is expected to study numerous more applications and prospects of CMTKG-based nanocomposites in the approaching period. The development of cost-effective ways for draining industrial wastewater treatment should also be a part of future nanocomposites study.

7.3 List of Publications

From Thesis

- Warkar, S.G., **Meena, J.** (2022). Synthesis and applications of biopolymer/FeO nanocomposites: A review. Journal of New Materials for Electrochemical Systems, Vol. 25, No. 1, pp. 7-16. **DOI:** https://doi.org/10.14447/jnmes.v25i1.a02
- **Jagram Meena**, Harish Chandra, Sudhir G. Warkar*, Carboxymethyl tamarind kernel gum /ZnO- biocomposite: As an antifungal and hazardous metal removal agent, Journal of New Materials for Electrochemical Systems, Vol. 25, No.3, July 2022, pp.57-64. https://doi.org/10.18280/jnmes.v25i3.a08
- **Jagram Meena**, Harish Chandra, Sudhir G. Warkar*, Antimicrobial and Ammonia sensor activity of novel carboxymethyl tamarind kernel gum/nano composites, Indian Journal of Engineering and Material Science (CSIR-NISCAIR) [Under Review]

Other Publications

- Verma D. K., **J. Meena** et al. "Synthesis, characterization and applications of chitosan based metallic nanoparticles: A review. Journal of Applied and Natural Science 13.2 (2021): 544-551. **DOI** https://doi.org/10.31018/jans.v13i2.2635
- **J. Meena**, S. K. Verma, R. Rameshwari and D. K. Verma, Polyaniline/carboxymethyl guar gum nanocomposites: As biodegradable, conductive film, Rasayan Journal of Chemistry, i.e. Vol. 15, No.2, 2022 issue. 1021-1027. DOI: http://doi.org/10.31788/RJC.2022.1526820
- Synthesis of nickel nanorods and their conversion in to nanoparticles" **(Accepted)** Journal of Chemistry and Environment.

Conference Presentation

1. Oral Presentation - International conference on Material Science and Technology (ICMT-2021) 12-14 th Nov. 2021 organized by Mahatma Gandhi University Kottayam, Kerala invited lecture entitled "Carboxymethyl tamarind kernel gum/ZnO biocomposite and its application

2. Oral Presentation International conference on Energy Science (ICES-2021) 10-12 th Dec. 2021 organized by Mahatma Gandhi University Kottayam, Kerala invited lecture entitled "Carboxymethyl tamarind kernel gum/Fe-O biocomposite and its characterization

IIETA International Information and Engineering Technology Association
Advancing the World of Information and Engineering

Journal of New Materials for Electrochemical Systems

Vol. 25, No.1, January 2022, pp. 07-16

Journal homepage: http://iieta.org/journals/jnmes

Synthesis and applications of biopolymer /FeO nanocomposites: A review

Sudhir G. Warkara and Jagram Meena*b

[ab]Department of Applied Chemistry, Delhi Technological University, Delhi 110042, India.

Corresponding Author Email: jrm.svc3@gmail.com

ABSTRACT

Magnetic oxide nanoparticles have engaged most consideration due to their rare character, such as easy separation, surface-to-volume ratio, paramagnetic and high surface area. Natural biopolymers, namely, (Chitosan, Guar-Gum, Tamarind, Alginate, Dextran, Pectin) have posed as an incredible host for the preparation of magnetic nanoparticles. Biopolymer based magnetic nanocomposites have been fabricated from long time using method like co-precipitations, green synthesis, in-situ, hydrothermal and wet chemical method. Properties of biopolymer magnetic nanocomposites draw attention to the researchers towards fabricating at the nano level for various applications like as adsorptions inorganic metal, organic impurity, targeted drug-delivery, bio-sensing, catalysis activity, antimicrobial activity, antifungal activity, antioxidant activity, anti-cancer activity, energy, environmental remediation, waste water treatment and textiles. This review is designed to report very firstly reported biopolymer magnetic nanoparticles (BMNPs) in last ten years and attractive approach in various applications.

Keywords: *Biopolymers; Biopolymer magnetic nanoparticles; Adsorptions, Antimicrobial activity, Antioxidant, Catalyst activity*

Received: September-2021 **Accepted**: November 29-2021 https://doi.org/10.14447/jnmes.v25i1.a02

1. INTRODUCTION

Implications and applications of nanomaterials have been widely explored. The improvement of nanotechnology has implement assets to numerous utilizations in the medical field, leading to important advances in terms of adsorptions, biological detection, diagnosis, , and drug delivery [1] The nanomaterials stand out as indispensable and superior in several fields, owing to their exclusive size-dependent properties.[2]

Generally, magnetic oxides are frequent, widely used as they are reasonable and play an essential role in various geological and biological processes. They are also predominantly usage by humans, for example, ores in catalysts, thermite , magnetic , durable pigments (colour concrete and coatings, paints,) and haemoglobin [3] Magnetic nanoparticles have been adsorbents catalysts, sensors, reducing agents and bactericides such as superparamagnetic iron oxide nanoparticles [4] The potential applications of magnetic nanoparticles in the bio-medical field, like as magnetic resonance imaging and magnetic separation, [5] targeted drug delivery, hyperthermia treatment for cancer, antibacterial activity and biomedical[6-8] have been of great interest, lately. They exhibit quick kinetics and appreciate adsorption capacity because of their high surface to volume ratio [9]. The metallic nanoparticles (MNPs) are especially attractive due to their exclusive properties and differing applications [10]. It has been approved that the dispersibility, morphology, size, , and physio-chemical character of MNPs are vigorously coordinate with their applications, which are afflicted by the synthetic access [11]. Biopolymers are naturally environmentally eco-friendly, abounding and, inexpensive polymers. Opportunity are extensively used in agricultural, industries, medical, and environmental because of their especially sustainable, renewable, and non-toxic characteristics [12]. This has also been reflected in the metal-polymer nanocomposites research area biopolymers, such as (chitosan, starch, alginate, tamarind gum, pectin. Cellulose, Gelatine, Guar gum, dextran, Mannan, PAA, PVA-A, Pectin etc.) [13-25]

Figure 1 shows magnetic nanoparticles' various properties as sorbents, reducing /oxidizing agents, nano-magnets, etc. The second step helps illustrates how individual imperfections of nanoparticles and bio polymeric host materials are abolished by using nanocomposites.

Biopolymer Magnetic Nanoparticles have been synthesized using different methods such as Green synthesis[12] electrodeposition [26] Combustion[27] in situ[28] ex-situ [29] wet method[81] (hydrothermal[46] co-precipitation [30] Incorporation of natural biopolymer into magnetic nanoparticles increases its application on a massive scale like Biomedical [101], Adsorption[31] Environmental[32] (Liang Drug delivery[33] Antimicrobial activity [34] Antioxidant activity[35] Anti-cancer activity[36] and catalyst activity [37].

The prime focus of the present article is the synthesis of biopolymer based magnetic metal nanoparticles/ nanocomposites and their applications. The review shall more over its readers with a knowledge of recent methods that are being employed for the synthesis of BMNPs and their biomedical applications.

Journal of New Materials for Electrochemical Systems
Vol. 25, No.3, July 2022, pp.57-64
Journal homepage: http://iieta.org/journals/jnmes

Carboxymethyl tamarind kernel gum /ZnO- biocomposite: As an antifungal and hazardous metal removal agent

Jagram Meena[ab], Harish Chandra[b], Sudhir G. Warkar*[a]

[a] Delhi Technological University, Delhi India 110042
[b] Gurukul Kangri (Deemed to be University) Haridwar-249404, Uttarakhand, India-249404

*Author for correspondence: sudhirwarkar@gmail.com

https://doi.org/10.18280/jnmes.v25i3.a08

Received: May 25-2022
Accepted: July 22-2022

Keywords:
Carboxymethyl tamarind kernel gum, zinc oxide NPs, antifungal, adsorption, chromium etc

ABSTRACT

ZnO nanoparticles (ZnO NPs) were in situ mixed with carboxymethyl tamarind kernel gum to generate the new biocomposite. High-resolution transmission electron microscopy (HR-TEM), field emission scanning electron microscopy (FE-SEM), Fourier transform infrared (FTIR), x-ray diffraction analysis (XRD), and dynamic light scattering (DLS)were used to characterize the CMTKG/ZnO nanocomposites. Numerous characterizations were utilized to prove that ZnO NPs had been integrated into the biopolymer matrix. The standard size of the CMTKG/ZnO nanocomposites was developed to be greater than 32–40 nm using high-resolution transmission electron microscopy and x-ray analysis de-Scherer methods. Chromium (VI) was removed from the aqueous solution using the nanocomposite (CMTKG/ZnO) as an adsorbent. The nanocomposite reached its maximum adsorption during 80 minutes of contact time, 30 mg/L chromium (VI) concentration, 2.0 g/L adsorbent part, and 7.0 pH. Further research into the antifungal activity of CMTKG/ZnO nanocomposites against *Aspergillus flavus* MTCC-2799 was conducted.

1. INTRODUCTION

In recent years, aquatic contamination has gained international attention as a deliberate environmental concern, particularly for a number of pollutants that are entering aquatic systems as a result of the unplanned rapid rise in the world's population, industrialization, urbanization, and the excessive use of agricultural fertilizers and chemical hazards [1]. Chromium is a substance that is used in paints and the chemical industry that poses a serious risk to the atmosphere [2]. It results in water supply contamination. Chromium exists in two oxidation states in hydrated situations: one is trivalent Chromium (III) and the other is hexavalent Chromium (VI) [3]. Due to the fact that ionic compounds containing Chromium (VI), like CrO_4^{2-} and H_2CrO_4, are more transportable and soluble than Cr (III). While chromium (III)-containing phases form a feeble cell barrier, chromium (VI)-containing phases more easily penetrate through cell membranes [4-5]. In fluid conditions, Cr (VI) is thought to be 100 times more dangerous than Cr (III) [6-7]. Cr (VI) has significantly higher mobility in water and so it can be converted into a variety of reactive and hazardous intermediates, eventually compromising human health due to its accumulating properties *[8-9]*.

Chromium can be taken out of contaminated water through co-precipitation, chemical reduction, coagulation, ion exchange, and adsorption methods. Most of these techniques are often expensive. On the other hand, adsorption techniques are a good choice because they are safe for the environment, effective, and non-toxic. [10]. ZnO NPs showed distinctive chemical and physical characteristics. [11]. Due to their novel uses in adsorptions [12], sensor activity [13], heat treatment [14], antimicrobial activity [15], antifungal activity [16], wound healing [17], ultra-violet filtering [18], and excessive catalytic and photochemical activity [19–20], ZnO NPs have attracted the attention of researchers. Nearly all researchers concur that it's critical to create green nanomaterial in an aqueous medium. This is due to the fact that it is simple to conduct and has no effect on the environment.

Natural, non-toxic, renewable, and sustainable polymer alternatives include biopolymers. They are extensively employed in industry, medicine, agriculture, and the environment. Some of the biopolymers that find use in the biomedical and pharmaceutical sectors include chitin, chitosan, cellulose, tamarind, starch, and pectin [21]. Biopolymers such as alginate, chitosan, and starch provide excellent alternatives for matrix polymers because they contain a high concentration of hydroxyl groups in their chains, which offer a favorable environment for the formation of nanoparticles. [22] Biopolymers have also been demonstrated to be bio and mucoadhesive, biocompatible, biodegradable and non-aggravating hence explored in biomedical applications such as drug delivery, bio nanoreactors, nanofiltration, biosensors, and antibacterial activity. In two other studies [26, 27], polysaccharides extracted from Tamarindus indica seeds were modified to carboxymethyl tamarind seed kernel polysaccharide (CMTSP) and then used for drug delivery [26] and as enzyme [27].

RJC

RASĀYAN *J. Chem.*
Vol. 15 | No. 2 |1021-1027| April - June | 2022
ISSN: 0974-1496 | e-ISSN: 0976-0083 | CODEN: RJCABP
http://www.rasayanjournal.com
http://www.rasayanjournal.co.in

POLYANILINE/CARBOXYMETHYL GUAR GUM NANOCOMPOSITES: AS BIODEGRADABLE, CONDUCTIVE FILM

J. Meena[1], S. K. Verma[2], R. Rameshwari[3] and D. K. Verma[4,✉]

[1]Department of Chemistry, Gurukul Kangri (Deemed to be University), Haridwar-249404 (Uttarakhand), India

[2]Department of Chemistry, Dayalbagh Educational Institute (Deemed University), Agra, India.

[3]Department of Biotechnology, Manav Rachna International Institute of Research and Studies, Faridabad, India

[4]Department of Chemistry, Sri Venkateswara College, University of Delhi (South Campus), Delhi, India.

✉Corresponding author: vermadev148@gmail.com

ABSTRACT

Biomaterial-based nanocomposites have been increased in demand in industries for a purpose of packaging and sensing because of their low cost and environmentally friendly nature. But less work has been done on conductive, biodegradable film preparations. This article is devoted to the preparation of Polyaniline/ Carboxymethyl guar gum nanocomposites film and their applications. Controlled synthesis of polyaniline in the presence of carboxymethyl guar gum solution has been carried out for the synthesis of these nanocomposites. Then nanocomposite films have been obtained by solution casting method in one step. The object of this research work was to prepare a conductive, biodegradable, flexible film. Such made nanocomposites film has been further tested for FTIR, SEM, UTM, Conductivity, Swelling behavior and biodegradability. The results have been concluded that by this method a fine flexible, conductive, biodegradable film may be prepared that can be applied in different fields for further study.

Keywords: Carboxymethyl Guar Gum, Polyaniline, Biodegradable, Nanocomposites Film.

RASĀYAN *J. Chem.*, Vol. 15, No.2, 2022

INTRODUCTION

A variety of nanostructure materials have been prepared so far with different synthesis approaches. Some of the research findings show that electrical stimulation affects a lot of cellular activities.[1-2] On this basis, conductive polymers like polyaniline, polypyrrole, etc. have been used in biomedical applications.[3] Polyaniline is the most studied polymer because of its easy synthesizing, low cost of formation, and easy combining property.[4] But even this, polyaniline has some drawbacks like non-biodegradability, not being soluble in common salts, and being unable to form thin films. This limits polyaniline in biomedical applications, but it has been found that this problem can be removed by replacing polyaniline with short chains aniline oligomers.[5] This short-chain oligomers may be obtained by control synthesizing. Researchers have found that conductivity, yield, and chain length may be controlled by using different doses of initiator, monomer, pH value of the medium, viscosity of the medium, temperature, and time of the reaction[6]. Polysaccharides have been found very useful for biomedical applications because of their biocompatibility and biodegradable behavior. CMGG (Carboxymethyl guar gum) is also a polysaccharide.[7] It has also a guar gum-based backbone.[8-9] Among the derivatives of the guar gum, CMGG has some specific properties which make this suitable for use in biomedical and drug delivery.[9-11] Some of the specific properties include good film-forming property, low cost, easy to synthesize, good stabilizing and reducing agent, biodegradable and biocompatible, soluble in acidic water, and vicious than guar gum. In this research article Polyaniline/ Carboxymethyl guar gum (PANI/CMGG) nanocomposites biodegradable, flexible, conductive film was prepared by controlled synthesizing, which might be used in biomedical application like tissue engineering and control drug delivery applications. For these, following points were considered:

Rasayan J. Chem., 15(2), 1021-1027(2022)
http://doi.org/10.31788/RJC.2022.1526820